ANALYSES OF POWER SYSTEM VULNERABILITY

AND TOTAL TRANSFER CAPABILITY

A Dissertation

by

XINGBIN YU

Submitted to the Office of Graduate Studies of
Texas A&M University
in partial fulfillment of the requirements for the degree of

DOCTOR OF PHILOSOPHY

December 2005

Major Subject: Electrical Engineering

ANALYSES OF POWER SYSTEM VULNERABILITY

AND TOTAL TRANSFER CAPABILITY

A Dissertation

by

XINGBIN YU

Submitted to Office of Graduate Studies of
Texas A&M University
in partial fulfillment of the requirements for the degree of

DOCTOR OF PHILOSOPHY

Approved by:

Chair of Committee,   Chanan Singh
Committee Members,   Garng M. Huang
                                  Andrew K. Chan
                                  Bryan L. Deuermeyer
Head of Department,   Costas N. Georghiades

December 2005

Major Subject: Electrical Engineering

ABSTRACT

Analyses of Power System Vulnerability

and Total Transfer Capability. (December 2005)

Xingbin Yu, B.S., Shanghai Jiao Tong University;

M.S., Shanghai Jiao Tong University

Chair of Advisory Committee: Dr. Chanan Singh

Modern power systems are now stepping into the post-restructuring era, in which utility industries as well as ISOs (Independent System Operators) are involved. Attention needs to be paid to the reliability study of power systems by both the utility companies and the ISOs. An uninterrupted and high quality power is required for the sustainable development of a technological society. Power system blackouts generally result from cascading outages. Protection system hidden failures remain dormant when everything is normal and are exposed as a result of other system disturbances. This dissertation provides new methods for power system vulnerability analysis including protection failures. Both adequacy and security aspects are included.

The power system vulnerability analysis covers the following issues: 1) Protection system failure analysis and modeling based on protection failure features; 2) New methodology for reliability evaluation to incorporate protection system failure modes; and, 3) Application of variance reduction techniques and evaluation. A new model of current-carrying component paired with its associated protection system has been proposed. The model differentiates two protection failure modes, and it is the foundation of the proposed research. Detailed stochastic features of system contingencies and corresponding responses are considered. Both adequacy and security reliability indices are computed. Moreover, a new reliability

index ISV (Integrated System Vulnerability) is introduced to represent the integrated reliability performance with consideration of protection system failures. According to these indices, we can locate the weakest point or link in a power system. The whole analysis procedure is based on a non-sequential Monte Carlo simulation method. In reliability analysis, especially with Monte Carlo simulation, computation time is a function not only of a large number of simulations, but also time-consuming system state evaluation, such as OPF (Optimal Power Flow) and stability assessment. Theoretical and practical analysis is conducted for the application of variance reduction techniques.

The dissertation also proposes a comprehensive approach for a TTC (Total Transfer Capability) calculation with consideration of thermal, voltage and transient stability limits. Both steady state and dynamic security assessments are included in the process of obtaining total transfer capability. Particularly, the effect of FACTS (Flexible AC Transmission Systems) devices on TTC is examined. FACTS devices have been shown to have both positive and negative effects on system stability depending on their location. Furthermore, this dissertation proposes a probabilistic method which gives a new framework for analyzing total transfer capability with actual operational conditions.

To my wife and my parents

ACKNOWLEDGMENTS

I would like to take this opportunity to express my heartfelt gratitude to everyone who has made it possible for me to successfully complete this dissertation. First, I would like to thank the Department of Electrical Engineering and its faculty for admitting me to the Ph. D. program in 2001, which opened the door to my Ph.D. studies here at Texas A&M University.

I am deeply indebted to my advisor, Professor Chanan Singh, for taking me as his student and giving me all the motivation and guidance I needed in my research work. His influence was instrumental to my academic performance, especially in making me realize the importance of striking a proper balance between theory and practice in my research. It amazes me how he is able to view research problems from many perspectives, and develop a variety of new techniques to solve them. Because he is never short of insight and creative ideas, it is always very enlightening to have a conversation with him.

I would like to thank Professor Andrew K. Chan, and Professor Bryan L. Deuermeyer who served on my oral examination committee. I am particularly grateful to Professor Garng M. Huang, who is also on my committee, for his advice and insight about my dissertation research. I would also like to thank all the staff in the Department of Electrical Engineering who assisted me with many administrative issues pertaining to my research work. The funding from Texas Advanced Technology Program has also been essential in supporting my research financially.

In addition, I am grateful to Dr. Yishan Li and Dr. Hyungchul Kim for taking time to discuss my research work with me, and for the many helpful suggestions they have given to improve the efficiency of the computer programs that I wrote in the course of my research. I am also grateful to Dr. Yan Ou, Dr. Nader Samaan and Dr. Jiansheng Lei for all the useful knowledge I have gained from them.

TABLE OF CONTENTS

LIST OF FIGURES

Figure   Page

LIST OF TABLES

I.   INTRODUCTION

1.1 Introduction

Modern power systems are now stepping into the post-restructuring era, in which utility industries as well as ISOs are involved. It is understood that attention needs to be paid to the reliability of power systems both by the utility companies and the ISOs. Reliability analysis is an important part of power systems. An uninterrupted and high quality power is required for the sustainable development of a technological society. The reliability of composite power systems consists of two basic aspects, adequacy and security [1][2][3][4]. Adequacy is mainly concerned with the ability of the electric systems to supply the aggregate electrical demand and energy requirements of customers at all times taking into account scheduled and reasonably expected unscheduled outages of system elements. Security deals with the ability of the system to withstand sudden disturbances such as short circuits or unanticipated loss of system element [1].

Protective relaying is an important branch of electric power engineering concerned with the principles of design and operation of equipment which detect abnormal power system conditions, and initiate action as quickly as possible in order to isolate the faulted component and return the rest of the system to the normal condition. The primary purpose of protection system consists of correct diagnosis of trouble, quickness of response, and minimum disturbance to the power system. Due to the requirement of quick response, human intervention in the protection system operation is not possible. System protection has evolved, over the years, from relatively primitive devices with limited capacity, to complex systems that involve extensive hardware. The modern protective systems are more selective in their detection and operation, and often require greater analytical effort in their application [5]. We must further examine the possibility

This dissertation follows the style and format of *IEEE Transactions on Power Systems.*

that protective relaying equipment itself may fail to operate correctly. It should be clear that extensive and sophisticated equipments and schemes are needed to accomplish these tasks.

In most reliability analysis, protection systems are assumed to be perfectly reliable. However, protection system itself is a complicated system comprising of a number of components, each of which has probability of failure. During the development of the modern power systems, protection system dependability has taken priority over global system security. While reinforcing the protection complexity to guarantee the system dependability, the risk of incorrect operation of protection system increases as well. There is more and more evidence that protection systems play a role in the origin and propagation of major power system disturbances. Studies show that protective relays are involved in about 75 percent of major disturbances. Power system blackouts generally result from cascading outages. Protection system hidden failures, which remain dormant when everything is normal and are exposed as a result of other system disturbances [6], are the main cause of cascading outages. Admittedly, large-scale power system blackout is a rare event. However, when it occurs, the impact on the system is catastrophic [7]. Though considerable progress has been made in power system reliability modeling and computational methods, not much effort has been spent on the study of the cascading events resulting from protection system malfunction. It is only recently that serious efforts were initiated to study the effect of protection system on power system reliability.

Some studies have been made on the origin and development of cascading outages, their impact and preventive action [7][8][9][10]. Most of the work was based on adequacy reliability analysis without considering the transient behavior of cascading outages. As a matter of fact, transient impact might interact with particular protection and control mechanisms in such a way that could cause or worsen cascading outages. Furthermore, stability is an important index that represents the system tolerance to contingencies. Therefore it is necessary to develop an integrated reliability study methodology concerning the protection system failures.

Total Transfer Capability (TTC) is another important topic in terms of planning, dispatch and control in system operation. In deregulated power system, TTC is the transmission limit for reserving and scheduling energy transactions in competitive electric markets. Accurate evaluation of TTC is essential to maximize utilization of existing transmission grids while maintaining system security. The TTC is a function of thermal, voltage and transient stability limits of the system. The previous work on calculating TTC considers only the first two constraints, i.e. thermal limit and voltage magnitude limit. The results without considering transient stability limit are prone to be somewhat optimistic and could not represent the actual system performance. Following those values in operation may lead to system instability in case of contingencies.

1.2 Research Objectives

The proposed research is focused on reliability analysis considering protection failures and calculation of transfer capability including stability. Both adequacy and security aspects are included. Following objectives are expected to be achieved.

1.2.1 Protection System Failure Analysis and Modeling

Based on protection failure features, a new model of current-carrying component paired with its associated protection system is established. This model differentiates 2 protection failure modes. This model is the foundation of the proposed research. Based on this model, we can obtain protection system failure probability with regard to its operation and inspection.

A new methodology for reliability evaluation to incorporate protection system failure modes is proposed. The cascading outage procedure is simulated including the effect of protection system hidden failures. In the process of cascading outages, hidden failure probability varies depending on system fault and operating condition. Detailed stochastic features of system contingencies and corresponding responses are considered. Both adequacy and security reliability indices are computed. Moreover, a new reliability index

IOV is introduced to represent the integrated reliability performance with consideration of protection system failures. According to these indices, we can locate weakest point or link in a power system. The whole analysis procedure is based on non-sequential Monte Carlo simulation method.

1.2.2 Variance Reduction Technique Application and Evaluation

Protection failures are rare events in a power system. Some variance reduction technologies could be applied to reduce simulation time. The candidate technologies include dagger, importance sampling, etc. In reliability analysis, especially with Monte Carlo simulation, computation time is a function not only of often large number of simulations, but also of time consuming system state evaluation, such as OPF and stability assessment. Theoretical and practical analysis will be conducted for the application of variance reduction techniques.

1.2.3 Total Transfer Capability Analysis

Total Transfer Capability (TTC) is defined as the amount of electric power that can be transferred over the interconnected transmission network in a reliable manner while meeting all of a specific set of defined pre- and post-contingency system conditions. TTC may be limited by the physical and electrical characteristics of the systems including thermal, voltage, and stability limits. The calculation of TTC must incorporate all three constraints – thermal, voltage, and security. In this dissertation, security analysis is emphasized in TTC calculation since it has been rarely considered in previous studies. It is well known that Flexible AC Transmission System (FACTS) technology can control voltage magnitude, phase angle and circuit reactance, so it can redistribute the load flow and regulate bus voltage. One objective of this research is to investigate the impacts of the two most popularly used FACTS devices – Thyristor Controlled Series Compensator (TCSC) and Static Var Compensator (SVC) on TTC. Because of the essentially stochastic nature of power system behavior, it is very important to calculate ATC in a probabilistic framework. The third objective of this research is to develop methodology to compute and

analyze probabilistic TTC. In order to provide more realistic and complete information to various market participants, the statistical analysis and risk assessment associated with TTC are proposed. Probabilistic TTC methodology is expected to yield more realistic results.

1.3 Organization of Dissertation

Section II provides the literature review of techniques for power system reliability evaluations. The review includes power system reliability theory, protection system history and trend, blackouts and their causes and precautions. Total Transfer Capability analysis is also discussed. Section III describes component-protection system model and introduces hidden failure modes and mathematical models for adequacy and security analysis. Section IV proposes the methodology formulation of Monte Carlo simulation. Both adequacy and security analyses are implemented. Numerical simulations are included to demonstrate the application of the proposed methodology. Section V introduces two innovative approaches for power system reliability simulation: Importance Sampling Monte Carlo Simulation (IS-MCS) and integration of Self-Organizing Map and Importance Sampling Monte Carlo Simulation (SOM-IS-MCS) methods. The concepts and applications of both approaches are introduced and evaluated. Case studies with adequacy and security analyses are performed. Section VI analyzes the effect of FACTS devices on TTC with security constraints and deals with probabilistic TTC calculation with consideration of security constraints. Numerical case studies are conducted and practical applications are evaluated. Section VII summarizes the research contribution and suggests the future work.

II.   REVIEW

2.1 Power System Reliability Considerations

The primary role of a power system is to provide reliable and continuous electrical energy to satisfy system load. Power system reliability, in a broad sense, can be defined as the ability of the system to provide an adequate supply of electric power with satisfactory quality. Power systems have three main components: generation, transmission and distribution systems. The generation systems generate electricity and transmission systems deliver the generated electricity to distribution systems for supplying load. The generation systems together with transmission systems are usually called the composite system or the bulk power system.

The reliability of a composite power system is comprised of both adequacy and security assessments [11-13]. Adequacy assessment relates to the ability of the system to supply energy requirements of customers in a satisfactory manner. Since adequacy assessment deals with static condition, it does not include the evaluation of the system response to transient disturbances. Security assessment deals with the ability of the electric systems to survive sudden disturbances such as electric short circuits or unanticipated loss of system elements. This includes the response of the system caused by the loss of generations and transmission lines.

The typical indices used in power system reliability evaluation are the following

Loss of Load probability (LOLP) is the probability that some portion of load demand may not be satisfied by the available generating capacity under the specified operating conditions and policies. LOLP is currently the most widely used reliability index.

Daily *Loss of Load Expectation* (LOLE) is the expected period of time during a given period, in which the daily peak load is expected to exceed the available generating

capacity. The hourly LOLE in *h/y* can be obtained by multiplying the LOLP by 8760 hours. LOLP and LOLE are often used interchangeably.

Loss of Load Frequency (LOLF) is the expected number of occurrence during a given period of time that the system may fail to meet its load demand.

Expected Unserved Energy (EUE) is the expected amount of energy during a given period of time that the system may be unable to supply to the consumers due to the loss of generation or load uncertainty. Typical unit is MW*h/year*.

Shrinking transmission margins for reliability makes the preservation of system reliability a harder job than it used to be. The system is being operated closer to the edge of reliability that it was just a few years ago. Table 2.1 represents some of the changed conditions that make the reliability situation more challenging [14].

Table 2.1 Changing Conditions That Affect System Reliability

Previous Conditions	Emerging Conditions
Fewer, relatively large resources	Smaller, more numerous resources
Long-term, firm contracts	Contracts shorter in duration More non-firm transactions, fewer long-term firm transactions
Bulk power transactions relatively stable and predictable	Bulk power transactions relatively variable and less predictable
Assessment of system reliability made from stable base (narrower, more predictable range of potential operating states)	Assessment of system reliability made from variable base (wider, less predictable range of potential operating states)
Limited and knowledgeable set of utility players	More players making more transactions, some with less interconnected operation experience; increasing with retail access
Unused transmission capacity and high security margins	High transmission utilization and operation closer to security limits
Limited competition, little incentive for reducing reliability investments	Utilities less willing to make investments in transmission reliability that do not increase revenues

Table 2.1 (Continued)

Previous Conditions	Emerging Conditions
Market rules and reliability rules developed together	Market rules undergoing transition, reliability rules developed separately
Limiting wheeling	More system throughput

2.2 Protection System History and Trend

Protection system plays an important role in power system operation in terms of safety and security. During the development of modern power systems, protection system dependability (the ability to function correctly when required) has taken priority over consideration of global system security (the ability to refrain from unnecessary operations). While reinforcing the protection systems to guarantee system dependability, the probability of their incorrect operation may increase as a result of higher complexity. It has been observed that protection system hidden failures commonly lead to multiple or cascading outages, which consequently can cause large-scale power system blackouts. A study by NERC (North American Electric Reliability Council) shows that protective relays are involved in about 75 percent of major disturbances [15]. There have been several large-scale cascading failures in recent times effecting large populations of customers in the Western United States. All of these blackouts are related to protection system hidden failures, which remain dormant when everything is normal and manifest as a result of other system disturbances [6]. There are two major failure modes in protection system: "failure to operate" and "undesired tripping" [16]. The former means that when a fault occurs in a power system, the protection system fails to clear the fault. The latter refers to either spontaneous operation in the absence of a fault or trip for faults outside the protection zone. Large-scale power system blackout is a rare event. However, when it occurs, the impact on the system is catastrophic [7]. Therefore, study of the origin and propagation of cascading outages, their impact and preventive actions are becoming more and more imperative.

Many studies have been conducted regarding hidden failures in protective relays and their impact on power system reliability [7][8][9][10][16][17]. Some of this work has proposed

methods for system vulnerability analysis. However, all of the work was mainly focused on adequacy analysis with the assumption that during cascading outages, system transits from one steady state to another. As a matter of fact, transient impact might interact with protection and control mechanisms in a way that could cause or worsen the impact of cascading outages. Furthermore, stability is a critical index that represents the system tolerance to contingencies. Vulnerability analysis ignoring the transient processes cannot represent the system behavior accurately and therefore the corresponding results may not give us the appropriate information. It is necessary to incorporate dynamic reliability analysis in a realistic vulnerability study as well. In this paper, while considering protection system failures, we conduct vulnerability research with consideration of both adequacy and security aspects, and provide a more realistic approach as applied to the power systems.

Protection systems are complicated in terms of principle, function, setting, operation, and maintenance. We use a simple example (Figures 2.1 & 2.2) to illustrate protection system failure features [5].
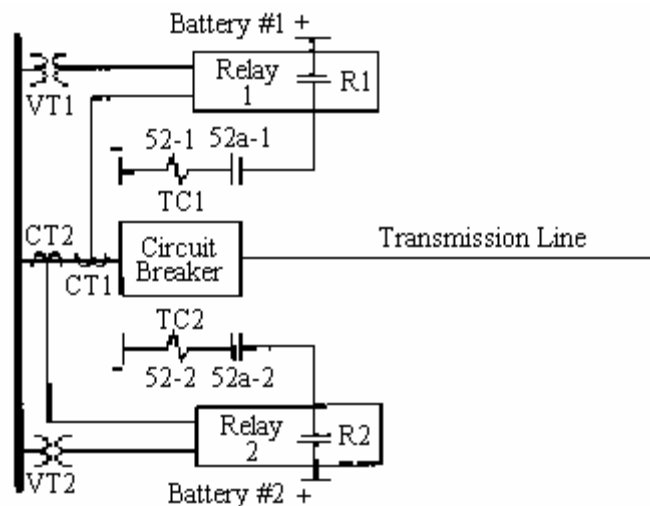
Figure 2.1 Transmission Line Protections with Redundant Components
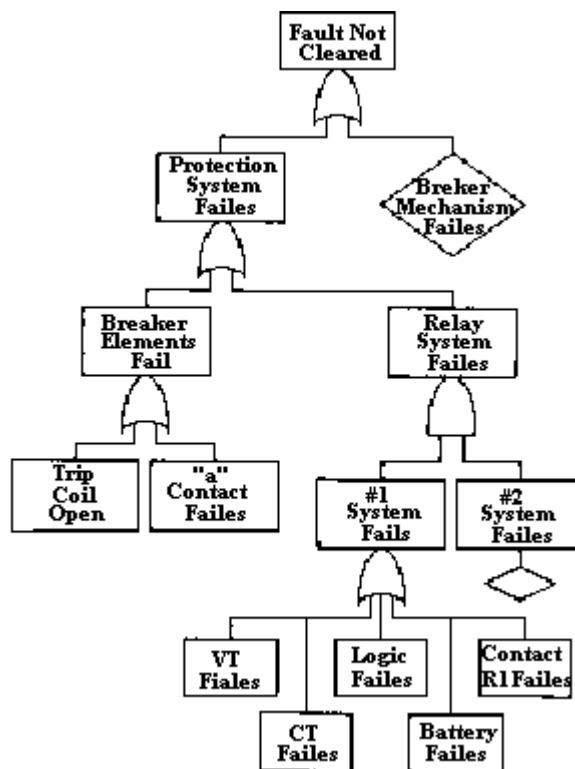
Figure 2.2 Fault Tree for One of the Protective System of Figure 2.1

As an example of fault tree construction, Figure 2.2 shows a fault tree for failure of the protective system shown in Figure 2.1. Almost the entire fault tree is constructed of OR gates, which indicates that there are many different items that can cause the failure of a protective system. The only requirement for the AND gate is in connection with the relays themselves, which are fully redundant. The nature of this type of failure may be different for breakers of different designs.

2.3 Blackouts, Causes and Precautions

Major blackouts are rare, and no two blackout scenarios are the same. The initiating events will vary, including human actions or inactions, system topology, and load/generation balances. Other factors that will vary include the distance between generating stations and

major load centers, voltage profiles across the grid, and the types and settings of protective relays in use.

Some wide-area blackouts start with short circuits (faults) on several transmission lines in short succession – sometimes resulting from natural causes such as lightening or wind or, as on August 14, 2003, resulting from inadequate tree management on right-of-way areas [14]. A fault causes a high current and low voltage on the line containing the fault. A protective relay for that line detects the high current and low voltage and quickly trips the circuit breakers to isolate that line from the rest of the power system.

A cascade is a dynamic phonemic phenomenon that cannot be stopped by human intervention once started. It occurs when there is a sequential tripping of numerous transmission lines and generators in a widening geographic area. A cascade can be triggered by just a few initiating events. Power swings and voltage fluctuations caused by these initial events can cause other lines to detect high currents and low voltages that appear to be faults, even if faults do not actually exist on those other lines. Generators are tripped off during a cascade to protect them from severe power and voltage swings. Protective relay systems work well to isolate them from the system under normal and abnormal system conditions.

But when power system operating and design criteria are violated because several outages occur simultaneously, commonly used protective relays that measure low voltage and high current cannot distinguish between the currents and voltages seen in a system cascade from those caused by a fault. This leads to more and more lines and generators being tripped, widening the blackout area [14].

System-wide disturbances that effect many customers across a broad geographic area are rare, but they occur more frequently than a normal distribution of probabilities would predict. North American power system outages between 1984 and 1997 are shown in

Figure 2.3 by the number of customers affected and the rate of occurrence. In Figure 2.3, the circles represent individual outages in North America between 1984 and 1997, plotted against the frequency of outages of equal or greater size over that period. (Source: Adapted from John Doyle, California Institute of Technology, "Complexity and Robustness," 1999. Data: NERC). While some of these were widespread wealth-related events, some were cascading events that, in retrospect, were preventable. Electric power systems are fairly robust and are capable of withstanding one or more contingency events, but they are fragile with respect to multiple contingency events unless the systems are readjusted between contingencies. With the shrinking margin in the current transmission system, it is likely to be more vulnerable to cascading outages than it was in the past, unless effective countermeasures are taken [14].
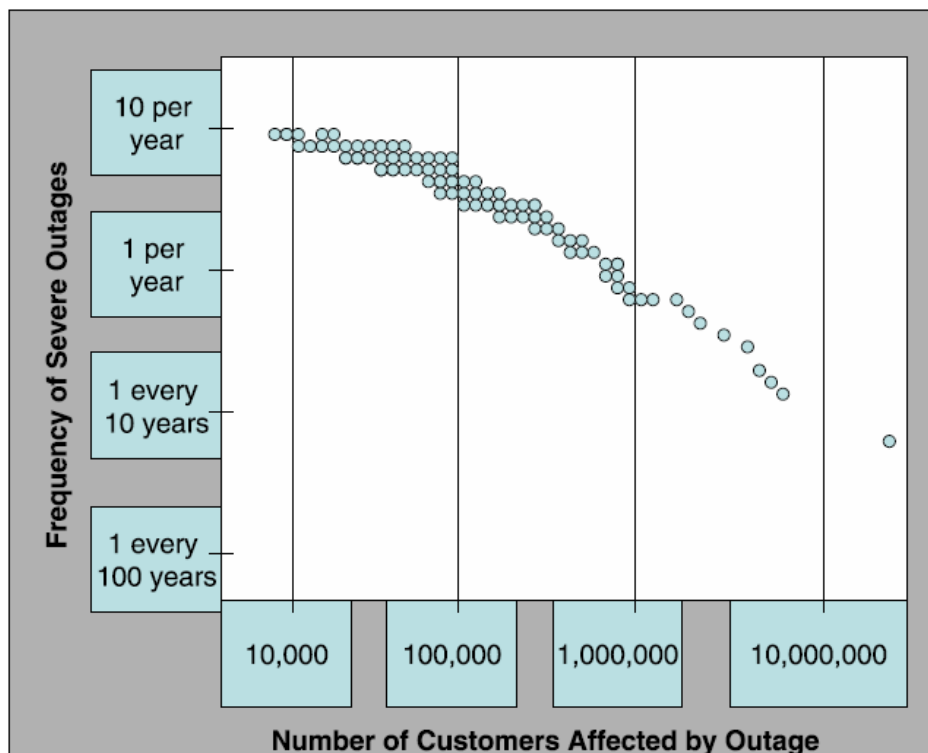
Figure 2.3 North American Power System Outages, 1984-1997

Some representative catastrophic events are listed below.

2.3.1 November 9, 1965: Northeast Blackout

This disturbance resulted in the loss of over 20,000MW of load and affected 30 million people. Virtually all of New York, Connecticut, Massachusetts, Rhode Island, small segments of northern Pennsylvania and northeastern New Jersey, and substantial areas of Ontario, Canada, were affected. Outages lasted for up to 13 hours. This event resulted in the formation of the North American Electric Reliability Council in 1968. A backup protective relay operated to open one of five 230-kV lines taking power north from a generating plant in Ontario to the Toronto area. When the flows redistributed instantaneously on the remaining four lines, they tripped out successively in a total of 2.5 seconds. The resultant power swings resulted in a cascading outage that blacked out much of the Northeast.

The major causal factors were as follows:
- Operation of a backup protective relay took a 230-kV line out of service when the loading on the line exceeded the 375-MW relay setting.
- Operating personnel were not aware of the operating set point of this relay. Another 230-kV line opened by an over current relay action, and several 115- and 230-kV lines opened by protective relay action.
- Two key 345-kV east-west (Rochester-Syracuse) lines opened due to instability, and several lower voltage lines tripped open.
- Five of 16 generators at the St. Lawrence (Massena) plant tripped automatically in accordance with predetermined operating procedures.
- Following additional line tripouts, 10 generating units at Beck were automatically shut down by low governor oil pressure, and 5 pumping generators were tripped off by over speed governor control.
- Several other lines then tripped out on under-frequency relay action.

2.3.2 July 13, 1977: New York City Blackout

This disturbance resulted in the loss of 6,000 MW of load and affected 9 million people in New York City. Outages lasted for up to 26 hours. A series of events triggering the separation of the Consolidated Edison system from neighboring systems and its subsequent collapse began when two 345-KV lines on a common tower in Northern Westchester were struck by lightning and tripped out. Over the next hour, despite Consolidated Edison dispatcher actions, the system electrically separated from surrounding systems and collapsed. With the loss of imports, generation in New York City was not sufficient to serve the load in the city.

Major causal factors were:

- Two 345-kV lines connecting Buchanan South to Millwood West experienced a phase B to ground fault caused by a lightning strike.
- Circuit breaker operations at the Buchanan South ring bus isolated the Indian Point No. 3 generating unit from any load, and the unit tripped for a rejection of 883 MW of load.
- Loss of the ring bus isolated the 345-kV tie to Laden Town, which had been importing 427 MW, making the cumulative resources lost 1,320 MW.
- 18.5 minutes after the first incident, an additional lightening strike caused the loss of two 345-kV lines, which connect Sprain Brook to Buchanan North and Sprain Brook to Millwood West. These two 345-kV lines share common towers between Millwood West and Sprain Brook. One line (Sprain Brook to Millwood West) automatically reclosed and was restored to service in about 2 seconds. The failure of the other line to reclose isolated the last Consolidated Edison interconnection to the Northwest.
- The resulting surge of power from the Northwest caused the loss of the Pleasant Valley to Millwood West line by relay action.
- 23 minuets later, the Leeds to Pleasant Valley 345-kV line sagged into a tree due to overload and tripped out.

- Within a minute, the 345 kV to 138 kV transformer at Pleasant Valley overloaded and tripped off, leaving Consolidated Edison with only three remaining interconnections.

- Within 3 minutes, the Long Island Lighting Co. system operator, on concurrent of the pool dispatcher, manually opened the Jamaica to Valley Stream tie.

- The two remaining external 138-kV ties to Consolidated Edison tripped on overload, isolating the Consolidated Edison system.

- Insufficient generation in the isolated system caused the Consolidated Edison island to collapse.

2.3.3 December 14, 1994: West Coast Blackout

At 1:25 A.M. on December 14, 1994, electric power flowed much heavier than normal from southern California to northern California and from northern California to the Northwest. A single phase-to-ground fault on a 345-kV line at the three-terminal substation Midpoint-Borah in Idaho caused the inadvertent tripping of an additional 345-kV line in the same station. Due to the substation configuration, the remaining line became open-ended, which is equivalent to being off-line. Overload and under voltage condition for some lines developed within the system due to the weakened network. The lines tripped one after another in a domino effect style, which led to the formation of four separate islands, 5,020 MW power was lost and 1,500,000 customers affected in this single phase-to-ground fault initiated event [18].

2.3.4 July 2-3, 1996: West Coast Blackout

This disturbance resulted in the loss of 11,850 MW of load and affected 2 million people in the West. Customers were affected in Arizona, California, Colorado, Idaho, Montana, Nebraska, Nevada, New Mexico, Oregon, South Dakota, Texas, Utah, Washington, and Wyoming in the United States; Alberta and British Columbia in Canada; and Baja California Norte in Mexico. Outages lasted from a few minutes to several hours.

The Outage began when a 345-kV transmission line in Idaho sagged into a tree and tripped out. A protective relay on a parallel transmission line also detected the fault and incorrectly tripped a second line. An almost simultaneous loss of these lines greatly reduced the ability of the system to transmit power from the nearby Jim Bridge plant. Other relays tripped two of the four generating units at that plant. With the loss of those two units, frequency in the entire Western Interconnection began to decline, and voltage began to collapse in the Boise and Idaho area, affecting the California-Oregon AC inter tie transfer limit.

For 23 seconds the system remained in precarious balance, until the Mill Creek to Antelope 230-kV line between Montana and Idaho tripped by zone 3 relay, depressing voltage at Summer Lake Substation and causing the inter tie to slip out of synchronism. Remedial action relays separated the system into five pre-engineered islands designed to minimize customer outrages and restoration times. Similar conditions and initiating factors were present on July 3; however, as voltage began to collapse in the Boise area, the operator shed load manually and contained the disturbance.

2.3.5 August 10, 1996: West Coast Blackout

This disturbance resulted in the loss of over 28,000 MW of load and affected 7.5 million people in the West. Customers were affected in Arizona, California, Colorado, Idaho, Montana, Nebraska, Nevada, New Mexico, Oregon, South Dakota, Texas, Utah, Washington, and Wyoming in the United States; Alberta and British Columbia in Canada; and Baja California Norte in Mexico. Outages lasted from a few minutes to as long as nine hours.

Triggered by several major transmission line outages, the loss of generation from McNary Dam, and resulting system oscillations, the Western Interconnection separated into four electrical islands, with significant loss of load and generation. Prior to the disturbance, the transmission system from Canada south through the Northwest into California was heavily loaded with north-to-south power transfers. These flows were due to high Southwest

demand caused by hot weather, combined with excellent hydroelectric conditions in Canada and the Northwest.

Very high temperatures in the Northwest caused two lightly loaded transmission lines to sag into untrimmed trees and trip out. A third heavily loaded line also sagged into a tree. Its outage led to the overload and loss of additional transmission lines. General voltage decline in the Northwest and the loss of Mcnary generation due to incorrectly applied relays caused power oscillations on the California to Oregon AC inter tie. The inter tie's protective relays tripped these facilities out and caused the Western Interconnection to separate into four islands. Following the loss of the first two lightly loaded lines, operators were unaware that the system was in an insecure state over the next hour, because new operating studies had not been performed to identify needed system adjustments.

2.3.6 August 14, 2003: US Midwest and Northeast/Canada

Before the blackout, a sequence of line trappings in northeast Ohio after 15:05 EDT caused heavily loadings on a number of transmission lines. The weakened system quickly started a cascading blackout at 16:05:57 (East Standard Time) after the Sammis-Star 345-kV relayed. In less than ten minutes, more than 508 generating units at 265 power plants were lost. The northern part of the whole eastern interconnection was broken apart into five islands. The blackout affected about 50 million people and caused the loss of 61,800 MW of electric load in the state of Ohio, Michigan, Pennsylvania, New York, Vermont, Massachusetts, Connecticut, New Jersey and the Canadian province of Ontario [14].

2.4 Total Transfer Capability (TTC)

2.4.1 Problem Definition

Total Transfer Capability (TTC) is defined as the amount of electric power that can be transferred over the interconnected transmission network in a reliable manner while meeting all of a specific set of defined pre- and post-contingency system conditions. TTC may be limited by the physical and electrical characteristics of the systems including

thermal, voltage, and stability limits. Total Transfer Capability is an important indicator of how much power can be transferred between two buses in the power system without compromising the system security [19][20]. The accurate TTC provides critical information for power system planners, operators and marketers. Planners need to know where the system bottlenecks are. Operators need to identify transmission congestions based on TTC, and marketers need to know if the transaction along certain route in the grid is feasible or not. The accurate TTC calculation is needed to ensure that power system can operate without reliability risks. Excessive conservative TTC, of course, may limit the power transfer unnecessarily and make the system operate inefficiently. In other words, TTC is the largest value of power transfer that causes no limit violations, with or without a contingency. The objective is to determine the maximum real power transfers from sending areas to receiving area.

Mathematically the TTC calculation procedure can be simplified as following:
- establish a base case without any violations;
- Define a transfer, which includes a power source and sink;
- Increase power input in the source and load in the sink until one of the limit is violated.

Find out the maximum delivered power from source to sink though the transmission network.

2.4.2 Existing Methods of TTC Calculation

2.4.2.1 Continuation Power Flow Approach

Continuation power flow method can be used to calculate TTC [21][22][23]. Starting from a solved base case, this method obtains a series of power flow solutions by increasing the transfer parameter without singularity of the Jacobian by way of a prediction-correction scheme. The amount of the transfer is a scalar parameter in the problem model.

2.4.2.2 Optimal Power Flow Approach

The application of Optimal Power Flow (OPF) in power system congestion management has been studied by some researchers [24][25][26][27]. In the mean time, TTC calculation by OPF approach has been proposed since 1999[28][29][30]. The basic concept of OPF approach is formulating the TTC calculation as an optimization problem, with equity constraints of power flow, inequality constraints from basic operation and equipment limits to more detailed approximation of transient stability security requirements. The objective function, obviously, is the maximum power flow on the specified transmission route.

2.4.2.3 Repeated Power Flow Approach

Repeated power flow approach starts from a base case, and repeatedly solves the power flow equations each time increasing the power transfer by a small increment until an operation limit is reached [31]. The advantage of this approach is its simple implementation and the ease to take security constraints into consideration. In this dissertation, this method is adopted to solve TTC problem.

III.   RELIABILITY MODEL[*]

Power system blackouts result from cascading outages. Protection system failures are the main cause of cascading outages. To facilitate reliability analysis with consideration of protection system failures, in this section, component-protection system model, together with hidden failure modes and mathematical formulation are proposed. Based on these models, adequacy and security analysis can be conducted successfully.

3.1 Introduction

Protection system plays an important role in power system operation in terms of safety and security. During the development of modern power systems, protection system dependability (the ability to function correctly when required) has taken priority over consideration of global system security (the ability to refrain from unnecessary operations). While reinforcing the protection systems to guarantee system dependability, the probability of their incorrect operation may increase as a result of higher complexity. It has been observed that protection system hidden failures commonly lead to multiple or cascading outages, which consequently can cause large-scale power system blackouts. A study by NERC (North American Electric Reliability Council) shows that protective relays are involved in about 75 percent of major disturbances [14]. There have been several large-scale cascading failures in recent times affecting large populations of customers in the Western United States. All of these blackouts are related to protection system hidden failures, which remain dormant when everything is normal and manifest as a result of other system disturbances [6]. Large-scale power system blackout is a rare event. However, when it occurs, the impact on the system is catastrophic [7]. Therefore, study of the origin and propagation of cascading outages, their impact and preventive actions are becoming more and more imperative.

In conventional power system reliability analysis, following assumptions are normally made:

- Protection system is 100% reliable
- Circuit is treated as single element
- Terminal station is considered as a single a busbar.

Figure 3.1 shows the typical single busbar representation of a terminal station, which includes protection system. When simultaneous outages are studied, the term "common mode contingency" is usually used. Common mode contingency is an event having a single external cause with multiple failure effects which are not consequences of each other. The concept of station-originated outages is used to handle simultaneous outages for terminal stations. In Figure 3.1, for instance, the failure of breaker 2 can cause outage of both L2 and L3.
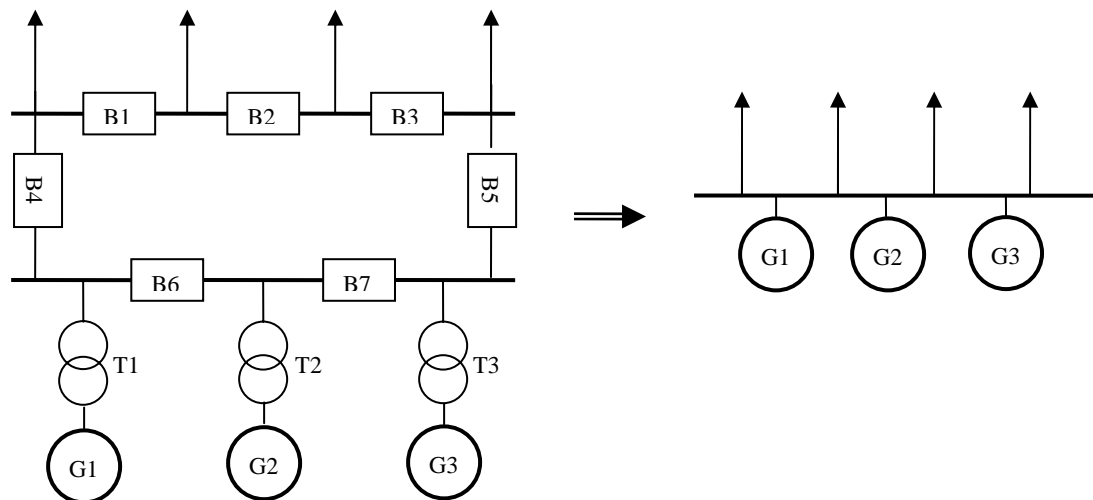
Figure 3.1 Conventional Assumption of a Terminal Station

Even if the probability of individual outage is high, the product can become quite small. The probability of a protection related outage resulting in a similar event can, however, be

many times larger. Therefore, the effect of such outages on reliability indices can be significant as compared with second and higher order simultaneous independent outage.

3.2 Protection Failure Modes and Cascading Outages

Protection system has two major failure modes: "failure to operate" and "undesired tripping" [15]. The former means that when a fault occurs in a power system, the protection system fails to clear the fault. The latter refers to either spontaneous operation in the absence of a fault or trip for faults outside the protection zone. In practice, phenomenon of stuck breaker is included in "failure to operate" mode.

A cascading outage refers to a series of trips initiated by one component failure in the system. When a fault occurs, the impact on the system such as over-current or voltage drop may cause some protection devices to operate incorrectly. Two types of protection system failures mentioned above are the major cause of cascading outages. Based on real life protection scenario, "failure to operate" will directly cause at least one bus isolation in the system. There are 2 types of "undesired tripping", one is "spontaneous unwanted tripping" that occurs in the absence of a fault, and another is "tripping for faults outside the protection zone". Since spontaneous unwanted tripping can be remedied immediately by auto-reclose and the system is designed to withstand the loss of any single element without a fault, this case does not have significant effect on the system reliability. Tripping for faults outside the protection zone is the main cause of the cascading outages. We will only focus on this kind of undesired trip in this research.

3.3 Models and Assumptions

3.3.1 Component-Protection Model

There have been a number of models established to facilitate the reliability evaluation including protection system failures. The model of current-carrying component paired with its associated protection system proposed by Singh and Patton [15] [16] is effective for general reliability analysis. However, it does not differentiate protection failure modes. In

this dissertation, the model is expanded to include the failure modes of protection system as shown in Figure 3.2, where we have the following:

State 1: the current-carrying component and the protection system are both good.

State 2: the component is good but the protection is at risk for "undesired trip".

State 3: the component is good but the protection is exposed to "failure to operate".

State 4: the component is good and the protection system is being inspected.

Stage 5: the component is failed while the protection system is still under "undesired trip"

State 6: the component is failed but the protection system is good.

State 7: the component is failed while the protection system has experienced "failure to operate".
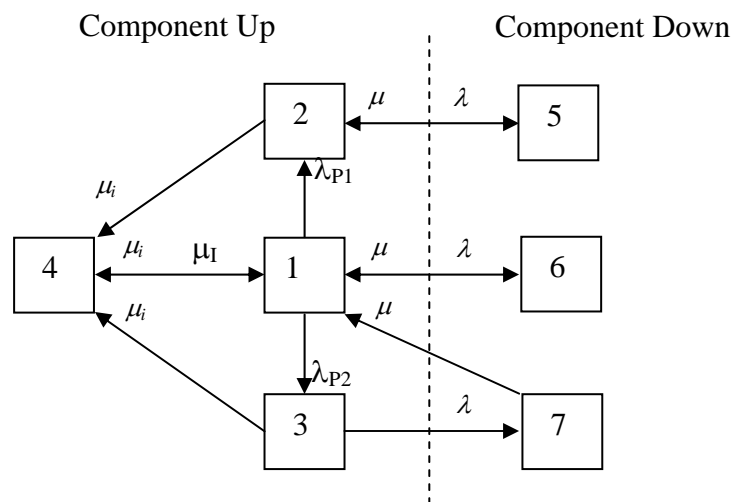
Figure 3.2 State Transition Diagram of a Component and Its Protection System

The notations in Figure 3.2 are as below:

μ_i inspection rate of protection system.

μ_I repair rate of protection system.

μ repair rate of component.

λ failure rate of component.

λ_{P1} failure rate of protection system to exposure to "undesired trip".

λ_{P2} failure rate of protection system to state of "failure to operate"

This model differentiates the two protection failure modes and represents them as two states: "undesired trip" and "failure to trip". When a component is in these two states, its protection system is suffering from hidden failure and can cause malfunction. Different failure modes will lead to different responses to contingencies and therefore have different contributions to system vulnerability. We adopt this model to derive probability of each state as basic input for subsequent simulation.

3.3.2 Protection System Failure Models

The "failure to operate" may occur after the fault is initiated. When "failure to operate" happens, the faulted line will be isolated by backup protection. Normally we use the phrase "stuck breaker" to represent this case. "Failure to operate" phenomenon is not very complicated since it is only related to the protection device itself rather than system operating condition. The probability of "failure to operate" is the probability of state 3 in the component/protection model (Figure 3.2).

The "undesired tripping" is more complicated since in this case the occurrence of cascading outages results not only from the existence of hidden protection failures, but is also related to system fault and operating conditions. "Failure to operate" and "undesired tripping" may occur simultaneously during the fault period. After the fault is cleared, "undesired tripping" will be the sole cause of cascading outages. In the following discussion we emphasize the "undesired tripping" properties.

We use distance protection and overcurrent protection to reveal the protection hidden failures "during fault" and "post fault" periods respectively. Since distance protection zone 3 and overcurrent protection overload have the lowest faulty parameter setting values, they

are more sensitive to the fault and abnormal operating conditions, Therefore, distance protection zone 3 and overcurrent protection overload are used to represent protection hidden failure properties in the study.

Reference [8] proposed a model of hidden failure probability of exposed line tripping as a function of impedance seen by the relay. In this paper, we adopt some simplification for the probability properties. For distance protection scheme, this property is shown in Figure 3.3 that suits the situation during the fault period.
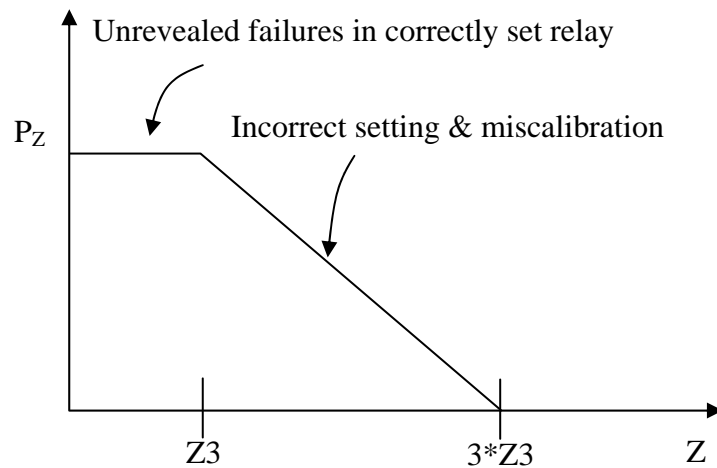
P_Z:	Distance protection failure probability
Z3:	Impedance zone 3 setting
Z:	Impedance seen by relay

Figure 3.3 Distance Protection Failure Probability of Exposed Line

On the other hand, after the initial fault is cleared, power flow in the system would change due to the changing topology. This might lead to redistribution of load on certain lines, which are then at risk to trip subsequently [9]. To represent the post-fault situation, we introduce over-current protection failure probability property as shown in Figure 3.4.

P_I: Over-current Protection failure probability
I3:   overload setting
I: Current seen by relay
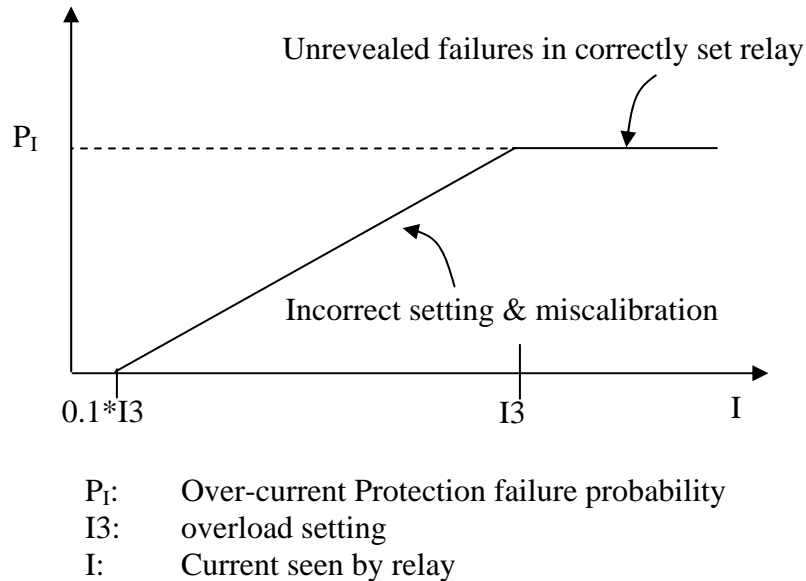
Figure 3.4 Over-current Protection Failure Probability of Exposed Line

In Figure 3.3 and Figure 3.4, P_Z and P_I are the probability of state 2 in the component/protection model (Figure 3.2). P_Z and P_I are protection system failure properties that are used "during fault" period and "post-fault" period respectively. Although P_Z and P_I refer to different protection devices, they are similar in type (either electromechanical, static, or digital). For simplicity of calculations we use the same numerical values for P_Z and P_I. This is however not an inherent limitation and different values can be used if available. Nevertheless, during the simulation process, the probability of exposed line tripping incorrectly is not simply a fixed value. On the contrary, it is also dependent on the fault and operating conditions as shown in Figure 3.3 and Figure 3.4. Each line may have a different probability of incorrect trip.

3.3.3 Mathematical Models

3.3.3.1 Cascading Outages

Traditional power system fault calculation is conducted in "during fault" period to figure out the outages in addition to the faulted line. Fault analysis here first calculates fault currents in all transmission lines and voltages in all buses. Based on these fault parameters the impedance seen by relay at each bus can be calculated. The impedance values then can be used as inputs of Figure 3.3 to determine the hidden failure probabilities "during fault" period.

Similarly, in "post-fault" period, Newton-Raphson power flow method is used to examine further line outages due to overload. The current values are inputs of Figure 3.4 to determine the hidden failure probability in "post-fault" period.

These two procedures control the process of cascading outages for both adequacy and security analysis.

3.3.3.2 Adequacy Analysis

An optimization procedure to determine the occurrence and the amount of load curtailment is formulated for adequacy assessment. The formulation is shown as below:

Objective:
$$\min \sum_{i=1}^{n} (Load\_Curtailment)_i \qquad (3.1)$$

$$\text{where } (Load\_Curtailment)_i = P_{di} - P_{li}$$

subject to:

$$P_{gi} - P_{li} - \sum_{j=1}^{n} U_i U_j (G_{ij} \cos \delta_{ij} + B_{ij} \sin \delta_{ij}) = 0$$

$$Q_{gi} - Q_{li} - \sum_{j=1}^{n} U_i U_j (G_{ij} \cos \delta_{ij} - B_{ij} \sin \delta_{ij}) = 0 \qquad i=1,...,n$$

$$P_{gi\min} \le P_{gi} \le P_{gi\max}$$

$$Q_{gi\min} \le Q_{gi} \le Q_{gi\max} \qquad\qquad i=1,...,n_g$$

$$0 \le P_{li} \le P_{di}$$

$$0 \le Q_{li} \le Q_{di} \qquad\qquad i=1,...,n_d$$

$$U_{i\min} \le U_i \le U_{i\max} \qquad\qquad i=1,...,n$$

$$P_{ij}^2 + Q_{ij}^2 \le S_{ij\max}^2 \qquad\qquad ij \in [1,...,n_b]$$

where

n, n_g, n_d, n_b:	the number of node, generator node, load node and branch;
P_{gi}, Q_{gi}:	the real and reactive output of the generator;
P_{gimin}, P_{gimax}:	the min/max real power of the generator;
Q_{gimin}, Q_{gimax}:	the min/max reactive power of the generator;
P_{li}, Q_{li}:	the load after rescheduling of generation;
P_{di}, Q_{di}:	the actual demand;
U_i:	the voltage magnitude;
U_{imin}, U_{imax}:	the voltage magnitude limits;
P_{ij}, Q_{ij}:	the line flow;
S_{ijmax}:	the line flow limit.

3.3.3.3 Security Analysis

We examine system transient stability for security analysis. Due to the shortcomings of the commonly used CCT (Critical Clearing Time) method for transient analysis including random fault location and auto-reclosing [32], we choose swing equation model to handle stability analysis directly. A typical swing-equation model includes second-order

differential equations associated with generator buses and algebraic equations for other buses. For the generator buses, we have equation (3.2):

$$M_i \ddot{\delta}_i + D_i \dot{\delta} = P_{mi} - P_{gi} \qquad\qquad i=1,\dots,n \qquad\qquad (3.2)$$

where δ_i : the generator rotor angle.

P_{mi} : the mechanical power input

P_{gi} : the electrical power output

n : the number of generators.

M_i : the ith-generator's inertia coefficient

D_i : the ith-generator's damping coefficient

Mechanical power P_{mi} is equal to the pre-fault electrical power, which can be obtained by power flow calculation. Electric power output is given as (3.3):

$$P_{gi} = \sum_{j=1}^{n} |V_i| |V_j| |Y_{ij}| \cos(\theta_{ij} - \delta_i + \delta_j) \qquad\qquad i=1,\dots,n \qquad\qquad (3.3)$$

where Y_{ij} is the reduced bus admittance matrix.

The transient stability criterion is that within a certain period after the occurrence of fault, the difference of any two rotor angles does not exceed the maximum secure relative swing angle, which is set as 180°. Since transient stability is only examined in a short time period after the occurrence of a fault, the assumption is made that the series of cascading outages occur within that short period.

3.3.4 Stochastic Features

To evaluate power system reliability, especially for security analysis, probabilistic factors must be taken into consideration [11]. There are many uncertainties in terms of system contingencies and corresponding responses. The following stochastic features are considered in our vulnerability evaluation.

- Type of fault: A variety of contingencies might happen in a power system. As for the vulnerability analysis, however, we assume all faults to be three-phase, either transient or permanent. This strategy will yield somewhat conservative results.

- Location of fault: The fault probabilities of transmission lines are calculated from their forced outage data. On the particular faulted line, the fault location is assumed to follow uniform distribution model.

- Fault clearing time: A normal probability distribution model is used to represent the fault clearing time.

- Reclosing time: The probabilities associated with the auto-reclosing time are assumed to be normally distributed.

- Fault duration: The distribution of fault duration is assumed Rayleigh.

3.3.5 Assumptions

Following assumptions are made in the vulnerability analysis.

- "Failure to operate" and "undesired trip" of the protection system failure do not overlap. That means, these two protection system failure do not occur simultaneously.

- Only first order initial contingencies are considered.

- The protection system failure does not happen when the current carrying component is in failure state.

- All failures are mutually independent. Failures of the protection system are independent from the failures of the components.

- Generator mechanical power P_{mi} is constant during the transient procedure.

IV.   IMPLEMENTATION OF VULNERABILITY ANALYSIS METHODOLOGY[*]

In this section, detailed cascading outage sequences are described and analyzed. Comprehensive Monte Carlo simulation methodology is implemented to simulate cascading outages. Some crucial reliability indices are calculated. Integrated System Vulnerability (ISV), including both adequacy and security effects, is proposed to represent the integrated vulnerability of a power system. Numerical results of simulations are also included.

4.1 Cascading Outage Sequences

Due to the complicated stochastic features of cascading outages, we use a sample network (Figure 4.1) to describe the basic simulation principle. The event tree in Figure 4.2 just illustrates a certain possible cascading outage sequence, in which there are nine events listed. In real simulation, other cascading outage sequences might happen also.
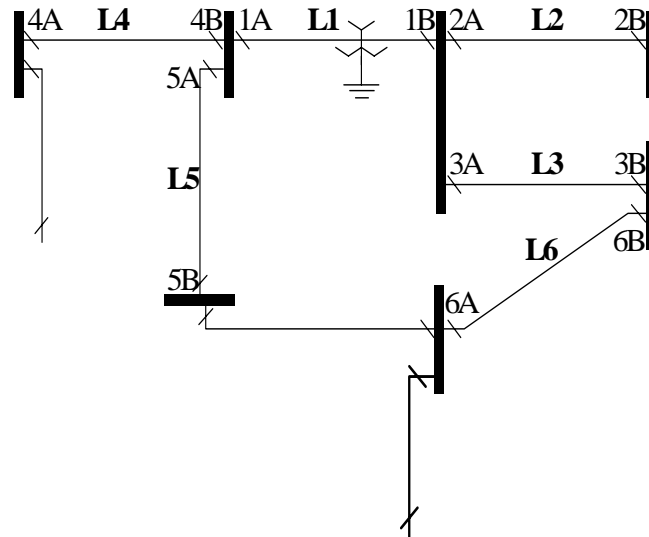
Figure 4.1 Sample Network.
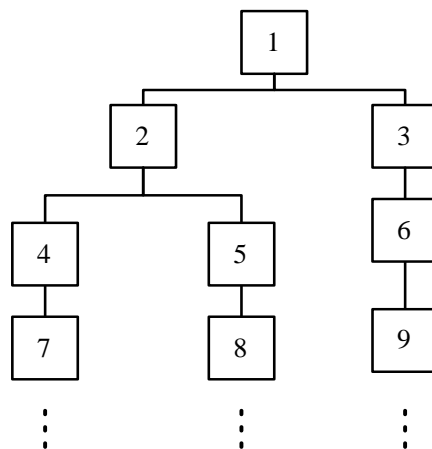
Figure 4.2 Possible Event-tree for Cascading Outages.

These nine possible events in Figure 4.2 are explained as below:

1) A fault occurs on transmission line L1. All lines connected to the faulted line are exposed lines. So lines L2, L3, L4 and L5 are exposed lines and are at risk to misoperate.

2) Breaker 1A and 1B trip, no hidden failure for protection system associated with line L1. Fault is cleared.

3) Breaker 1A trips whereas 1B does not due to "failure to operate", such as stuck breaker mode.

4) Breaker 1A and 1B reclose successfully for temporary fault.

5) Breaker 1A and 1B reclose unsuccessfully for permanent fault.

6) Backup protection operates to trip breakers 2A and 3A.

7) L1 back to service. Breaker 2A and 2B trip provided there is "undesired tripping" hidden failure exists on the protection system associated with line L2

8) Breaker 1A and 1B trip again. Breaker 2A and 2B trip provided there is "undesired tripping" hidden failure exists on the protection system associated with line L2

9) Breaker 6A and 6B trip provided there is "undesired tripping" hidden failure on the protection system associated with line L6

Event tree in Figure 4.2 does not exhaust all possible event paths. In fact, it just presents an example to describe the sequence of cascading outages due to protection system failure. In Figure 4.2, events 6), 7), 8) and 9) indicate the cascading outages resulting from protection system hidden failures. In simulation, the series of outages would keep on extending in the inherent probabilistic manner until no more new outage occurs or certain criterion is reached.

4.2 Process of Analysis

4.2.1 During Fault

Fault remains in the system and protection system takes action under fault condition. During the fault period, all neighboring components in the system are suffering from impact as well. This is the most dangerous period for the exposure of unrevealed failures. Therefore, fault analysis is conducted in this period till the fault is eventually cleared. The events in this period include events 1)~6) in Figure 4.2.

4.2.2 Post-Fault

After the fault is cleared, system enters after-fault period, in which transient phenomenon is still going on but no fault exists any longer. In this period, cascading outage probability is mainly associated with the exposed lines' over-current resulting from network topology changes. Therefore we apply power flow analysis in this period to figure out following cascading events.

4.3 Reliability and Vulnerability Indices

4.3.1 Bus Isolation Probability (BIP)

Bus isolation is a major disturbance to the power system. BIP shows the weakness of system in which a single component outage might result in bus isolation.

The mathematical description is as equation (4.1).

$$BIP = \sum_i \frac{I_i}{N} \qquad (4.1)$$

where i : an element of the set of simulations conducted.

               I_i : 1 if there is bus isolation in simulation i, otherwise it is 0.

               N : the total number of simulations.

In simulation, "bus isolation" is the criterion to stop for a series of outages. This means that as the series of outages progress, it is stopped as soon as a bus is isolated.

4.3.2 Loss of Load Probability (LOLP)

LOLP is a typical reliability index indicating the likelihood that service to electricity customers will be curtailed. Normally, a power system can withstand one component outage without adequacy and security violation. Based on our assumptions, here the LOLP represents the load curtailment resulting from protection system failure. The series of outages is stopped as soon as loss of load occurs.

LOLP is described mathematically in equation (4.2)

$$LOLP = \sum_i \frac{L_i}{N} \qquad (4.2)$$

where i : an element of set of simulations conducted.

               L_i : 1 if there is load curtailment in simulation i, otherwise it is 0.

               N : the total number of simulations.

4.3.3 Expected Power Loss (EPL)

EPL is the average load curtailment quantity of a power system. This index with units of "MW" can numerically show the impact of cascading outages on the system. There is no artificial stopping criterion for a series of outages being used for calculating this index. The series of outage will keep extending until no more new outages occur.

$$EPL = \sum_i \frac{C_i}{N}$$ (4.3)

where i : an element of set of completion of cascading outages.

          C_i : the load curtailment during simulation i.

          N : the total number of simulations.

In the analysis of this dissertation, EPL indicates the impact of hidden failures on system reliability. It should be normalized to differentiate the effects on various power systems. The normalized EPL can be defined as nEPL in (4.4)

$$nEPL = \frac{EPL}{SL}$$ (4.4)

where SL is the total system load.

4.3.4 Probability of Stability (POS)

POS shows the likelihood of system stability. The aim of power system stability study is to check the system's ability of maintaining synchronism under system contingencies. At the end of each cascading outage, security analysis is performed based on the series of outages just occurred to check if any generator in the system loses synchronization. The result of evaluation is recorded to facilitate the derivation of *POS*. Similarly, POS is defined as equation (4.5).

$$POS = \sum_i \frac{S_i}{N} \tag{4.5}$$

where I : an element of set of simulations.

S_i : 1 if the system is stable in simulation i, otherwise it is 0.

N : the total number of simulations.

4.3.5 Integrated System Vulnerability (ISV)

In a power system, each transmission line has different component failure phenomena, protective device hidden failure probability and protection system scheme. Because of these variations, *BIP*, *LOLP*, *EPL* or *POS* separately might locate different weak links for the same system. *ISV*, with effects of both adequacy and security performance, represents the integrated vulnerability of a particular system. After obtaining *BIP*, *LOLP*, n*EPL* and *POS*, we can calculate *ISV* by choosing proper weighting factors (4.6).

$$ISV = \alpha_1(BIP) + \alpha_2(LOLP) + \alpha_3(nEPL) + \alpha_4(1 - POS) \tag{4.6}$$

where α : the weighting factors.

The selection of the weighting factors depends on the emphasis of the study and the specific requirements of the power systems. In this dissertation, we propose the set of weighting factors be 0.25, 0.10, 0.15 and 0.50 with the balanced importance of adequacy and security. Specifically, security factor is 0.50 and total adequacy factor is 0.50, in which three adequacy indices have shares of 0.25, 0.10 and 0.15 respectively.

4.4 Simulation Algorithm

The simulation consists of two procedures. The first one is analytical procedure generating protection system hidden failure probabilities and the second one is non-sequential Monte Carlo simulation calculating reliability indices.

4.4.1 Hidden Failure Probability Calculation

In a power system, each transmission line has its own protection system, which has its own hidden failure probability as well. From Markov chain in Figure 3.2, based on known state transition rates, we can figure out the hidden failure probability of each protection system.

First we form the transition rate matrix as (4.7) according to the Markov chain. Then the state probabilities can be calculated by solving the equations in (4.8) [13]. Particularly, probabilities of state 2 ("undesired trip") and state 3 ("failure to operate") are of our interest. The probability of "undesired trip" (P_Z and P_I) will be denoted to Figure 3.2 and Figure 3.3 therefore the dynamic properties of hidden failure probability can be established. They will be used in the simulation in following section 4.4.2.

$$R = - \begin{bmatrix} -\left(\lambda_{P1} + \lambda_{P2} + \mu_i + \lambda\right) & \lambda_{P1} & \lambda_{P2} & \mu_i & 0 & \lambda & 0 \\ 0 & -\left(\mu_i + \lambda\right) & 0 & \mu_i & \lambda & 0 & 0 \\ 0 & 0 & -\left(\mu_i + \lambda\right) & \mu_i & 0 & 0 & \lambda \\ \mu_I & 0 & 0 & \mu_I & 0 & 0 & 0 \\ 0 & \mu & 0 & 0 & -\mu & 0 & 0 \\ \mu & 0 & 0 & 0 & 0 & -\mu & 0 \\ \mu & 0 & 0 & 0 & 0 & 0 & -\mu \end{bmatrix} \quad (4.7)$$

$$\begin{cases} pR = 0 \\ \sum_i p_i = 1 \end{cases} \quad (4.8)$$

where p is a row vector whose i^{th} element p_i is the steady state probability of being in the ith state.

4.4.2 Monte Carlo Simulation

Non-sequential Monte Carlo simulation is used to calculate all reliability indices. In essence, the non-sequential Monte Carlo simulation consists of sampling states

proportional to their probabilities of occurrence [13]. This is achieved by drawing a random number between 0 and 1 and then comparing it with the probability of occurrence of a state. If the random number is less than or equal to the probability of occurrence, then the state is considered as occurred and evaluation of this stage for adequacy and security is performed. This information is then translated into the estimation of indices using the equations outlined in Section 4.3. Monte Carlo simulation generally takes much longer time to converge than analytical reliability assessment methods. However, it can handle complicated problems in a more realistic manner.

Our task comprises of both adequacy and security analysis. The basic methodology is explained as follows:

1) Select a faulted line using the fault probabilities of transmission lines calculated from their forced outage data.

2) List all exposed lines that are likely to mis-operate.

3) Check if fault is cleared. If yes, compute the currents on the exposed lines by conducting power flow calculation. Go to step 8

4) Compute the impedance seen by relays for the exposed lines by conducting fault calculation.

5) Check if "failure to operate" occurs by comparing the random numbers generated and protection failure probabilities. If "failure to operate" occurs, auto-recloser will not be activated and backup protection will clear the fault therefore additional lines will be out. Update exposed line list. Go to step 7

6) Return the faulted line into the system if auto-reclosing is successful.

7) Figure out tripping probability for each exposed line during the fault as a function of the impedance seen by relays (Figure 3.2) computed in step 4, Go to step 9

8) Figure out tripping probability for each exposed line after the fault as a function of current (Figure 3.3) computed in step 3.

9) Determine k (the number of lines that will trip) out of n (the total number of exposed lines) undesired trip by comparing the random numbers generated and the tripping probabilities derived in last step (either step 7 or step 8).

10) Update the list of exposed lines based on newly tripped lines.

11) If new lines trip, go to step 3.

12) Record the cascading outages and

    a. For adequacy analysis, use OPF to determine the amount of load curtailment.

    b. For security analysis, use stability evaluation algorithm to check if the system is stable.

13) Calculate reliability indices

14) Check if either indices are converged or the maximum number of simulations is reached. If yes, stop. Otherwise go to step 1.

Repeating the above simulation with randomly selected initial faulted lines will give us the system-wide indices. On the other hand, by specifying the initial faulted line during the simulation, we can get individual reliability indices so as to locate the weakest point in the system. Detailed Monte Carlo simulation flowchart is presented in Figure 4.3.

4.5 Numerical Results of Simulation

4.5.1 Test System and Data

The 24-bus IEEE Reliability Test System (RTS) as Figure A.1 in Appendix A is used to demonstrate the results.
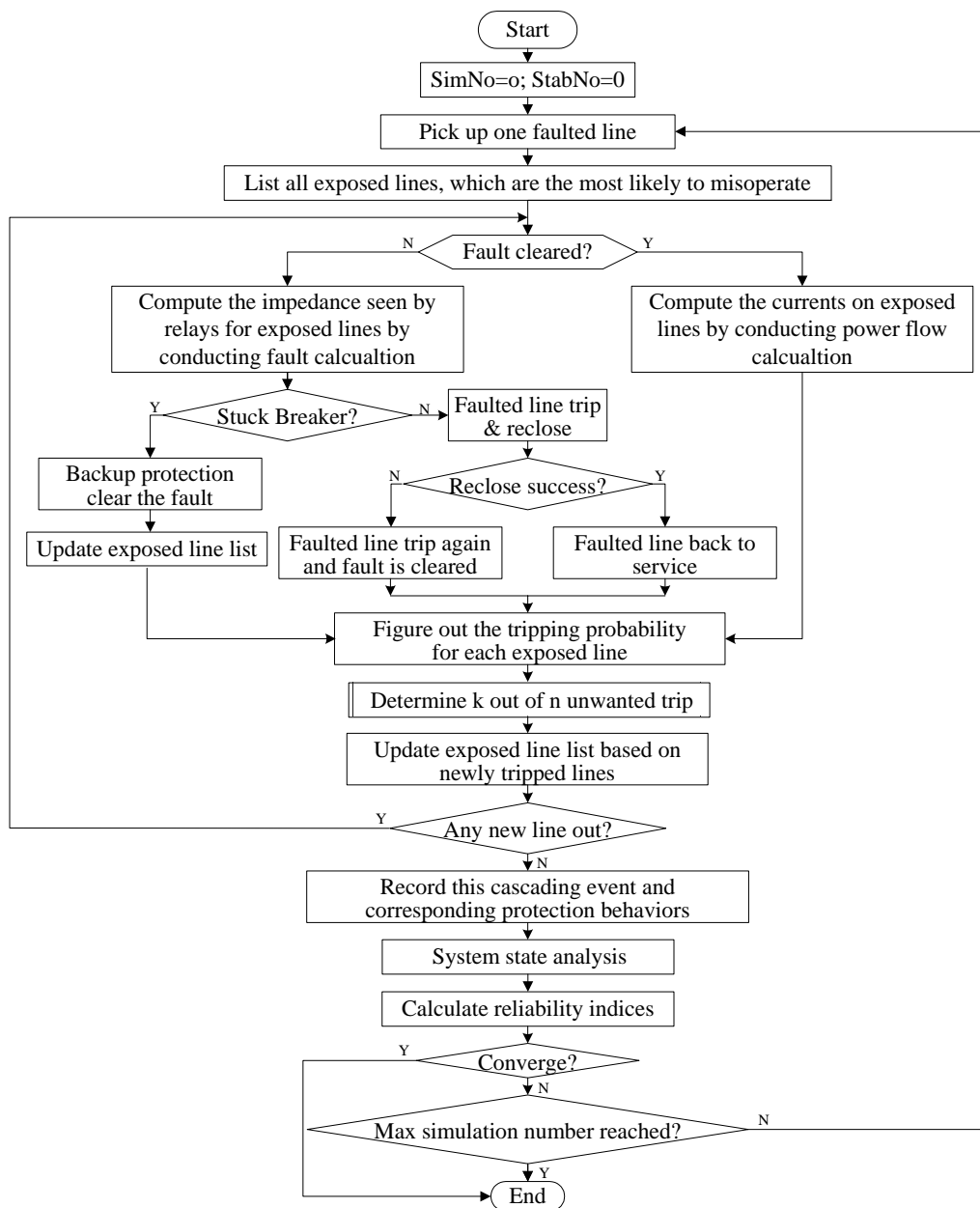
Figure 4.3 Flowchart for Calculating Reliability Indices

The basic data for the RTS system can be found in [33]. In addition, the transition rates of components and protection systems are listed in Table A.1 in Appendix A. Those transition rates are corresponding to the ones in Figure 3.2. According to the data, the hidden failure probability of each protection system can be calculated by (4.7) and (4.8) and the results are shown in the right-most column of Table A.1 in Appendix A.

Some other important simulation parameters are summarized in Table A.2 in Appendix A.

4.5.2 Simulation Process

4.5.2.1 Adequacy Indices

Figures 4.4 – 4.6 illustrate the Monte Carlo simulation process for calculating BIP, LOLP, and nEPL respectively.
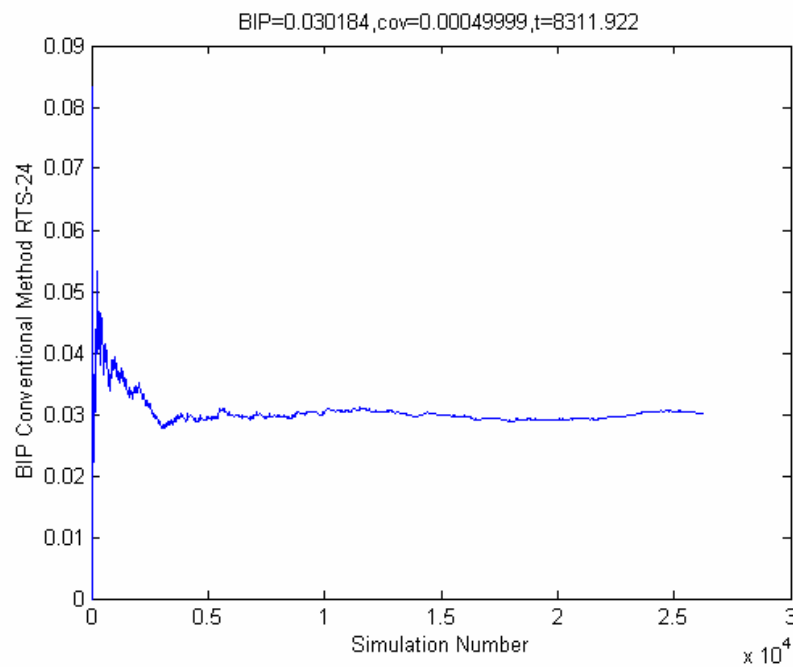
Figure 4.4 BIP by Monte Carlo Simulation
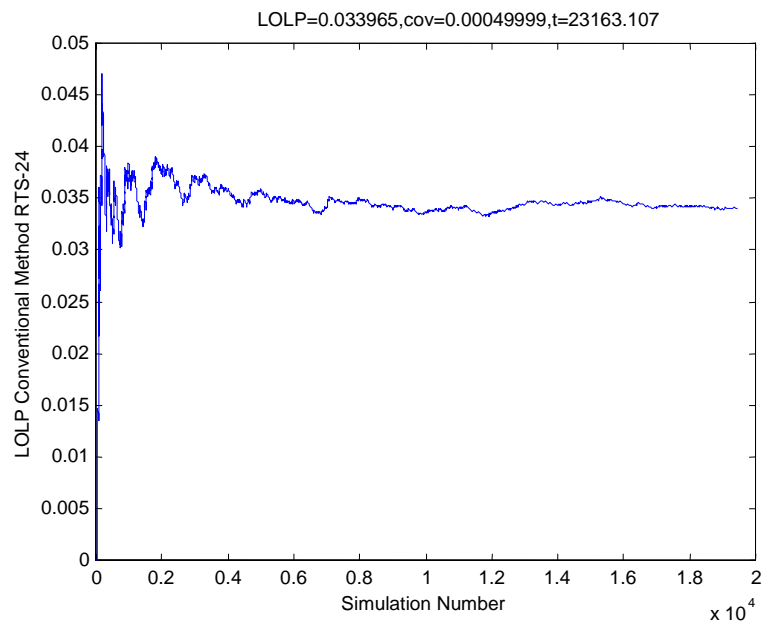
Figure 4.5 LOLP by Monte Carlo Simulation
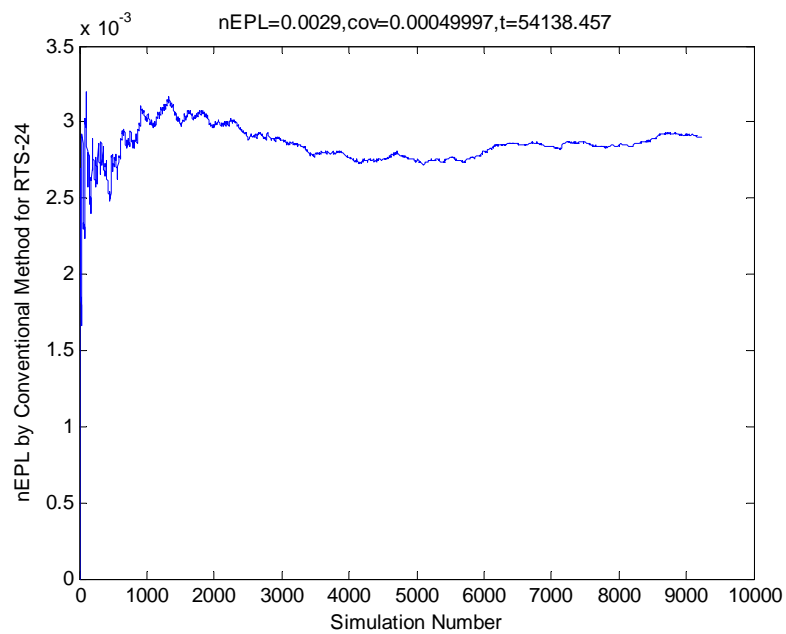
Figure 4.6 nEPL by Monte Carlo Simulation

4.5.2.2 Security Index

Stability evaluation is included in individual Monte Carlo simulation process. Two typical cases are selected and the corresponding stability evaluations are demonstrated as below:

Case-1: Fault at 0.7 of line 11-14, fault cleared at 0.065sec, successful reclosing at 0.739sec, cascading outages:

    a) Line 9-11.

    b) Line 3-9 and 4-9.

    c) Line 1-3.

The listed cascading outages are assumed to occur immediately after the successful reclosing. The evaluation result indicates the system is still stable after the cascading outages (Figure 4.7).
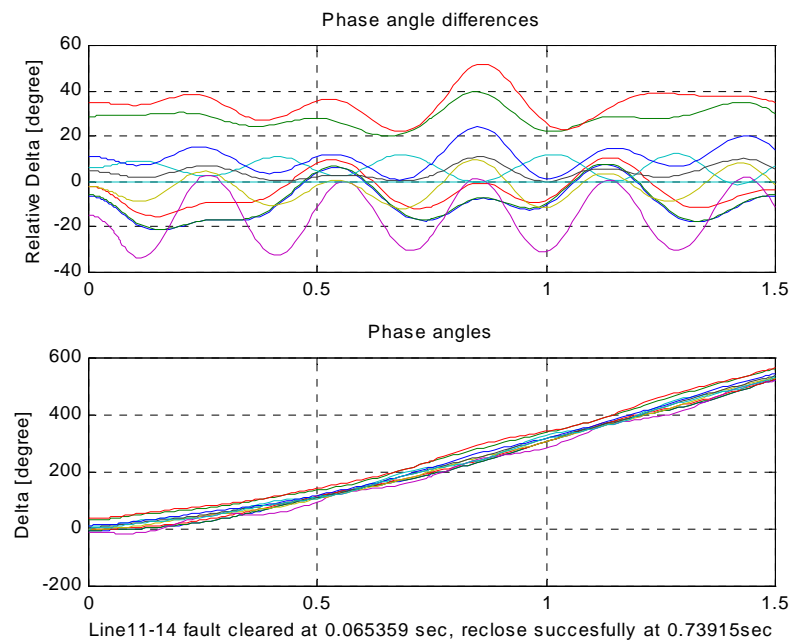
Figure 4.7 Case-1: Machine Phase Angle

Case-2: Fault at 0.4 of line 8-9, fault cleared at 0.066sec, unsuccessful reclosing at 0.698sec. The sequence of cascading outages is:

a) Line 3-9 and 4-9.

b) Line 2-4, 1-3, 9-11, and 9-12.

c) Line 1-3, and 2-4.

d) Line 1-2.

The system is unstable with the series of cascading outages. Specifically, generator 2 loses synchronism from the others. The simulation result is shown in Figure 4.8.
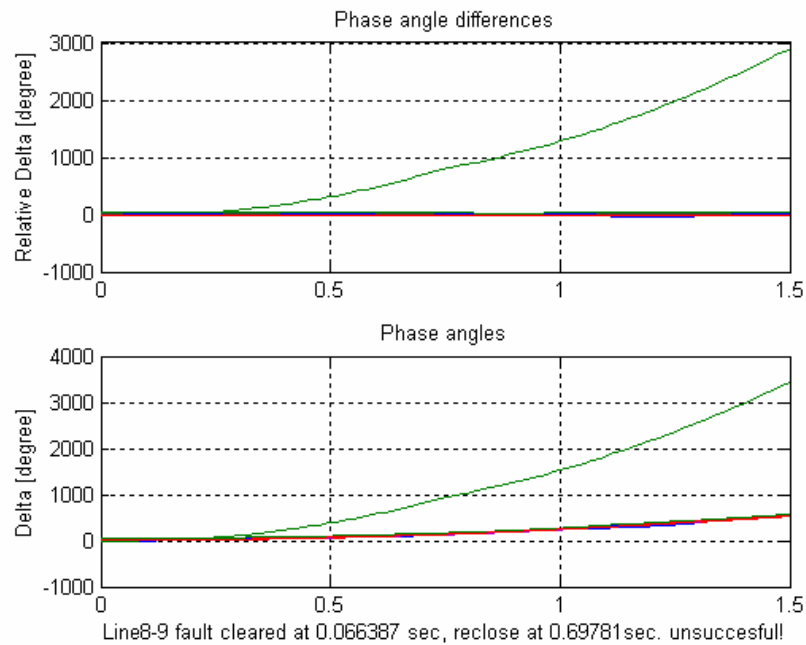
Figure 4.8 Case-2: Machine Phase Angle

The Monte Carlo simulation process for calculating the Probability of Stability (POS) is illustrated in Figure 4.9.
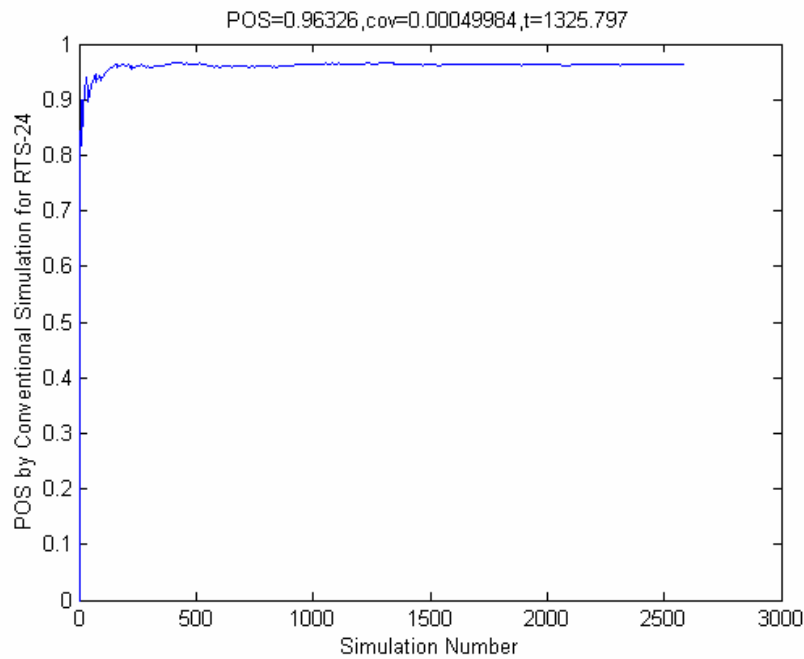
Figure 4.9 POS by Monte Carlo simulation

4.5.3 Numerical Results and Analysis

System-wide reliability indices are listed in Table 4.1. The results represent the degree of vulnerability when a particular system suffers from cascading outages.

Table 4.1 System-wide Simulation Results

BIP $(\times 10^{-2})$	LOLP $(\times 10^{-2})$	nEPL $(\times 10^{-2})$	POS	ISV $(\times 10^{-2})$
3.02	3.40	5.13	0.9633	2.76

We also calculated the individual reliability indices with the specified faulted lines. The results are shown in Table 4.2. These indices help us to learn which part of the system is the weakest link according to our criteria.

Table 4.2 Individual Simulation Results

Faulted Line	BIP (x10^{-2})	LOLP (x10^{-2})	nEPL (x10^{-2})	POS	ISV (x10^{-2})
1-2	2.68	2.29	9.03	0.9641	2.74
1-3	1.37	1.37	6.36	0.9915	1.93
1-5	0.80	0.74	0.82	0.9941	0.89
2-4	1.50	1.59	2.26	0.9965	1.37
2-6	2.31	2.20	3.70	0.9856	1.85
3-9	5.31	5.09	5.13	0.9668	3.09
3-24	2.53	2.31	1.64	0.9819	1.60
4-9	**6.87**	**6.85**	11.09	0.9673	**4.55**
5-10	4.11	4.12	7.19	0.9720	3.00
6-10	2.24	3.34	3.29	0.9750	1.88
7-8	3.37	3.34	8.42	0.9758	2.93
8-9	2.52	2.69	4.31	**0.9423**	2.02
8-10	3.00	2.99	5.54	0.9594	2.36
9-11	4.02	3.99	5.13	0.9548	2.65
9-12	4.30	5.61	10.68	0.9496	3.71
10-11	**6.59**	**6.30**	10.68	0.9491	**4.35**
10-12	5.12	**6.06**	**16.01**	0.9515	**4.76**
11-13	**5.67**	5.72	7.39	0.9557	3.58
11-14	5.52	5.72	6.16	**0.9436**	3.35
12-13	**5.64**	**6.49**	4.11	**0.9490**	3.15
12-23	3.83	5.47	10.27	0.9673	3.53
13-23	3.62	4.64	3.49	0.9756	2.38
14-16	2.93	2.69	2.26	0.9825	1.83
15-16	4.53	5.87	**14.58**	**0.9381**	**4.38**
15-21	3.32	3.27	**15.40**	0.9592	3.95
15-21	3.52	3.55	**16.01**	0.9658	4.12
15-24	3.00	3.56	5.75	0.9749	2.46
16-17	5.31	3.24	2.46	**0.9447**	2.49
16-19	4.13	4.59	10.06	0.9809	3.49
17-18	1.40	0.33	0.82	0.9801	1.00
17-22	1.90	0.24	2.05	0.9746	1.29
18-21	3.84	3.36	13.14	0.9573	3.75
18-21	4.11	2.98	**15.19**	0.9577	4.08
19-20	1.82	1.80	2.26	0.9921	1.47
19-20	1.98	1.79	2.26	0.9920	1.51
20-23	3.58	3.35	3.29	0.9873	2.22
20-23	3.05	3.45	3.49	0.9875	2.12
21-22	2.88	0.78	4.52	0.9694	1.96

In Table 4.2, the top four significant values in each index are highlighted, which are the weakest links in terms of the corresponding indices. We further summarize them in Table 4.3.

Table 4.3 Weakest Links as per Indices

Index	Top 4 weakest links			
BIP	4-9	10-11	11-13	12-13
LOLP	4-9	12-13	10-11	10-12
nEPL	10-12	15-21*	18-21	15-16
POS	15-16	8-9	11-14	12-13
ISV	10-12	4-9	15-16	10-11

* either of the double lines

From Table 4.3 we learn that the line 4-9 is the weakest link from the viewpoint of *BIP* and *LOLP*. Line 10-12 is the weakest link with respect to *nEPL*. *POS* locates line 15-16 as the weakest link. In this case, reliability indices in terms of adequacy and security analysis give different weakest link information. As we discussed before, there are a number of variations corresponding to system configuration, operating situation, especially protection system hidden failure probability.

The integrated vulnerability index *ISV*, combining all aspects of reliability analysis, shows the most reasonable weakest link in the system. In this case, *ISV* indicates that line 10-12 is the weakest link by adopting weighting factors of 0.25, 0.1, 0.15 and 0.5. Obviously different sets of weighting factors may give different results.

Figure 4.10 demonstrates the ISV with respect to various fault locations. This type of figure visualizes the locational vulnerability index.
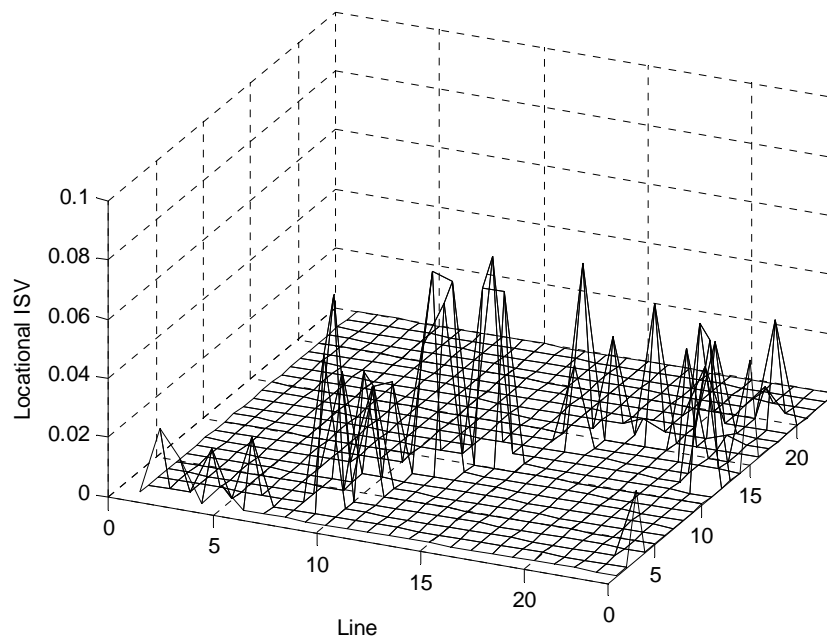
Figure 4.10 Locational ISV

In Figure 4.10, x-axis and y-axis denote buses in the system therefore the lattices represent grid component, either transmission line or transformer.

4.6 Conclusion

Based on a more explicit model of components paired with protection system, a Monte Carlo simulation approach is developed to simulate system behavior including cascading outages. Besides evaluating common adequacy reliability indices *BIP*, *LOLP*, and *nEPL*, we also analyze the transient stability with the occurrence of cascading outages in the power system.

Different reliability indices show different weakest links in the system. We could estimate the system vulnerable point based on individual reliability index with particular emphasis. However, the newly introduced vulnerability index *ISV* can depict the overall severity of the impact of cascading outages.

Protection failures are rare events in a power system. This can be noticed by the long simulation time to converge. Some variance reduction technology could be applied to reduce simulation time.

The methodology proposed in this section does not include the influence of voltage in cascading outages. Also, the power outage duration is not considered for system vulnerability analysis either. Future studies are intended to take account of these factors.

V.   INNOVATIVE APPROACHES FOR VULNERABILITY ANALYSIS

Since protection hidden failures are rare events, conventional Monte Carlo simulation method can consume large computation time, as demonstrated in section IV. In this section two simulation approaches for vulnerability analysis considering protection system failures are proposed and developed. The first one is Importance Sampling method, which uses varied probability to reveal more rare events. The second one is Self-Organizing Maps (SOM) method, which is based on the first one and integrates neural networking technology to further reduce the simulation time.

5.1 Importance Sampling Monte Carlo Simulation (IS-MCS) Approach

5.1.1 Introduction

This section introduces Importance Sampling Monte Carlo Simulation (IS-MCS) approach in concept and application. Importance Sampling is one of the "variance reduction" techniques for rare event simulation in reliability studies. In a power system, protection failures are rare events, which may result in cascading outages. This section demonstrates the application of Importance Sampling method in power system reliability analysis considering protection failures. The Importance Sampling technique is embedded into non-sequential Monte Carlo Simulation to implement the stochastic properties of contingencies, protective response and protection system failures. Therefore, the newly developed method here is called Importance Sampling based Monte Carlo Simulation scheme. To evaluate the efficiency of the new approach, both straightforward Monte-Carlo simulation approach and IS-MCS approach are demonstrated and compared. The WSCC-9 is used as the test system.

Since protection failures occur with a very low probability, the standard simulation suffers from long simulation time to converge. The properties of hidden failures in protective relays and their impact on power system reliability has been explored in [7][15][16]. However, there has been little systematic analytical or simulation methodology for considering cascading outages due to the complexity and difficulties. Thorp, Phadke,

Horowitz, and Tamronglak [34] first proposed the use of importance sampling to handle the difficulty encountered with rare events. Bae and Thorp [8] presented an importance sampling application regarding voltage related hidden failures and relay misoperations. However, this was not initiated from the viewpoint of reliability and some important reliability indices were not included.

Importance Sampling has been utilized in rare events reliability analysis by some researchers [9][10][35]. In their research, it has been claimed that computation time saving is mainly achieved by reducing the random numbers generated. However, computation time is the problem of not only large simulation numbers, but is also attributable to the tools of system state evaluation, such as OPF and stability analysis, which use enormous computation time.

In this section, Importance Sampling technique is embedded into non-sequential Monte Carlo simulation method to deal with protection system failures. The methodology itself is also evaluated through actual simulation.

5.1.2 Importance Sampling Principle

Importance sampling is a procedure for changing the probability density function of sampling in such a fashion that the events which make greater contributions to the simulation results have greater occurrence probabilities [36]. Reference [37] gives a rough introduction of the principle of importance sampling in simulation for reliability analysis. The application in simulation needs to alter the probabilities, which make the unlikely events more likely and processing the simulation results so that the correct answers are obtained.

Protection failures are rare events in a power system. A direct simulation of these rare events would require an unrealistic amount of computation. Also each simulation would require a number of random number draws, putting the long-term behavior of the random

number generator under scrutiny [35].

A fundamental parameter in Monte Carlo simulation method is the mathematical expectation of a given reliability index. Mathematically, importance sampling can be understood by expression (5.1).

$$
\begin{aligned}
Q_s &= P_r\{\psi(X)=1\} \\
&= \sum_X \psi(X)P_r\{X\} \\
&= E_X\{\psi(X)\} \\
&\approx \frac{1}{N}\sum_{i=1}^{N}\psi(x_i) \\
&= \sum_X \frac{\psi(X)P_r\{X\}}{PP_r\{X\}}PP_r\{X\} \\
&= E_X\left\{\psi(X)\frac{P_r\{X\}}{PP_r\{X\}}\right\} \\
&\approx \frac{1}{N}\sum_{i=1}^{N}\psi(x_i)\frac{P(x_i)}{PP_r(x_i)}
\end{aligned}
\tag{5.1}
$$

where

Q_s	System unavailability.
X	$(x_1, \ldots, x_k)$ is a basic event state vector.
$\psi(X)$	Binary function expressing the top event. of the fault tree (system failure).
P_r	Actual event probability.
PP_r	Altered (simulation) event probability

From (5.1), we can see that importance sampling enables the simulation to be run with altered probabilities so that the rare events occur more frequently. In brief, assume the

actual probability of one blackout is *p*, and the altered simulation probability is *pp*, we then form the estimated probability of this event as:

$$\hat{\rho} = \frac{N_{occuring}}{N_{total}} \cdot \frac{p}{pp} \qquad (5.2)$$

where $N_{occuring}$ is the number of times that this event occurs and N_{total} is the total number of simulation samples. The mean value of $\hat{\rho}$ is unbiased [38].

A simple example can demonstrate how efficient the importance sampling method is. In a 5-component system, each component has independent failure probability of *p*=0.03. The probability of 2 and more components failure is:

$$P=1-(5p(1-p)^4+(1-p)^5)=0.008472053 \qquad (5.3)$$

Now we use simulation methods to solve this problem. Figure 5.1 and Figure 5.2 show the simulation results of straightforward MCS method and IS-MCS respectively. Here we use a cov=0.001 as stop criteria for both methods.
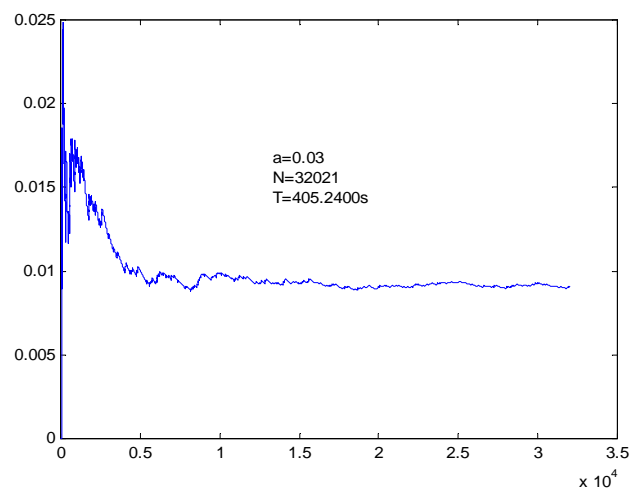
Figure 5.1 Result of Straightforward MCS Method
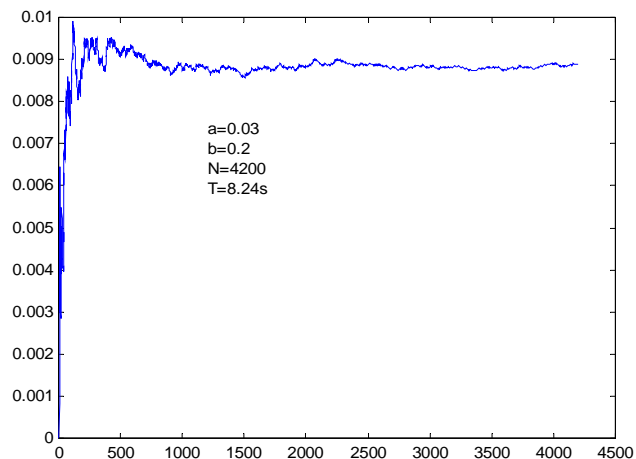
Figure 5.2 Result of IS-MCS Method

In IS-MCS method, altered simulation probability b=2 for the component failure is used. The IS-MCS method takes only 8.24s to solve the problem while straightforward MCS consumes 405s to complete the same work.

5.1.3 Path Probability Ratio

Unlike conventional Monte Carlo simulation in which we care only about the occurrence of top event, when importance sampling method is embedded, we should also record the probability ratio along the path to the top event. We use a simple example to illustrate the definition of path probability ratio in Figure 5.3.
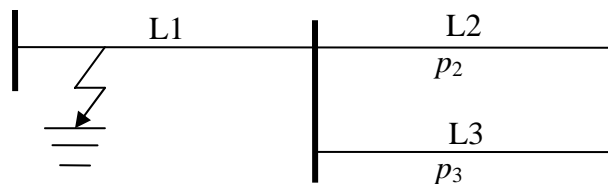
Figure 5.3 Cascading Outage Illustration

In Figure 5.3, suppose a fault occurs in L1, L1 trips by the correct response of its protection device. If L3 also trips due to hidden failure of its protection system (failure probability p3) and L2 does not trip with its hidden failure probability p_2, the cascading outage path is L1 and L3. And the path probability ratio of this event is defined as expression (5.4).

$$r = \frac{p_3}{pp_3} \cdot \frac{(1 - p_2)}{(1 - pp_2)}$$ (5.4)

where pp_3 and pp_2 are altered probabilities

In general, if cascading outages involve a series of N consecutive exposures of hidden failures, n out of N hidden failure lead to misoperation, the path probability ratio can be described as (5.5).

$$r = \prod_{i=1}^{n} \frac{p_i}{pp_i} \cdot \prod_{j=n+1}^{N} \frac{(1 - p_j)}{(1 - pp_j)}$$ (5.5)

Although the choice of the simulation probability pp is less critical than the direct importance sampling, some variation in the typical sample paths are observed as the rule for generating the pp is changed [8]. If all exposed lines are given the same probability (say 0.5) then the resulting sample paths are somewhat different from those obtained when the exposed probabilities are simply scaled so the largest is 0.5. A solution is to randomize the rule for generating the simulation probabilities as (5.6).

$$pp_j = 0.5 \left(\frac{p_j}{p_{max}} \right)^{\alpha_j}$$ (5.6)

where α_j are uniform random numbers between 0 and 1.

The value $\alpha_j = 1$ corresponds to uniform scaling while a value of 0 refers to setting all values to 0.5. Since the α_j are chosen at each step, all combinations are exposed [8].

5.1.4 Reliability Indices Definition in Simulation

In contrast to the definitions of reliability indices by straightforward MCS method in Section IV (equation 4.1-4.5), the corresponding reliabilities indices by IS-MCS can be defined as below.

$$BIP = \frac{1}{N}\sum_i r_i \tag{5.7}$$

$$LOLP = \frac{1}{N}\sum_i r_i \tag{5.8}$$

$$EPL = \frac{1}{N}\sum_i (C_i \cdot r_i) \tag{5.9}$$

$$POS = \frac{1}{N}\sum_i r_i \tag{5.10}$$

where i : an element of set of simulations conducted.
r_i : path probability ratio up to the occurrence of the studied event in simulation i, otherwise it is 0.
C_i : load curtailment during simulation i
N : the total number of simulations.

5.1.5 Simulation Algorithm

Although Monte Carlo simulation can handle complicated reliability problems in a more realistic manner, some rare events may not get sampled during the process of convergence. To alleviate this difficulty, a new algorithm is proposed here to embed importance-sampling concept into Monte Carlo simulation, which is named as importance sampling

based Monte Carlo simulation, or IS-MCS. In this paper, our task is reliability adequacy analysis. The IS-MCS algorithm is described as below:

1) Select a faulted line.

2) Compute the impedance seen by relays for the exposed lines by conducting fault calculation.

3) Resume the faulted line into the system if auto-reclosing is successful.

4) Figure out tripping probability for each exposed lines during the fault.

5) Determine which exposed line(s) will trip. If no new lines trips, go to step 9.

6) Update exposed lines based on newly tripped lines.

7) Rearrange the power injections if necessary and compute the currents on the exposed lines by conducting power flow calculation.

8) Figure out tripping probability for each exposed line after the fault. Go to step 6.

9) Record the path of cascading outages and determine the tripping probability ratio following the path as per equation (5.4).

10) System evaluation. This is to judge the occurrence of reliability problem, such as Bus Isolation, Load Curtailment, or System Stability.

11) Calculate the reliability indices using correspondent probability ratio multiply $N_{occurring}$ over N_{total}.

Repeating the above simulation with randomly selected initial faulted lines will give us the system-wide indices. The cov (coefficient of variation) is used as the convergence criterion in the simulation.

Figure 5.4 shows the flowchart to demonstrate the IS-MCS procedure for LOLP calculation. Other reliability indices can be obtained by the similar process.
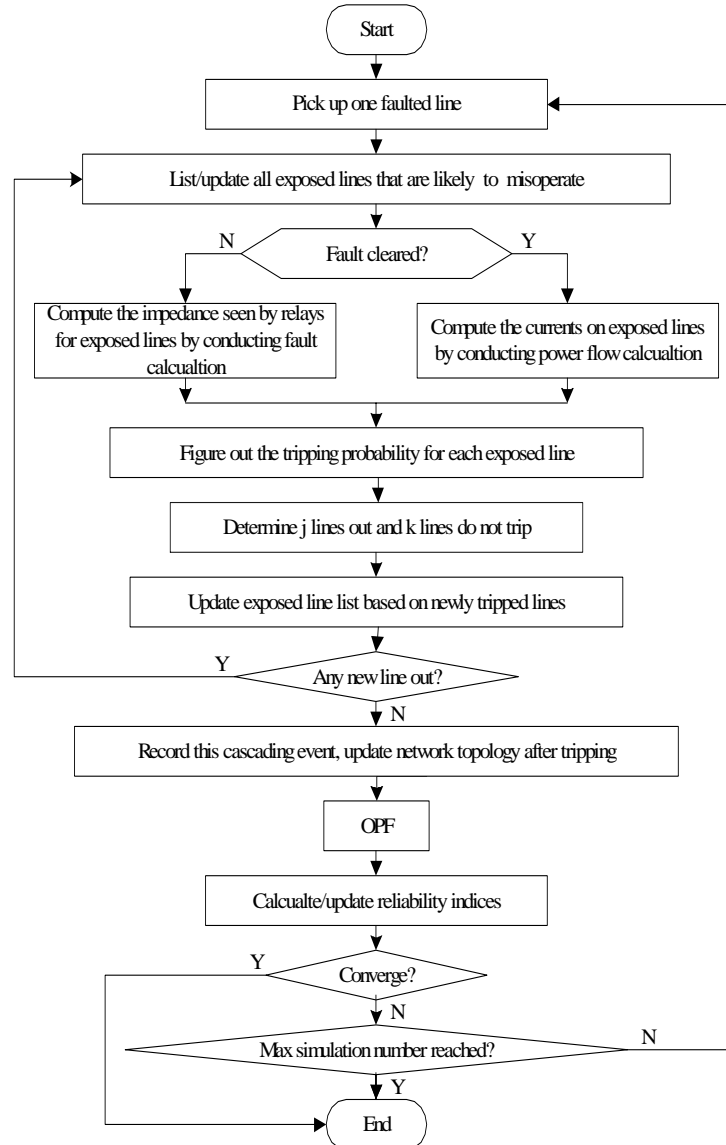
Figure 5.4 Flowchart for IS-MCS Method

5.1.6 Numerical Simulation Case Study

5.1.6.1 Test System

The WSCC-9 bus system is used as the test system (shown in Figure 5.5). Since it is not complex, it can easily provide insights into cascading outages and the application of new methodology.
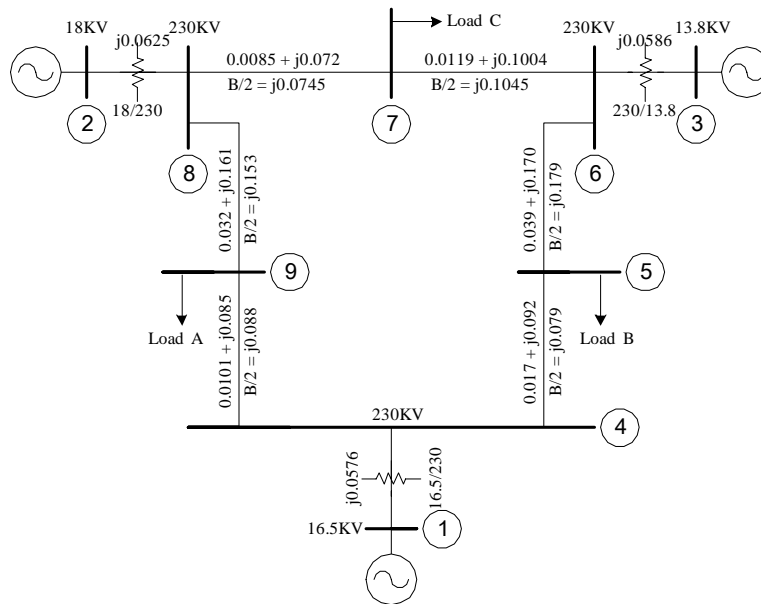
Figure 5.5 WSCC-9 Bus System

The typical failure rate and repair rate of each component and its protection system is listed in Table 5.1 [32] [39]. Here we assume that the protection devices on both ends of a given line have the same properties.

Table 5.1 Components and Associated Protection System Data

	Component		Protection System			
Line	λ (1/year)	μ (1/year)	λ_{p1} (1/year)	λ_{p2} (1/year)	μ_i (1/year)	μ_I (1/hour)
4-5	6	160	0.0113	0.34	4	0.25
5-6	12	130	0.0079	0.28	4	0.25
6-7	4	170	0.0088	0.31	4	0.25
7-8	3	170	0.0107	0.43	4	0.25
8-9	10	150	0.0080	0.45	4	0.25
4-9	3.5	170	0.0143	0.40	4	0.25

5.1.6.2 Simulation Results

The simulations are carried out in Dell Optiplex™ GX260, 2.40GH Pentium® 4 processor with 512MB RAM.

1) BIP

Figure 5.6 and Figure 5.7 show the process of straightforward and importance sampling based Monte Carlo simulation for BIP respectively.

BIP=0.011356,cov=0.00099996,t=559.453
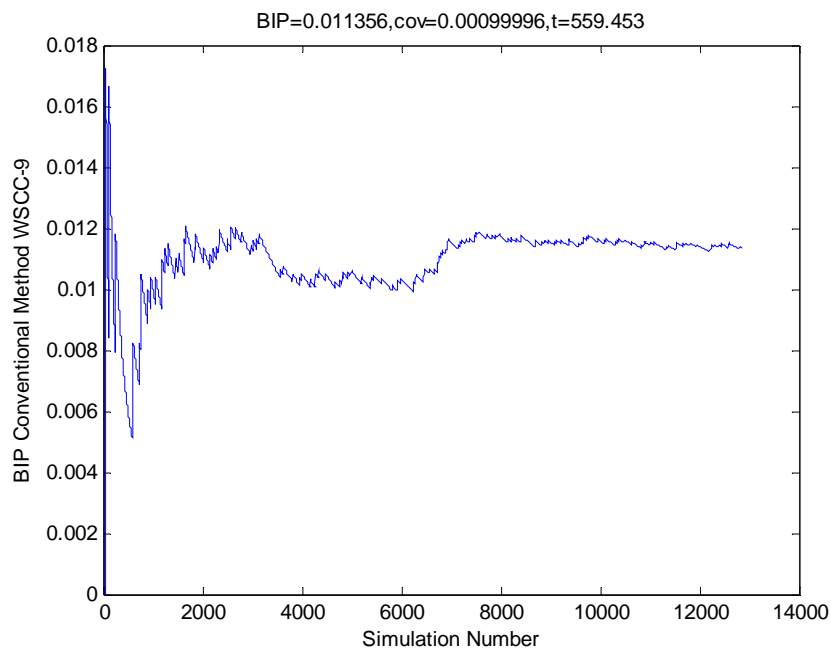
Figure 5.6 BIP by Straightforward Monte Carlo Simulation
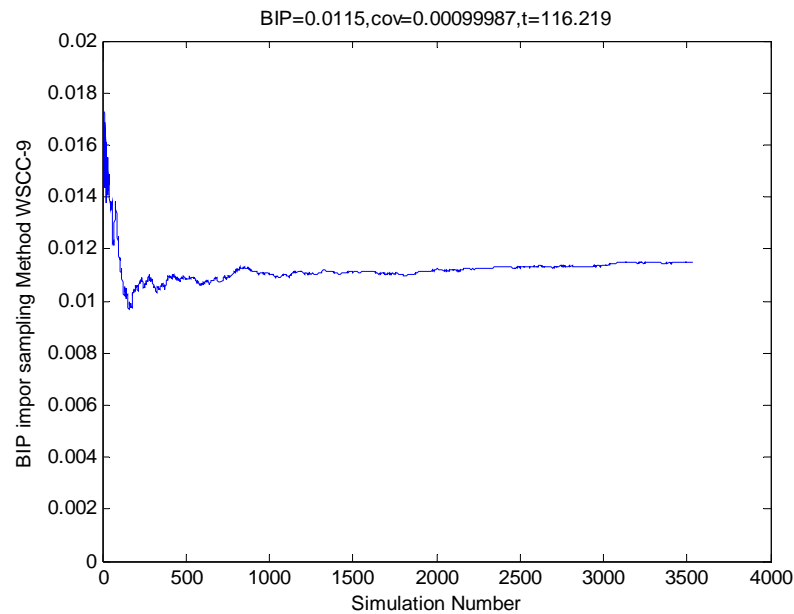
Figure 5.7 BIP by IS-MCS

Here we set coefficient of variation (cov) as 0.001. Both methods obtain the same results. Importance sampling based method only took 116.219sec to converge while straightforward method took 559.453sec.

2) LOLP

Figure 5.8 and Figure 5.9 show the process of conventional and importance sampling based Monte Carlo simulation for LOLP.
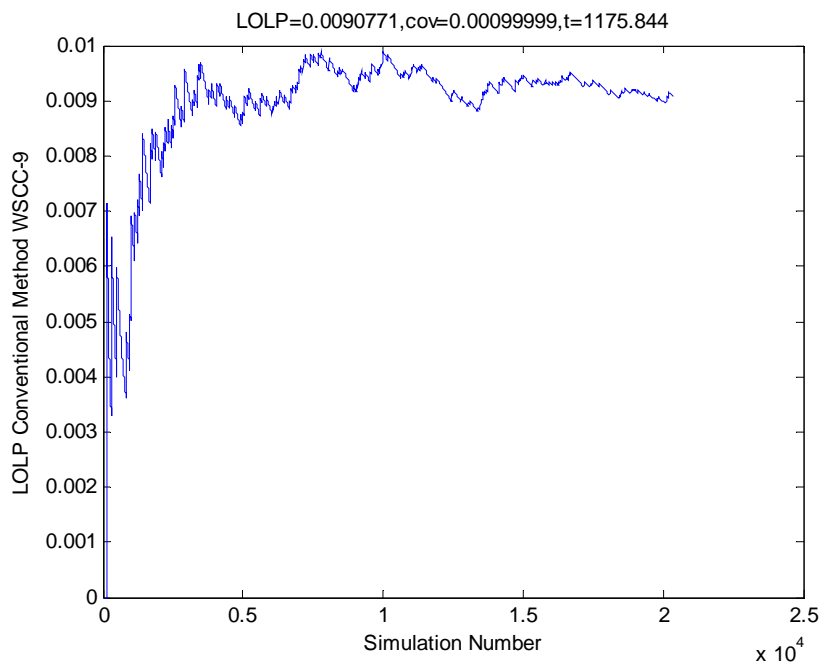
Figure 5.8 LOLP by Straightforward Monte Carlo Simulation
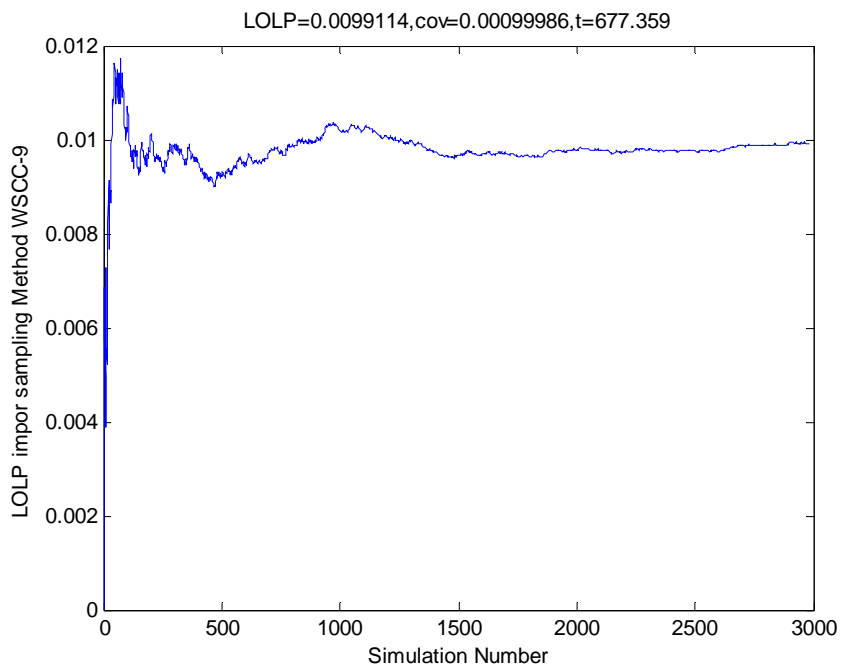
Figure 5.9 LOLP by IS-MCS

For LOLP the importance sampling based method takes less time to converge than the conventional method. Another observation is the difference in the simulation curves. In the finishing portion, the simulation curve by conventional Monte Carlo method has still some fluctuations whereas the one by importance sampling based method is pretty flat. In practice, for this case, straightforward Monte Carlo simulation should choose a smaller cov to achieve accurate result.

3) EPL

Figure 5.10 and Figure 5.11 show the process of conventional and importance sampling based Monte Carlo simulation for EPL.
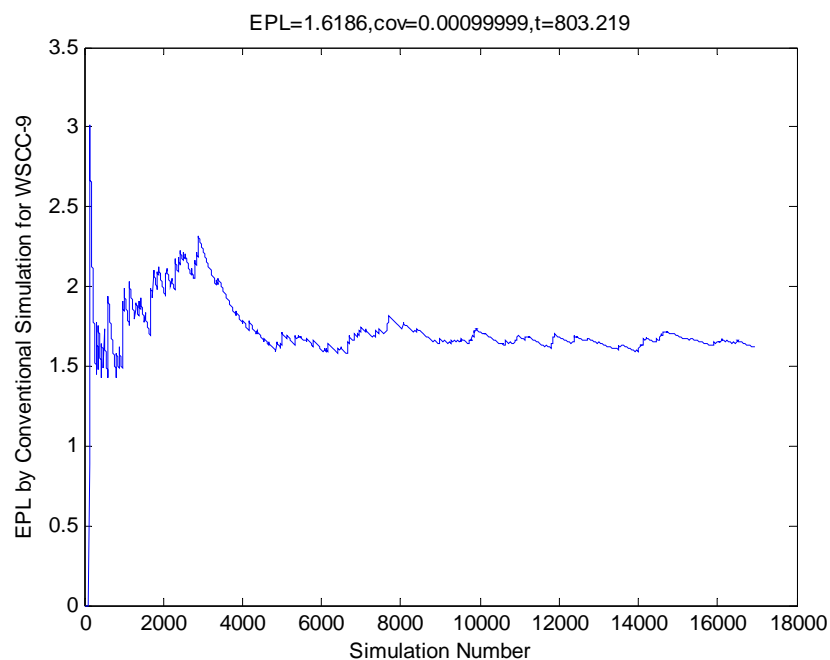
Figure 5.10 EPL by Straightforward Monte Carlo Simulation

EPL=1.5459,cov=0.00099991,t=612.797
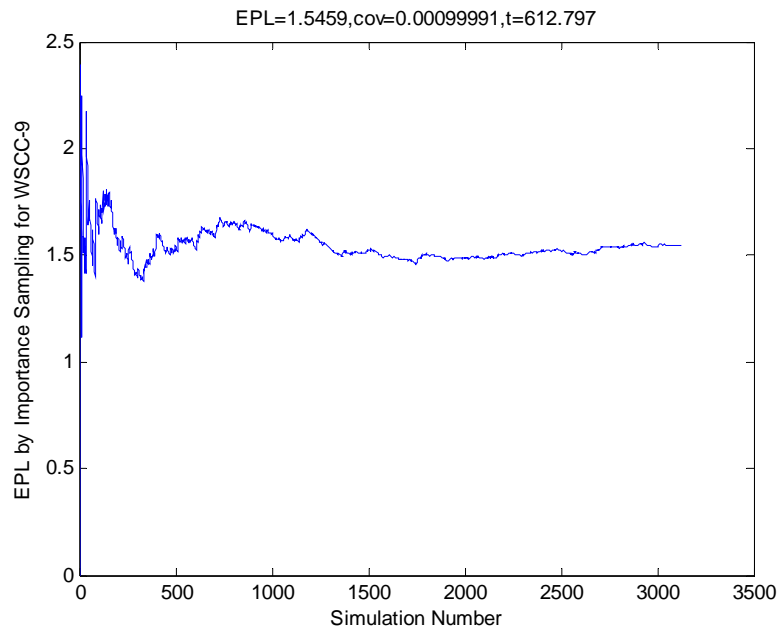
Figure 5.11 EPL by IS-MCS

The importance sampling based method spends less computation time in this case. However, the difference is not significant. The reason is that OPF, which is very time consuming, is used in evaluating loss of load in the simulation process. Since we use altered probability, which is much higher than the actual probability, the cascading outages occurs more frequently. Consequently, more OPF evaluation process is incurred. Also, importance sampling based method has better convergence performance.

4) POS

Figure 5.12 and Figure 5.13 show the process of conventional and Importance Sampling based Monte Carlo simulation for Probability of Stability.

POS=0.99043,cov=0.00099989,t=77.265
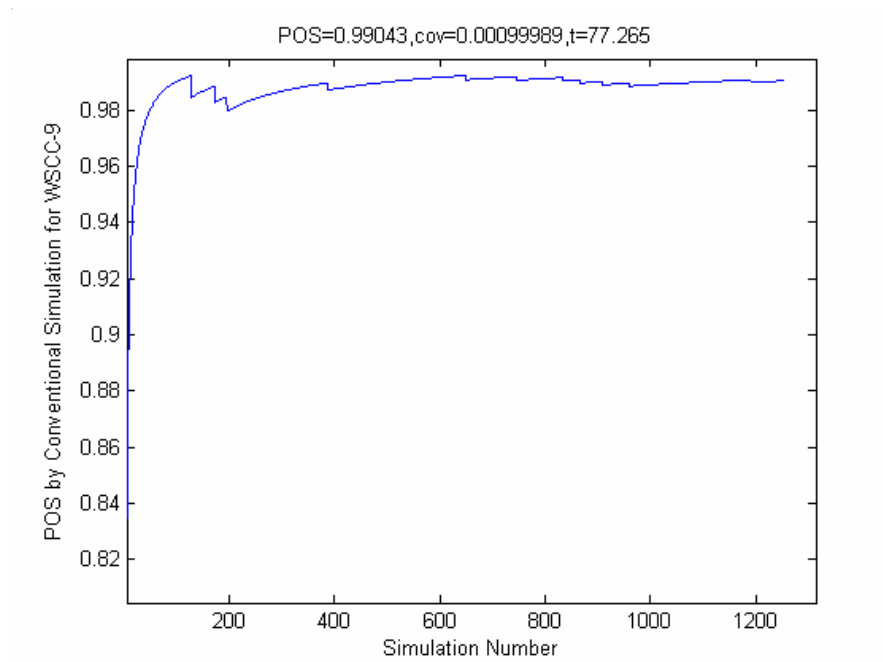
Figure 5.12 POS by Straightforward Monte Carlo Simulation

POS=0.9923,cov=0.00099982,t=145.5
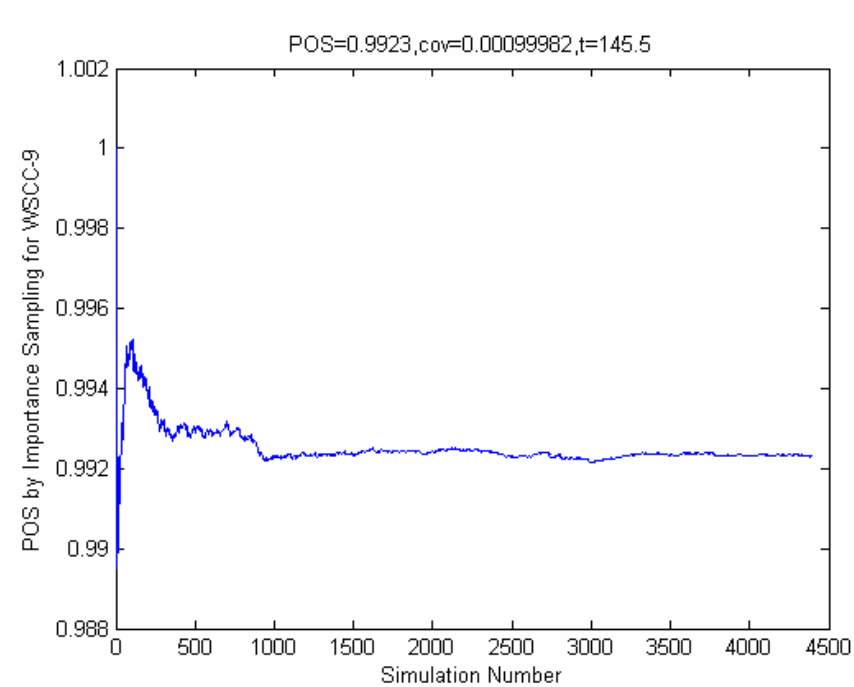
Figure 5.13 POS by IS-MCS

System stability analysis, like OPF, is a time consuming process too. The comparison of straightforward MCS and IS-MCS in calculating POS reveals one important case that the IS-MCS does not guarantee save computation time in all situations. The reason is that when we use altered probability, which is much higher than the actual probability, the cascading outages occurs more frequently. As a result, more system stability evaluation processes are triggered. This phenomenon also implies that WSCC-9 bus system is a stably reliable system which can withstand most contingencies. Again in this case, IS-MCS method has better convergence performance.

5.1.7 Conclusion

Protection failures are rare events in a power system. This can be noticed by the long simulation time to converge. Importance sampling technique can be applied to reveal more rare events and perhaps reduce simulation time.

Based on the explicit model of components paired with protection system, an importance sampling based Monte Carlo simulation approach is developed to simulate system behavior including cascading outages. Three typical adequacy reliability indices BIP, LOLP, EPL and POS are calculated to demonstrate the application. The new method is generally advantageous in terms of convergence.

Meanwhile, our research also shows that for simulation with heavy state evaluation tasks, which is time consuming and repetitive, like OPF and stability analysis, the saving in computation time is not significant. On the contrary, IS-MCS may lose time-saving advantage in some cases.

5.2 SOM-IS-MCS Approach

In this section, SOM theory and its application are introduced. Particularly, the integration of SOM and Importance sampling method to optimize the methodology in terms of computation time and probabilistic features for protection failure problems are implemented.

5.2.1 Motivation

Artificial neural network is one of the emerging and exciting developments in solving engineering problems such as computer vision, control and speech recognition. They mimic the human biological neural nets, which can learn how to recognize and classify pattern in an autonomous manner. In power systems, artificial neural networks have also been used in many areas, e.g. load forecasting, security assessment, fault diagnosis, system identification, and voltage control [40 - 46].

The clustering mechanism of human brain led researchers to the concept of Kohonen Networks. Kohonen networks, which were developed by Teuvo Kohonen during the early 1980s, can be used in classification problems [47 - 48]. Kohonen networks are divided into two main subgroups based on the learning philosophy: supervised and unsupervised learning. Supervised learning needs the correct desired output for a controlled adaptation to minimize the error between the neural output and the desired output. Learning Vector Quantization (LVQ) is a pattern classification method in the supervised learning class. In unsupervised learning, the learning process classifies similar data into clusters using similarity indices. Self-organizing maps (SOM) learn to recognize groups of similar input vectors in such a manner that neurons physically near each other in the neuron layer respond to similar input vectors. The combination of Self-organizing maps, Importance Sampling, and Monte-Carlo simulation is called the SOM-IS-MCS in this dissertation. SOM-IS-MCS overcomes the computation burden caused by repeated characterization of similar states in the power system reliability evaluation with protection failures.

This section proposes another new probabilistic method involving adequacy and security assessment by combining SOM, Importance Sampling, and Monte-Carlo simulation. The main disadvantage of the use of straight Monte-Carlo simulation for reliability and security analysis is the time required for the characterization of sampled states. Even for Importance Sampling based Monte Carlo simulation, due to the repetitive and time-consuming system evaluation processes, the improvement is not significant for some cases. The proposed

approach in this section overcomes the problem of a large amount of computation time required of straight Monte-Carlo simulation. Data classification by SOM can reduce sampling data. This reduces computation time for adequacy and security indices when using classified data.

Protection failures are rare events, which may result in cascading outages in power systems. From the last section, we already know that importance sampling is one efficient way for rare event simulation in reliability studies. However, in certain reliability analysis applications like OPF, importance sampling method reveals some disadvantages (Section 5.1), which can be overcome by the introduction of SOM (Self Organizing Map). This section demonstrates the application of combination of importance sampling and SOM in power system reliability analysis considering protection failures. Both importance sampling and SOM techniques are embedded into non-sequential Monte Carlo simulation implementing the stochastic properties of contingencies, protective response and protection system failures. This newly developed methodology can be called "SOM + importance sampling" based Monte Carlo Simulation method, or SOM-IS-MCS, which can deal with reliability analysis with rare events efficiently. The 24-bus IEEE RTS system is used as the test system to demonstrate the performance of this approach.

5.2.2 Self-Organizing Map (SOM)

5.2.2.1 Structure and Algorithm of Self-Organizing Map

The self-organizing map (SOM) is a method for unsupervised learning, based on a grid of artificial neurons whose weights are adapted to match input vectors in a training set. It was first described by the Finnish professor Teuvo Kohonen and is thus sometimes referred to as a Kohonen map.

The structure of SOM can be simplified as in Figure 5.14 [49]. SOM consists of a standard input layer and a Kohonen layer. Each input neuron is connected to every neuron in the Kohonen layer. This Kohonen layer learns to categorize its input vectors. After computing the distance between input vectors and weight vectors, Kohonen layer identifies a winner

neuron through competitive transfer functions. All neurons that lie within a neighborhood surrounding the winning neuron are allowed to adjust their weights. Neurons that are outside the neighborhood do not adjust their weights. All neurons within a certain neighborhood of the winning neuron are updated using the Kohonen-rule.
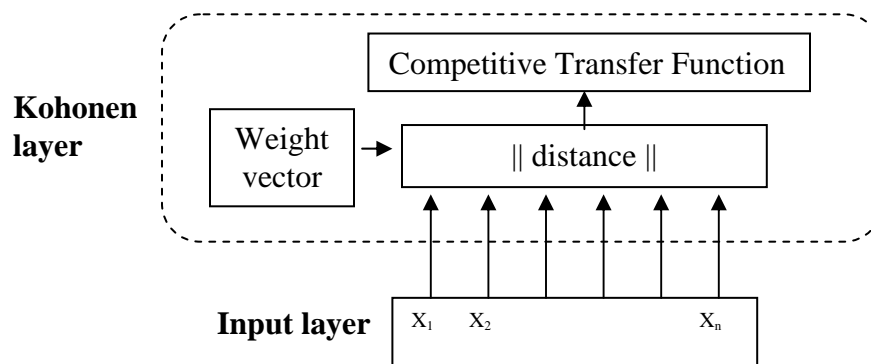
Figure 5.14 Structure of Self-Organizing Maps

The algorithm can be explained in terms of a set of artificial neurons, each having its own physical location on the output map, which take part in a winner-take-all process (a competitive network) where a node with its weight vector closest to the vector of inputs is declared the winner and its weights are adjusted making them closer to the input vector. Each node has a set of neighbors. When this node wins a competition, the neighbors' weights are also changed. They are not changed as much though. The further the neighbor is from the winner, the smaller its weight change. This process is then repeated for each input vector, over and over, for a number (usually large) of cycles. Different inputs produce different winners.

Each neuron j in the Kohonen layer is represented by an n-dimensional weight vector $w_j = [w_{j1} \; w_{j2} \; ---w_{jn}]$. The input vectors to the SOM are represented by $X = [X_1 \; X_2 \; --- \; X_i \; --- \; X_o]$ where o is the number of the input vectors. The dimension of each input vector is the

same as that of the weight vector. The input vector in our studies is the transmission line contingencies in the process of simulation in the next section. The dimension of weight vector is the same as the sum of the number of transmission lines (n). The algorithm to map the system states into the neuron is described below.

1) Initialize weight vectors and decide the parameters of SOM such as topology, distance function and learning rate.

2) Start learning while a stopping criterion is not reached. The stopping condition can be used as $w_j(t+1) \approx w_j(t)$.

3) For each input vector Xi, compute Euclidean distances between neurons and the input vector X_i.

$$d_j = \sqrt{\sum_{i=1}^{n} (X_i - w_j(t))^2}$$

(5.11)

where

X_i : the ith input vector.

$w_j(t)$: the jth weight vector at time t.

4) Find a winner neuron j with the minimum distance.

$$c = \arg \min d_j$$

(5.12)

5) Update weight vectors ($w_j(t)$) within a specified neighborhood for a winner neuron using Kohonen -rule.

$$w_j(t+1) = w_j(t) + a(t) \cdot h_{cj}(t) \cdot (X_i(t) - w_j(t)) \quad \text{for } j \in h_{cj}(t)$$

(5.13)

$$w_j(t+1) = w_j(t) \quad \text{for } j \notin h_{cj}(t)$$

(5.14)

where $a(t)$: learning rate

$h_{cj}(t)$: topological neighborhood

6) Update learning rate $a(t)$, which is a monotonically decreasing function.

7) Reduce the radius of topological neighborhood $h_{cj}(t)$.

8) Increase the iteration number $t = t+1$.

9) Check stopping condition. Go to Step-2.

The fundamental idea of SOM can be understood as the vicinity concept based on the distance between neurons and each input vector, which means input data near a neuron may match this neuron. Only a neuron with a minimum distance between input vectors and a weight vector is updated in the equation (5.13) or (5.14) until the current weight vector is the same as the previous. The state of neuron called by weight vectors changes its value during learning. The final weight vectors, called the state of neurons, are only taken as input data for the state characterization.

The selection of topology including the number of map units (the number of neurons), the lattice type and the map dimension is one of the most important factors to obtain satisfactory results. The number of map units and map dimension may increase as the number of input vectors increases. There are three different topologies for the original neuron locations such as grid, hexagonal, rectangular, and random topology.

The learning structure has important parameters such as the map initialization, the neighborhood function and the learning rate function. There are three kinds of map initialization; random, linear or hexagonal. If random initialization is chosen, a different result may be obtained. The neighborhood function has several possible choices such as bubble, Gaussian, cut Gaussian, and Ep function. The learning rate starts at the ordering-phase (Rough-tuning) and decreases until it reaches the tuning-phase (Fine-tuning). The learning rate continues to decrease very slowly during the tuning-phase. The neighborhood size shrinks and learning rate value within the neighborhood also decreases towards zero. Both the shrinkage of neighborhood and the decrease in the learning rate change slowly.

The optimal selection of topology and learning structure is based on the quantization error. The quantization error is defined as the mean of $\| x - w_c \|$ over all learning states where x is the input learning vector and w_c is the nearest weight vector to x.

5.2.2.2 Formulation of Self-Organizing Map

Based on the Self-Organizing Map algorithm introduced above, we will formulate Self-

Organizing Map with actual system data for reliability analysis.

1) Input Data

The input vector consists of the states of transmission lines, either up or down. Thus the dimension of each input data is the total number of transmission lines in the system. The number of learning pattern should be large enough to cover most cases occurs frequently.

2) Topology Structure

The number of map units (the number of neurons) and dimension will be determined by training process itself and may increase as the number of input vectors increases. The number of weighting vectors should be equal to that of map units. The lattice type can be chosen as either hexagonal or rectangular.

3) Learning Structure

Since the elements of input vectors are 1 and 0, linear initialization is chosen among random, linear and hexagonal initializations. There are several possible options for neighborhood function such as bubble function, Gaussian function, cut Gaussian function and ep function. The neighborhood distance starts as the maximum distance between two neurons, and decreases to the tuning neighborhood distance.

There are also several learning rate functions such as inverse function, linear function and power function. The learning rate starts from the ordering phase (rough tuning) learning rate and decrease until it reaches the tuning-phase (fine tuning) learning rate. The learning rate continues to decrease from the tuning phase learning rate, but very slowly.

5.2.3 Simulation Algorithm

Although Monte Carlo simulation can handle complicated reliability problem in a more realistic manner, as we pointed out before, it generally takes much longer time to converge than analytical reliability assessment methods. Moreover, when we focus on rare events, some of them may not get sampled during the process of convergence. To alleviate these difficulties, in this section, the importance sampling and SOM techniques are embedded into Monte Carlo simulation.

The simulation algorithm is composed of three modules; "system state generation", "SOM implementation" and "SOM utilization". Importance sampling is applied in both "system state generation" and "SOM utilization" modules.

5.2.3.1 System State Generation

System state generation module is shown in Figure 5.15. This module simulates power system state with all its stochastic features with consideration of protection failures. The system states generated will be used in following modules.
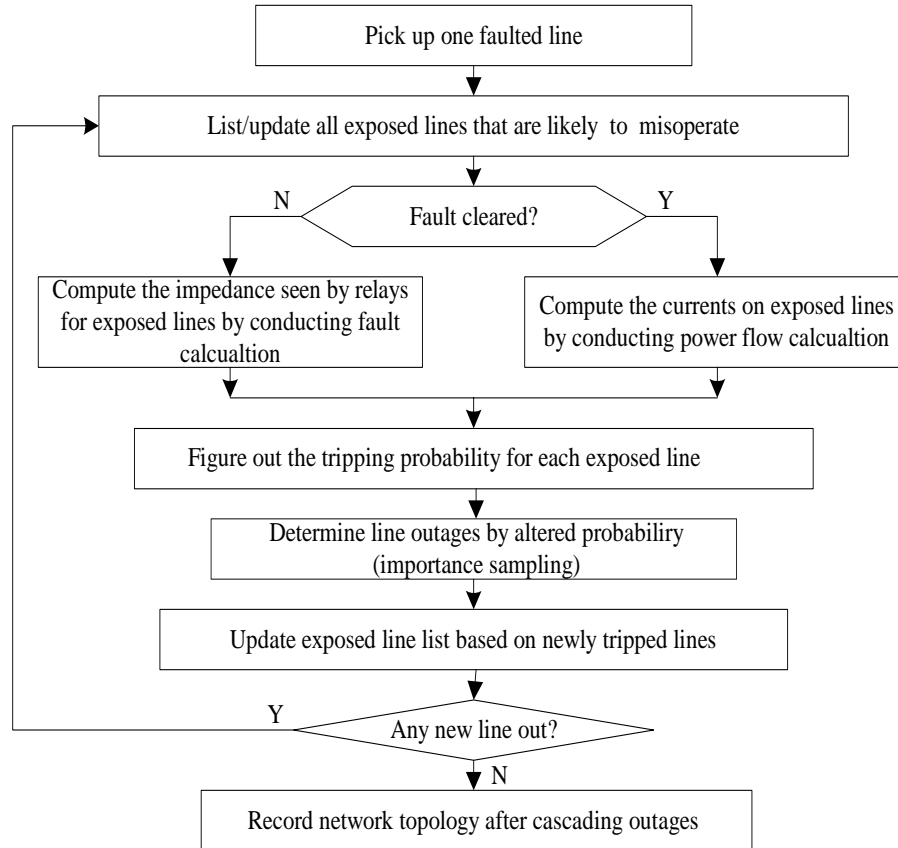
Figure 5.15 Flowchart of System State Generation

5.2.3.2 SOM Implementation

Flowchart in Figure 5.16 shows the implementation of SOM.

Input vectors represent component (transmission line) states. Learning set, composed of input vectors, should have sufficient information to identify patterns. Here, we use system state generation module rather than direct random state sampling to determine input vectors. In other words, the learning set is only those states that will actually occur in the simulation. As a result, the requirement for the number of learning set will be reduced.
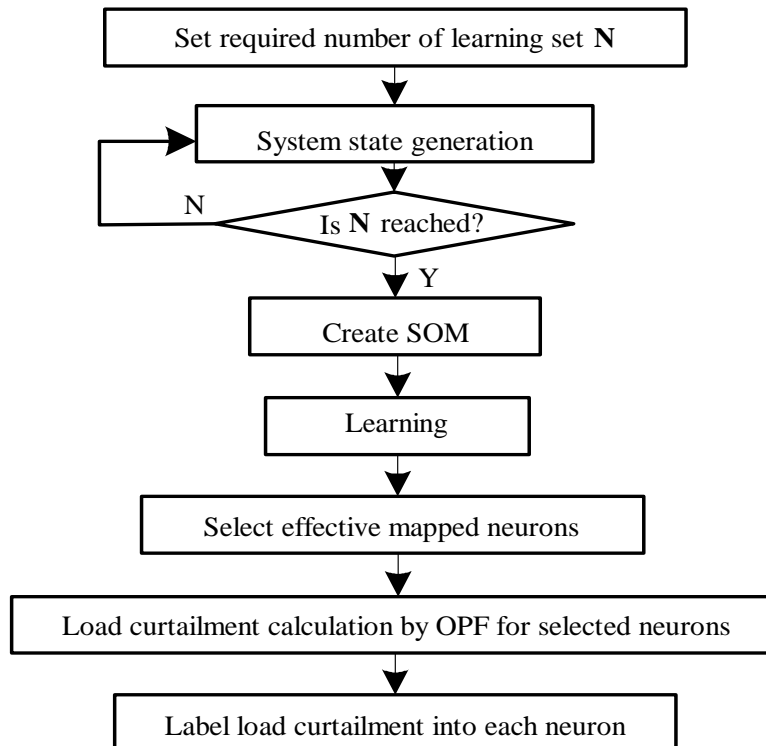
Figure 5.16 Flowchart of SOM Implementation

After the learning process, the mapped neurons are formed and the weighting vectors of neurons match the input vectors. Only those neurons that actually match learning set are taken as component states for system evaluation, i.e. OPF, by which the amount of load curtailment will be calculated. The evaluation results are labeled to the neurons.

5.2.3.3 SOM Utilization

The flowchart in Figure 5.17 shows the final simulation process to calculate nEPL. Other reliability indices can be obtained from the similar procedure.
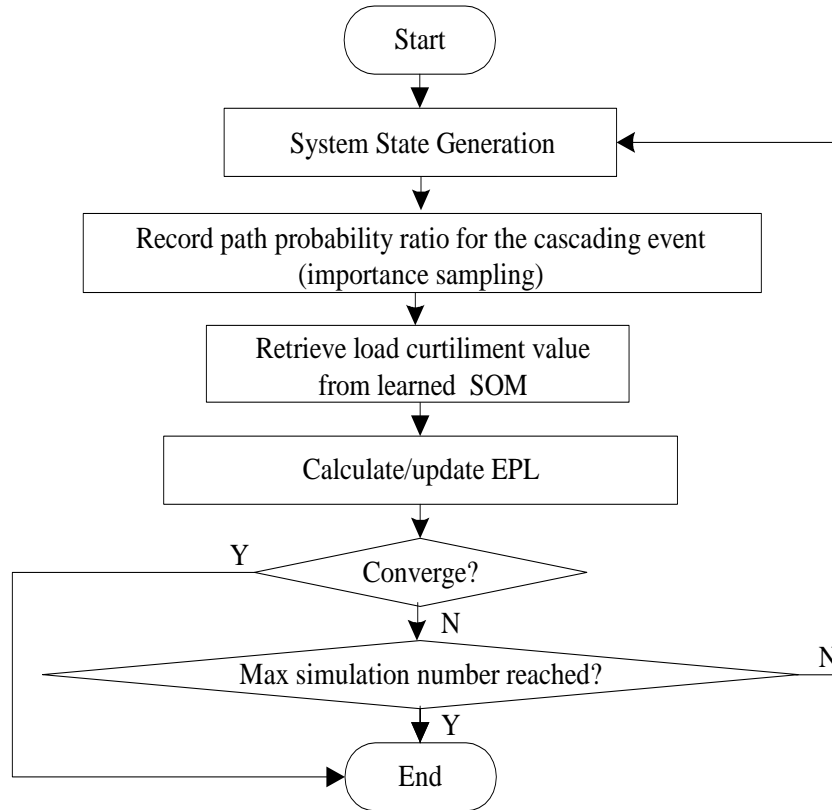
Figure 5.17 Flowchart of SOM Utilization

This procedure integrates both "system state generation" module and "SOM implementation" module. In calculating load curtailment, direct OPF calculation is not needed anymore generally. Instead, the results can be obtained from on-line use of SOM since the mapped neurons have been labeled with the amount of load curtailment already in the SOM implementation module. Nevertheless, for the cases that the neurons being matched has not been evaluated before, of course it is rare provided the number of learning set is big enough, extra OPF calculation will be performed and the result will be recorded for the next time use.

5.2.4 Case Study

The 24-bus IEEE Reliability Test System (RTS) [33] is used again here to demonstrate the calculation.

5.2.4.1 SOM Formulation

The selection of learning set is very important step for implementation of SOM [50]. Since we use real time system simulation rather than direct random sampling to generate input vectors, the requirement for the number of learning set can be small. Table 5.2 shows the key SOM parameters for IEEE RTS.

Table 5.2 Key SOM Parameters for 24-bus IEEE RTS

Input vector	Dimension	38
	No. of learning pattern	500
Topology	No. of map unit	112
	Lattice type	Rectangular
Learning structure	Map initialization	Linear
	Neighborhood type	Ep
	Learning rate function	Linear

5.2.4.2 Simulation Process

Figure 5.18 and Figure 5.19 show the simulation process of nEPL and POS calculation respectively, in which we choose coefficient of variance (cov) 0.001 as convergence criteria.
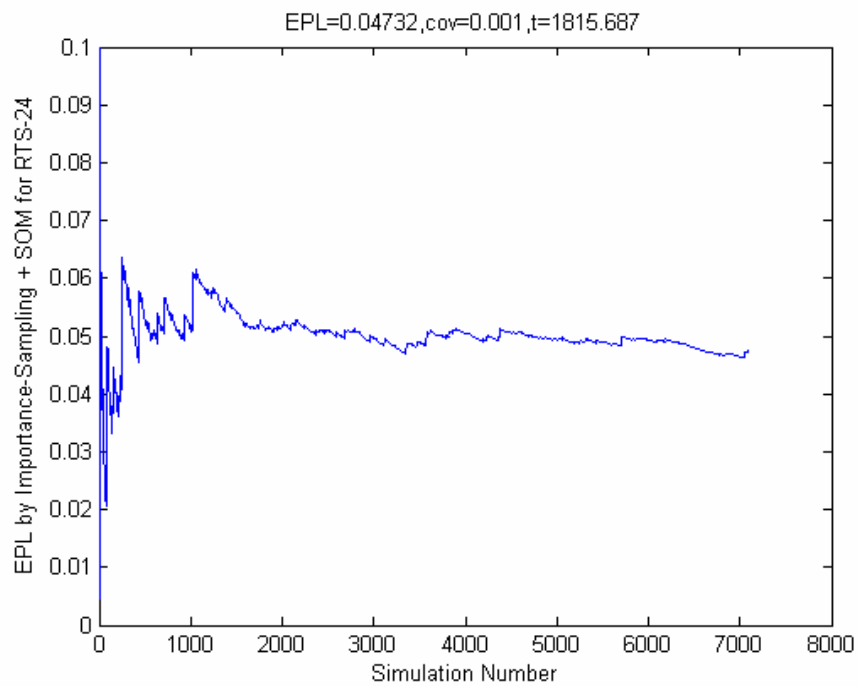
Figure 5.18 nEPL by SOM-IS-MCS
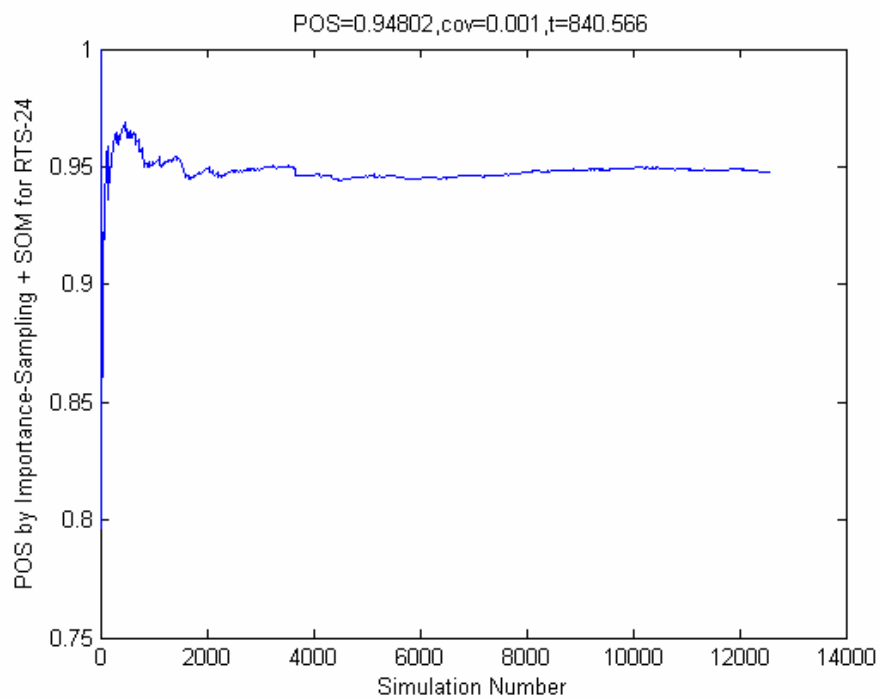
Figure 5.19 POS by SOM-IS-MCS

When the number of learning pattern is set as 500, the number of neurons is 112, of which only 82 neurons actually represent the learning patterns in the learning process. Only the weighting vectors of those 82 neurons are taken as input vectors for state evaluation (Load curtailment by OPF calculation). In the following SOM application process, 4 additional neurons need to be evaluated. Therefore, instead of 112 OPF calculations, we only conduct 86 OPF calculations for the entire simulation.

5.2.4.3 Comparison of Results and Observations

We calculate nEPL and POS by straightforward Monte Carlo simulation and importance sampling based Monte Carlo simulation also to compare the efficiency of the methodology newly proposed. All simulations are carried out in Dell Optiplex™ GX260, 2.40GH Pentium® 4 processor with 512MB RAM. The results are listed in Table 5.3.

Table 5.3 Simulation Comparison

Simulation Method	Coefficient of Variance	nEPL	Computation Time (Sec)	POS	Computation Time (Sec)
Straightforward MCS	0.001	0.0549	5654	0.9561	607
IS-MCS	0.001	0.0502	11309	0.9637	1719
SOM-IS-MCS	0.001	0.0473	1815	0.9480	840

From Table 5.3 we see that the importance sampling based simulation method spends much longer computation time. The reason is that OPF, which is very time consuming, is used in evaluating loss of load in the simulation process. Since we use altered probability, which is much higher than the actual probability, the cascading outages occurs more frequently. Consequently, more OPF evaluation process is incurred. The application of SOM can solve this problem efficiently.

Similarly for POS comparison, System Stability Evaluation, like OPF, is another time

consuming process. IS-MCS will cost more time than straightforward Monte Carlo Simulation. With SOM-IS-MCS, both accuracy and time-saving can be achieved.

5.2.5 Conclusion

Protection failures are rare events in a power system. This can be noticed by the long simulation time to converge. Importance sampling technique can be applied to reveal more rare events but not guarantee to reduce simulation time.

Based on the explicit model of components paired with protection system, an importance sampling + SOM based Monte Carlo simulation approach is developed to simulate system behavior including cascading outages. Reliability index nEPL and POS are calculated to demonstrate the application. The new method is advantageous in terms of convergence.

VI.   TOTAL TRANSFER CAPABILITY[*]

6.1 Introduction

Total Transfer Capability (TTC) is the largest value of electric power that can be transferred over the interconnected transmission network in a reliable manner without violation of specified constraints. TTC is the key component for calculating Available Transfer Capability (ATC). The relationship of TTC and ATC is described in NERC report [51]: ATC equals TTC less the sum of the Transmission Reliability Margin (TRM), Existing Transmission Commitments (ETS) and Capacity Benefit Margin (CBM).

There are a number of methods and algorithms for computing TTC. Only three of them are practical for large realistic applications [52]. These are

- Security Constrained Optimal Power Flow (SCOPF) method.
- Continuation Power Flow (CPF) method [53-54].
- Repeated Power Flow (RPF) method.

SCOPF method needs to calculate a large number of OPFs under different postulated system conditions. It is obviously a time consuming approach. The CPF method, whose implementation involves parameterization, predictor, corrector and step-size control, is mathematically complicated. The RPF method, which repeatedly solves power flow equations at a succession of points along the specified load/generation increment, is used in this paper for TTC calculation. Compared with SCOPF and CPF, the implementation of RPF is much easier and it also provides part of V-P, V-Q curves, which facilitates the potential analysis of voltage stability [55].

---

[*] Part of this section is reprinted with permission from "Total Transfer Capability Considering FACTS and Security Constraints" by Xingbin Yu, Chanan Singh, Sasa Jakovljevic, Dragan Ristanovic, and Garng Huang, 2003. *IEEE* PES *Transmission & Distribution Conference and Exposition*, Volume: 1. pp. 73-78. © 2004 by IEEE.

The TTC is a function of thermal, voltage and transient stability limits of the system. All three limits restrict the value of TTC. The previous work on calculating TTC considers only the first two constraints, i.e. thermal limit and voltage magnitude limit [52-55]. The results without considering transient stability limit are prone to be somewhat optimistic and would not represent the actual system performance. Following those values in operation may lead to system instability in case of contingencies. In this section, an algorithm that incorporates all three constraints to calculate the TTC is established. Therefore this approach is expected to yield more realistic results.

In this section, two topics are selected in analyzing TTC. The first one is the discussion of the effects of Flexible AC Transmission System (FACTS) devices on Total Transfer Capability (TTC). The second one is the probabilistic analysis of Total Transfer Capability considering security constraints.

6.2 Total Transfer Capability Considering FACTS and Security Constraints

6.2.1 Introduction

In the power industry term FACTS (Flexible AC Transmission Systems) covers a number of technologies that enhance the security, capacity and flexibility of power transmission systems. FACTS solutions enable power grid owners to increase existing transmission network capacity while maintaining or improving the operating margins necessary for grid stability. As a result, more power can reach consumers with a minimum impact on the environment, with substantially shorter project implementation times, and at lower investment costs - all compared to the alternative of building new transmission lines or power generation facilities. The two main reasons for incorporating FACTS devices in electric power systems are:

- Raising dynamic stability limits
- Provide better power flow control

Thyristor Controlled Series Capacitors (TCSC) provides a proven technology that addresses specific dynamic problems in transmission systems. TCSC's are an excellent tool to introduce if increased damping is required when interconnecting large electrical systems. Additionally, they can overcome the problem of Sub-Synchronous Resonance (SSR), a phenomenon that involves an interaction between large thermal generating units and series compensated transmission systems.

Electrical loads both generate and absorb reactive power. Since the transmitted load varies considerably from one hour to another, the reactive power balance in a grid varies as well. The result can be unacceptable voltage amplitude variations, a voltage depression, or even a voltage collapse. A rapidly operating Static Var Compensator (SVC) can continuously provide the reactive power required to control dynamic voltage swings under various system conditions and thereby improve the power system transmission and distribution performance. Installing an SVC at one or more suitable points in the network can increase transfer capability and reduce losses while maintaining a smooth voltage profile under different network conditions. In addition, an SVC can mitigate active power oscillations through voltage amplitude modulation.

6.2.2 Formulation of the Problem

6.2.2.1 TTC without TCSC and SVC

RPF formulation for TTC without TCSC and SVC (base case) is expressed as follows:

$$Max \quad P_{tie-lines} = f\left(P_{G_i(i \in Source)}, P_{D_j(j \in Sink)}, Q_{D_j(j \in Sink)}\right)$$

Subject to:

$$P_{Gi} - P_{Di} - \sum_{j=1}^{n} |U_i||U_j|\left(G_{ij}\cos\delta_{ij} + B_{ij}\sin\delta_{ij}\right) = 0 \tag{6.1}$$

$$Q_{Gi} - Q_{Di} - \sum_{j=1}^{n} |U_i||U_j|\left(G_{ij}\sin\delta_{ij} - B_{ij}\cos\delta_{ij}\right) = 0 \tag{6.2}$$

$$|U_i|_{\min} \leq |U_i| \leq |U_i|_{\max} \tag{6.3}$$

$$|S_{ij}| \leq |S_{ij}|_{\max} \tag{6.4}$$

$$|\delta_{Gi}(t) - \delta_{Gj}(t)| \leq \delta_{G\max} \tag{6.5}$$

where:

P_D : the total real power load on all load buses.

$P_{tie-lines}$: the summation of real power flow on tie lines

P_{Gi}, Q_{Gi} : real and reactive power generation at bus i

P_{Di}, Q_{Di} : real and reactive load at bus i

n : number of system buses

$|U_i|$: voltage magnitude at bus i

G_{ij}, B_{ij} : real and imaginary part of the ij^{th} element of bus admittance matrix.

δ_{ij} : voltage angle difference between bus i and bus j

S_{ij} : apparent power flow in line ij

$|U_i|_{\min}$: lower limit of voltage magnitude at bus i

$|U_i|_{\max}$: upper limit of voltage magnitud at bus i

$|S_{ij}|_{\max}$: thermal limit of line ij

$\delta_{Gi}(t)$: rotor angle of generator i

$\delta_{G\max}$: maximum secure relative swing angle.

In the process of calculation, P_{Gi}, P_{Di} and Q_{Di} are changed in following ways [41]

$$P_{Gi} = P_{G1}^0\left(1 + \lambda k_{Gi}\right) \tag{6.6}$$

$$P_{Di} = P_{D1}^0 \left(1 + \lambda k_{Di}\right) \tag{6.7}$$

$$Q_{Di} = Q_{D1}^0 \left(1 + \lambda k_{Di}\right) \tag{6.8}$$

where

P_{G1}^0 : base case real power generation at bus i

P_{D1}^0, Q_{D1}^0 : base case real and reactive load at bus i

λ : increment factor in bus load or generation

k_{Gi}, k_{Di} : constants specifying the rate of change in generation and load

According to (7.6)~(7.8), we can increase the apparent load with constant power factor at each bus in the sink area and increase injected real power at each generator bus in the source area in successive steps until one or more limits are reached.

6.2.2.2 TTC with TCSC

When TCSC is installed in a transmission line, the reactance of the line can be adjusted. Normally the adjustment range is 0.5X to 1.5X, where X is the reactance of the original line. The formulation of TTC can be expressed as below:

$$Max \quad P_{tie-lines} = f\left(P_{G_i(i \in Source)}, P_{D_j(j \in Sink)}, Q_{D_j(j \in Sink)}\right)$$

Subject to:

$$P_{Gi} - P_{Di} - \sum_{j=1}^{n} |U_i||U_j|\left(G_{ij}\cos\delta_{ij} + B_{ij}\sin\delta_{ij}\right) = 0 \tag{6.9}$$

$$Q_{Gi} - Q_{Di} - \sum_{j=1}^{n} |U_i||U_j|\left(G_{ij}\sin\delta_{ij} - B_{ij}\cos\delta_{ij}\right) = 0 \tag{6.10}$$

$$|U_i|_{min} \leq |U_i| \leq |U_i|_{max} \tag{6.11}$$

$$\left| S_{ij} \right| \leq \left| S_{ij} \right|_{\max} \tag{6.12}$$

$$-0.5X \leq X_{TCSC} \leq 0.5X \tag{6.13}$$

$$\left| \delta_{Gi}(t) - \delta_{Gj}(t) \right| \leq \delta_{G\max} \tag{6.14}$$

where:

$G_{ij-TCSC}$, $B_{ij-TCSC}$: real and imaginary part of the ij^{th} element of bus admittance

matrix when TCSC is installed.

X_{TCSC} : reactance of TCSC

X   : original reactance of the line where TCSC is installed

6.2.2.3 TTC with SVC

SVC is a shunt compensation component. When it is installed in the transmission line, it can be treated as a PV bus with zero generation of real power [9]. The formulation of TTC using RPF can be represented as follows:

$$Max \quad P_{tie-lines} = f\left(P_{G_i(i \in Source)}, P_{D_j(j \in Sink)}, Q_{D_j(j \in Sink)} \right)$$

Subject to:

$$P_{Gi} - P_{Di} - \sum_{j=1}^{n} \left| U_i \right| \left| U_j \right| \left(G_{ij} \cos \delta_{ij} + B_{ij} \sin \delta_{ij} \right) = 0 \tag{6.15}$$

$$Q_{Gi} - Q_{Di} - \sum_{j=1}^{n} \left| U_i \right| \left| U_j \right| \left(G_{ij} \sin \delta_{ij} - B_{ij} \cos \delta_{ij} \right) = 0 \tag{6.16}$$

$$\left| U_i \right|_{\min} \leq \left| U_i \right| \leq \left| U_i \right|_{\max} \tag{6.17}$$

$$\left| S_{ij} \right| \leq \left| S_{ij} \right|_{\max} \tag{6.18}$$

$$P_{SVC} = 0 \tag{6.19}$$

$$\left|\delta_{Gi}(t) - \delta_{Gj}(t)\right| \leq \delta_{G\max} \tag{6.20}$$

where:

G_{ij-SVC}, B_{ij-SVC} : real and imaginary part of the ij^{th} element of bus admittance matrix when SVC is installed.

P_{SVC} : real power output of the additional PV bus representing the SVC

6.2.2.4 Security Constraint Model

Among the three constraints in TTC calculation, thermal and voltage magnitude limits are easier to implement. However, transient stability constraint needs special procedure to deal with.

Power system stability considers the dynamic behavior of the power system after a contingency [56]. Power system stability denotes a condition in which various synchronous machines of the system remain "in synchronism" or "in step" with each other [57]. Therefore, the security assessment can be conducted by checking generator rotor angles in the n-1 contingency scenario. In this paper, swing equation model is used to handle stability analysis directly. A typical swing-equation model includes second-order differential equations associated with generator buses and algebraic equations for other buses. For generator buses, we have:

$$M_i\ddot{\delta}_{Gi} + D_i\dot{\delta}_{Gi} = P_{mi} - P_{gi} \qquad\qquad i=1,...,n \tag{6.21}$$

where

δ_{Gi} : the generator rotor angle.

P_{mi} : the mechanical power input

P_{gi} : the electrical power input

n : the number of generators

M_i : the ith-generator's inertia coefficient

D_i : the ith-generator's damping coefficient

Mechanical power P_{mi} is equal to the pre-fault electrical power, which can be obtained by power flow calculation. Electric power output is given as (7.22):

$$P_{gi} = \sum_{j=1}^{n} |V_i| |V_j| |Y_{ij}| \cos\left(\theta_{ij} - \delta_{Gi} + \delta_{Gj}\right) \qquad i=1,...,n \qquad (6.22)$$

where Y_{ij} is the reduced bus admittance matrix.

In this section, fixed typical fault clearing time is used in stability analysis. The transient stability criterion is that within a certain period after the occurrence of fault, the difference of any two rotor angles does not exceed the maximum secure relative swing angle, which is set as 180°.

6.2.3 Methodology and Implementation

The methodology suggested in this paper includes both steady state and dynamic security constraints. The general procedure to calculate TTC with TCSC/SVC can be described as follows:

1) If TCSC is installed, set initial TCSC=-0.5X. If SVC is installed, set initial position, normally at one line end.

2) Select the base case and solve the power flow.

3) Use RPF to make a step increase in generation and load.

4) Establish and solve the power flow problem according to the modified system condition; conduct stability assessment under the current condition.

5) Check the power flow solution to see whether thermal limit or voltage limit are violated. Check stability assessment result to see whether security limit is violated. If none of these limits are violated, go to step 3). Otherwise go to step 6).

6) Take opposite step of RPF to eliminate all violations in minimum steps. Compute the TTC level.

7) If TCSC is installed, increase the reactance of TCSC by a specified increment, go to step 2) until the reactance of TCSC reaches 0.5X. If SVC is installed, move the SVC location along the line in a certain step until the end of the line is reached. The maximum values of the TTC associated with each TCSC reactance or SVC location are the final results.

Based on the above procedure, a user-friendly software package is developed. The full software functionality is controlled by Graphical User Interface (GUI), which facilitates effective and flexible analysis for various system conditions. Different test systems, analysis types, operation modes and corresponding system conditions can be easily chosen. Both graphic and numerical outputs are available for assessment. Graphic output results include the relation of TTC and value of TCSC applied, relation of TTC and position of SVC installed, and swing curves of generator phase angles. One snapshot of the interface is shown in Figure 6.1.
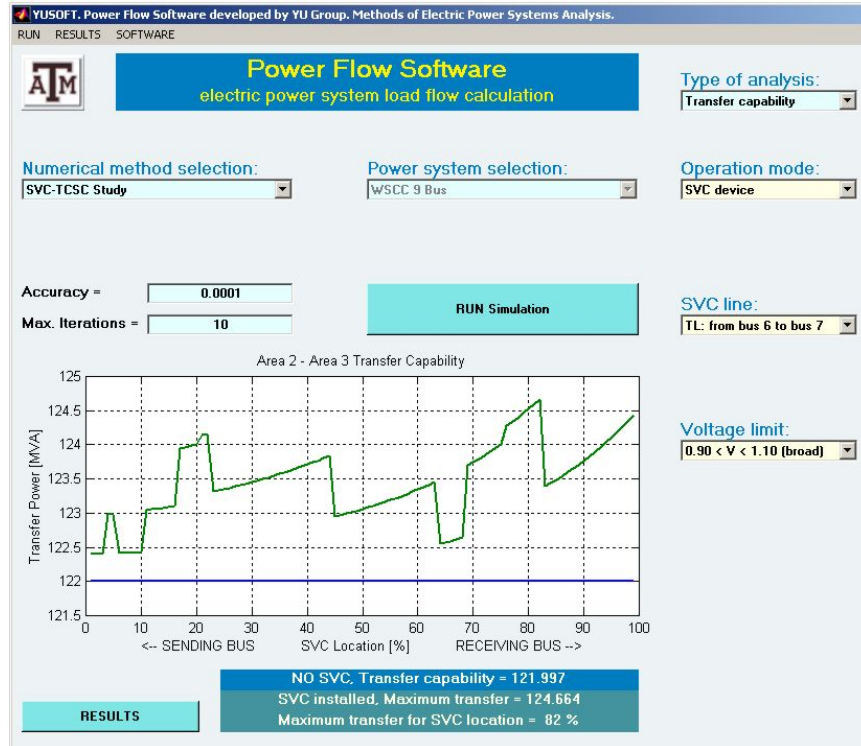
Figure 6.1 GUI of the Software Package

6.2.4 Case Study

6.2.4.1 Test System

The WSCC-9 bus system (shown in Figure 6.2) is used as the test. Three areas are identified for TTC analysis, in which we focus on the transfer capability from Area-2 to Area-3.

The transmission line parameters are shown in Figure 6.2 too. The base case system loads are listed in Table 6.1.

Fixed thermal limits for transmission lines are set as in Table 6.2. Transformers are assumed to have infinite thermal limit.

Protective zone II tripping time is used as typical fault clearing time for n-1 contingency stability analysis.
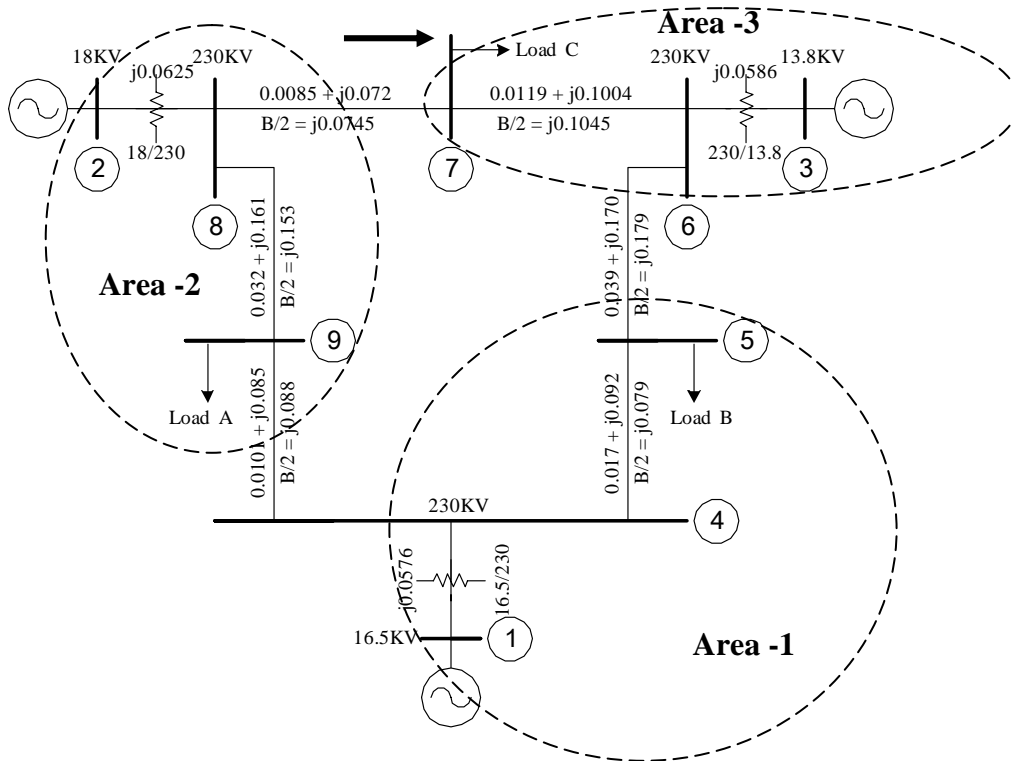
Figure 6.2 WSCC-9 Bus System

Table 6.1 WSCC-9 Base Case Load

Load A	Load B	Load C
90MW	100MW	125MW

Table 6.2 WSCC-9 Transmission Line Thermal Limits

Line	4-5	5-6	6-7	7-8	8-9	9-4
Thermal limit (MVA)	50	115	70	150	150	80

6.2.4.2 Impact of FACTS Devices on Stability

It has been known that FACTS devices are designed and installed to enhance system stability to some extent. However, this may not be true in all cases. In this section we demonstrate the negative influence of SVC and TCSC devices on power system stability in some particular cases. The location of SVC is set at 50% of transmission line under consideration and TCSC factor is set to -0.5X. The base case system load is applied.

1) Effect of TCSC

Figure 6.3 presents an example of negative influence of TCSC devices.

Two lines observed in this case are line 6-7 where SVC is installed and line 7-8 where the fault was applied. Fault clearing time that roughly corresponds to zone II tripping is selected as 0.48 sec. This corresponds to the delayed clearing from the remote end of the line 7-8 and gives greater influence of the system on the right-hand side of the fault. Since SVC is installed in line 6-7 and increases right-hand side fault in feed, the system is more prone to instability.
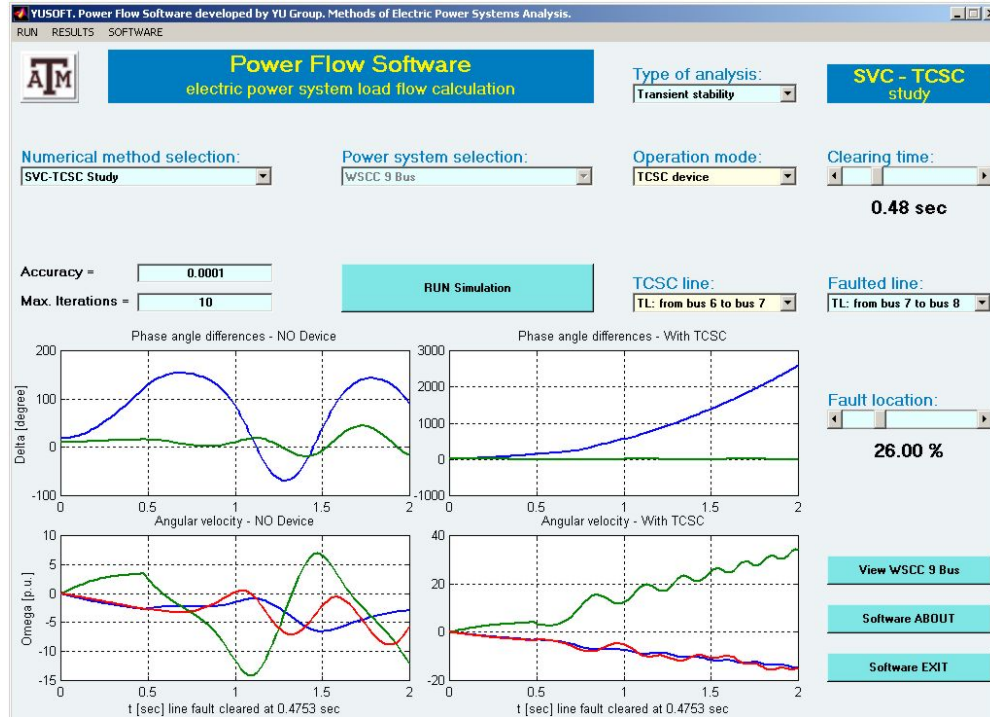
Figure 6.3 Negative Influence of TCSC on System Stability Illustration

2) Effect of SVC

The same fault and protection scenario is selected for SVC device as 1). In this case, the influence of SVC device proved to have negative impact on the system transient stability too. This is illustrated in Figure 6.4.
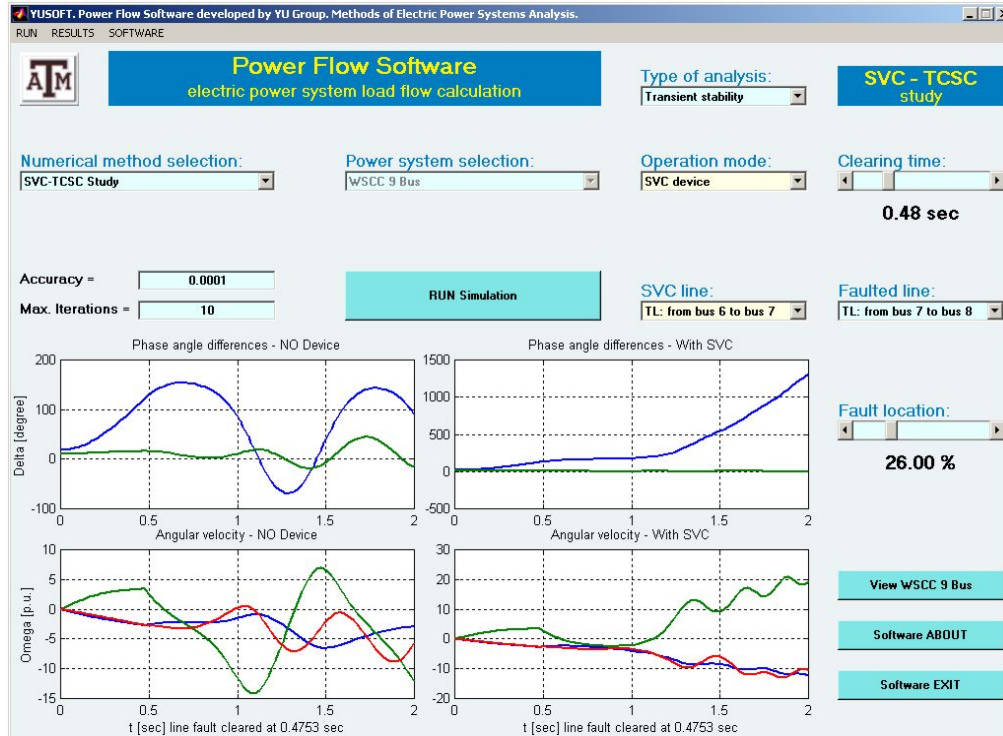
Figure 6.4 Negative Influence of SVC on System Stability Illustration

Another example that TCSC has greater impact on the system stability than SVC can be observed in comparison of the above two cases. In fact, in both cases, both TCSC and SVC cause system instability, but the magnitude of generator oscillations increased in the case when TCSC was applied.

6.2.4.3 TTC Analysis

Two sets of voltage limit, the broad one and the narrow one, are applied to analysis. The loose one is expected to allow the thermal limit violation to occur and we call it "thermal limit dominant" case. The narrow one, on the other hand, makes voltage magnitude violation normally happen and we call it "voltage limit dominant" case.

1) Effect of TCSC

Case-1: Voltage Limit 0.90<|V|<1.10

Table 6.3 gives two sets of results, one of which does not include stability constraint and the other does. Without considering stability constraint, the base case transfer capability is 122.0MVA and the installation of TCSC improves the transfer capability. The maximum improvement (16.1%) occurs when TCSC is installed on line 8-9.

Table 6.3 Effect of TCSC on TTC (Thermal Limit Dominant)

TCSC Installed on	Without considering stability		Considering stability	
	Transfer Capability	Violation	Transfer Capability	Violation
Null	122.0	Thermal: 8-9	102.3	Stability: 7-8
4-5	122.6	Thermal: 8-9	102.9	Stability: 7-8
5-6	140.7	Thermal: 8-9	102.9	Stability: 7-8
6-7	123.2	Thermal: 8-9	104.8	Stability: 7-8
7-8	128.7	Thermal: 8-9	104.1	Stability: 7-8
8-9	141.6	Thermal: 8-9	105.4	Stability: 8-9
4-9	123.1	Thermal: 8-9	102.9	Stability: 8-9

On the other hand, when considering stability constraint, the base case transfer capability is decreased to 102.3MVA. Stability violations occurred in all other cases and there is not much improvement for TTC by installing TCSC in these cases.

Without consideration of stability, TCSC could have significant effect on increasing the transfer capability, and this matches the conclusion from reference [55]. However, that conclusion may not always be true when stability limit is incorporated.

Case-2: Voltage Limit 0.95<|V|<1.05
Without considering stability constraint, this case would be a "pure" voltage limit dominant case. Table 6.4 shows the results. The base-case TTC is the same for both conditions. This

is because for either condition, the voltage limit always hits first. After installing TCSC, the transfer capability increases. When TCSC is installed in different lines, the effect varies. That also matches the conclusion in [55]. When considering stability constraint, either voltage limit or transient stability limit might hit for TTC calculation. This demonstrates the importance of taking the stability into account in TTC calculation. When TCSC is installed in line 4-9, which is connected to the bus-9 with voltage violation, the effect is significant. The case where TCSC is installed in line 5-6 also gives good effect. That is because the installation of TCSC in that line changes the power flow with positive effect on the transfer capability.

Table 6.4 Effect of TCSC on TTC (Voltage Limit Dominant)

TCSC Installed on	Without considering stability		Considering stability	
	Transfer Capability	Violation	Transfer Capability	Violation
Null	96.5	Voltage: 9	96.5	Voltage: 9
4-5	97.4	Voltage: 9	97.4	Voltage: 9
5-6	121.3	Voltage: 9	102.9	Stability: 7-8
6-7	103.8	Voltage: 9	103.8	Voltage: 9
7-8	107.9	Voltage: 9	104.1	Stability: 7-8
8-9	102.8	Voltage: 9	102.8	Voltage: 9
4-9	120.8	Voltage: 9	102.9	Stability: 8-9

2) Effect of SVC

Case-1: Voltage Limit 0.90<|V|<1.10

Table 6.5 shows the results of the effect of SVC on TTC. When considering stability constraints, the base case TTC decreased 16.2% from 122.0MVA to 102.3MVA. After installing SVC, no obvious improvement is found from the results in Table 6.5. Therefore,

the SVC cannot improve the transfer capability in thermal limit dominant cases. Stability limit further confines the TTC.

Table 6.5 Effect of SVC on TTC (Thermal Limit Dominant)

SVC Installed on	Without considering stability		Considering stability	
	Transfer Capability	Violation	Transfer Capability	Violation
Null	122.0	Thermal: 8-9	102.3	Stability: 7-8
4-5	123.3	Thermal: 8-9	102.3	Stability: 7-8
5-6	123.3	Thermal: 8-9	102.3	Stability: 7-8
6-7	124.7	Thermal: 8-9	102.3	Stability: 7-8
7-8	122.4	Thermal: 8-9	104.8	Stability: 8-9
8-9	122.4	Thermal: 8-9	102.3	Stability: 8-9
4-9	122.4	Thermal: 8-9	102.3	Stability: 7-8

Case-2: Voltage Limit $0.95<|V|<1.05$

Transfer capability without SVC decreases due to the narrow voltage limit margin. In both conditions the voltage limits are hit for base case TTC. The installation of SVC can fairly improve the TTC from Table 6.6

Table 6.6 Effect of SVC on TTC (Voltage Limit Dominant)

SVC Installed on	Without considering stability		Considering stability	
	Transfer Capability	Violation	Transfer Capability	Violation
Null	96.5	Voltage 9	96.5	Voltage 9
4-5	123.3	Thermal: 8-9	102.3	Stability: 7-8
5-6	116.2	Voltage 9	102.3	Stability: 7-8
6-7	110.6	Voltage 9	102.3	Stability: 7-8
7-8	122.4	Thermal: 8-9	104.8	Stability: 7-8
8-9	122.4	Thermal: 8-9	102.3	Stability: 8-9
4-9	122.4	Thermal: 8-9	102.3	Stability: 7-8

In this case, either thermal limit or voltage limit might be hit when stability constraint is not taken into account. When stability is considered, however, the stability limit becomes the bottleneck except for the base case.

3) Comparison of Results

Table 6.7 summarizes the TTC results with the most significant improvements under various conditions.

Table 6.7 Comparison of the Effect of TCSC and SVC on TTC

	Without considering stability		Considering stability	
	$0.90<|V|<1.1$	$0.95<|V|<1.05$	$0.9<|V|<1.1$	$0.95<|V|<1.05$
TTC (base case)	122.0	96.5	102.3	96.5
TTC with TCSC	141.6	121.3	105.4	104.1
Improvement	16.1%	25.7%	3.0%	7.9%
TTC with SVC	124.7	123.3	104.8	104.8
Improvement	2.2%	27.8%	2.4%	8.6%

From Table 6.7, it is observed that when transient stability is not considered, TCSC and SVC improve TTC significantly for voltage limit dominant cases while only TCSC improves TTC for thermal limit dominant cases. On the other hand, when stability constraint is considered the improvement drops.

6.2.5 Conclusion

A comprehensive approach for TTC calculation is established with consideration of thermal, voltage and transient stability limits. Based on this approach, both steady state and

dynamic security assessments are included in the process of obtaining total transfer capability. The studies reported indicate that TTC without considering transient stability limits is prone to give optimistic results.

The FACTS devices have both positive and negative effects on system stability depending on their location. In order to evaluate the effects of FACTS devices on TTC, all critical factors need to be taken into account simultaneously.

Fault conditions such as fault location and fault duration time are major factors in determining the system stability. In this paper, fixed fault location and fault duration time are used for stability analysis. However, a fault condition varies greatly based on the nature of fault and protection device/scheme applied. Therefore, probabilistic stability analysis is expected to give more realistic results in TTC calculations.

6.3 Probabilistic Analysis of Total Transfer Capability

6.3.1 Motivation

Due to the uncertainty of power system behavior, discrete events such as unexpected circuit or unit outage can result in a decrease of transfer capability considerably [58]. It is impossible to give a fixed TTC results under all conditions. Furthermore, in system operation, transmission risk analysis needs a statistical forecast for an expected range of transfer capability. Therefore, it is important to study TTC problem from a probabilistic point of view. Some research has been performed to include various probabilistic models for load and generation [59-62]. However, probabilistic transient stability analysis is seldom considered. Fault conditions such as fault location and fault duration time are major factors in determining the system stability. In fact, a fault condition varies greatly based on the nature of fault and protection device/scheme applied. Therefore, probabilistic stability analysis is one of the most important factors in calculating TTC.

In this section, we establish a probabilistic algorithm that incorporates all three constraints to calculate the TTC. This approach is expected to yield more realistic and useful results.

The formulation of the TTC calculation considering security constraints is the same as described in 6.2.2.1. In this section, we will focus on probabilistic methodology and its implementation.

6.3.2 Stochastic Features

For security analysis, probabilistic factors must be taken into consideration. There are many uncertainties in terms of system contingencies and corresponding responses. The following stochastic features are considered in security analysis.

6.3.2.1 Type of fault

A variety of contingencies might happen in a power system. As for the vulnerability analysis, however, we assume all faults to be three-phase, either transient or permanent. This strategy will yield somewhat conservative results.

6.3.2.2 Location of fault

The fault probabilities of transmission lines are calculated from their forced outage data. On the particular faulted line, the fault location is assumed to follow uniform distribution model

6.3.2.3 Fault clearing time

A normal probability distribution model is used to represent the fault clearing time.

6.3.2.4 Reclosing time

The probabilities associated with the auto-reclosing time are assumed to be normally distributed.

6.3.2.5 Fault duration

The distribution of fault duration is assumed Rayleigh.

All these five stochastic features influence the actual TTC value when security constraint is concerned

6.3.3 Methodology and Implementation

The methodology suggested in this section includes both steady state and dynamic security constraints. The general procedure to calculate TTC can be described as follows. The first step is to calculate TTC without considering the transient stability constraint. This TTC value is generally optimistic since the transient stability constraint is not considered yet. The second step is to perform transient stability analysis based on the TTC calculated in the first step by simulating stochastic features of the contingencies. For each selected contingency, opposite step of RPF may be taken to remove the transient stability violation if any. The second step will be carried out repeatedly until convergence is achieved.

As a matter of fact, the second step described above is the procedure of Monte Carlo simulation. The flowchart in Figure 6.5 shows the algorithm more clearly.
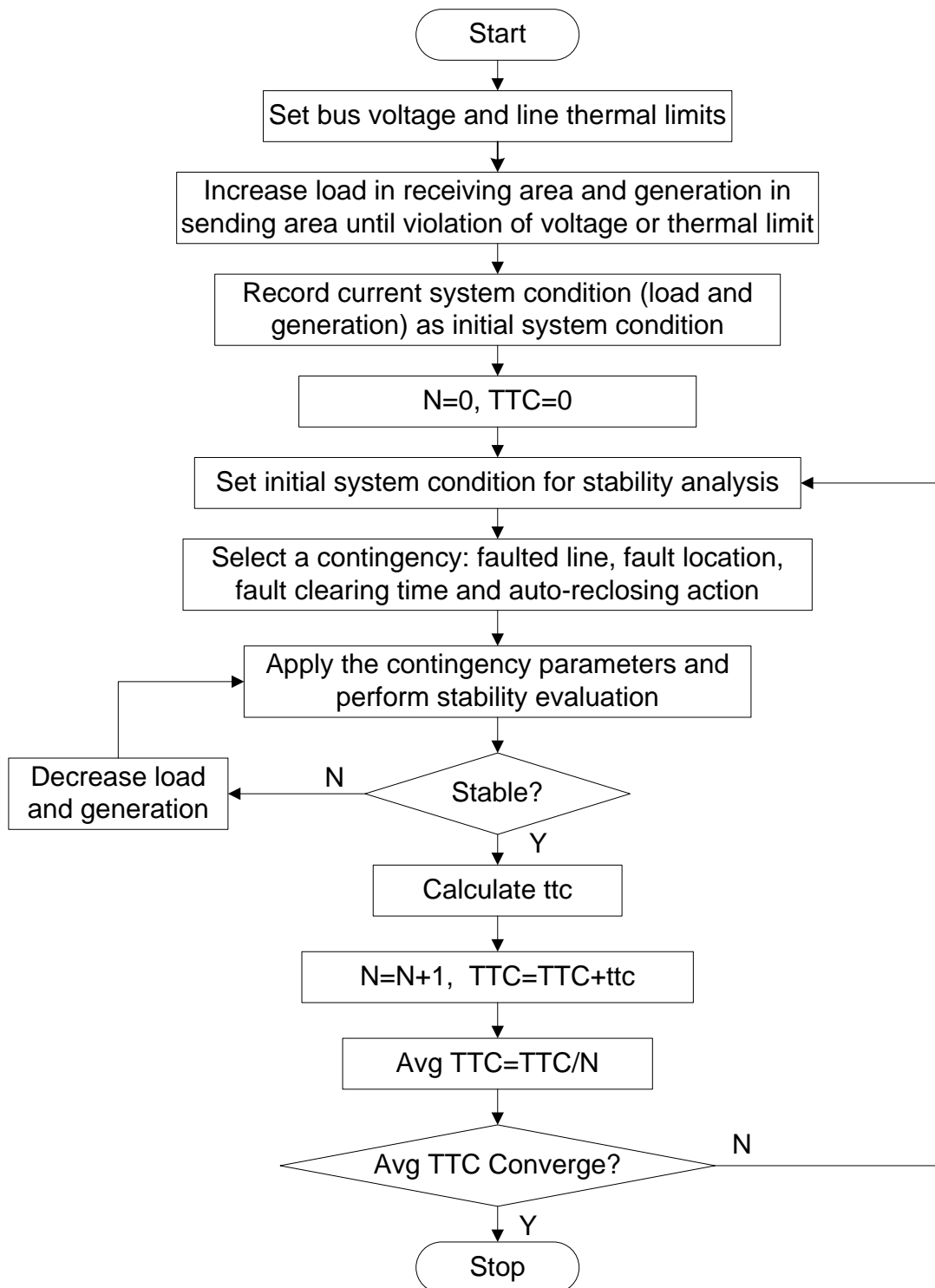
Figure 6.5 Flowchart of the Probabilistic TTC Algorithm

6.3.4 Case Study

6.3.4.1 Test System

The WSCC-9 bus system (shown in Figure 6.2) is used again here as the test system. Three areas are identified for TTC analysis, in which we focus on the transfer capability from Area-2 to Area-3. The transmission line parameters are shown in Figure 6.2 too.

The base case system loads are listed in Table 6.1.

Fixed thermal limits for transmission lines are set as in Table 6.2. Transformers are assumed to have infinite thermal limit. The voltage limits are set as $0.90<|V|<1.10$ for all buses.

In this section, we consider only the contingencies of transformers and transmission lines. The reliability data, such as the failure rate and repair rate of components, fault parameter etc, are given in the Appendix B.

6.3.4.2 The Effect of Transient Stability on TTC

System transient stability depends not only on contingency itself, but also system operating conditions such as generation and loads. On the other hand, TTC is determined by the corresponding system conditions too. Hence there are relationships between TTC and transient stability. The effect of transient stability on TTC can be seen by the following specific case.

Suppose the TTC is 145.46MW during a certain system condition without considering security constraint. Now a fault occurs with parameters described in Table 6.8. The stability evaluation is shown in Figure 6.6.

Table 6.8 Fault Parameters in a Specific Study Case

Fault line	8-9
Fault location	0.98% of line 8-9 to bus 8
Fault clearing time	0.055sec
Fault duration time	0.350sec
Reclosing time	0.781sec, successful
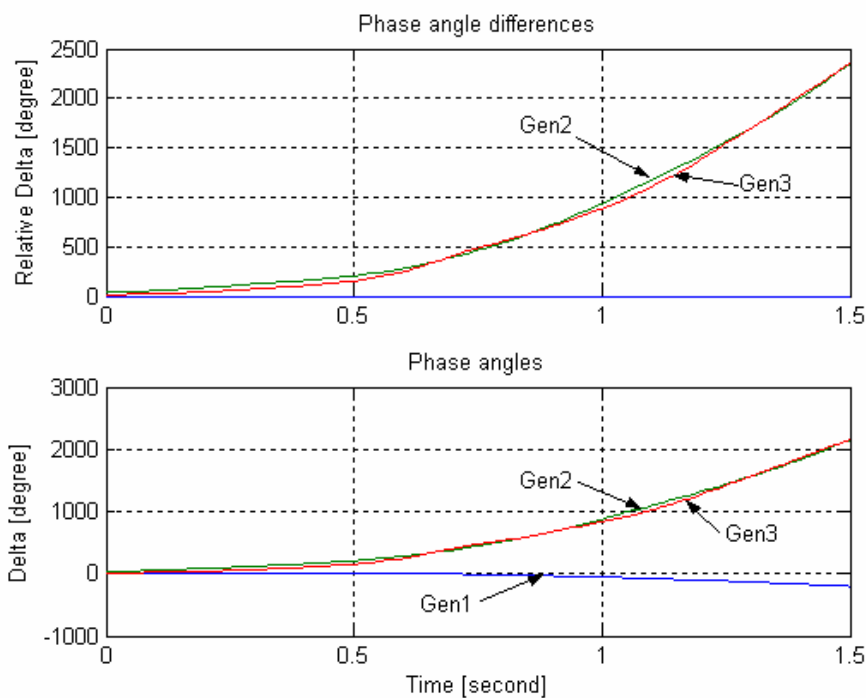
Figure 6.6 Stability Evaluation Illustration-1

From Figure 6.6 we can see that the angle differences between generator 2, 3 and generator 1 far exceed 180°. The system has lost synchronism. That means the current system condition cannot sustain the normal operation when a transient fault happens. As a result, the TTC (145.46MW) derived originally without considering security constraint is not appropriate.

When we rearrange the system condition with consideration of security constraint, the TTC reduces to 110.90MW. We test the system with exactly the same fault parameters in Table 6.8 and the stability evaluation is illustrated in Figure 6.7. Now the system is stable since the angle difference of any two generators does not exceed 180°.
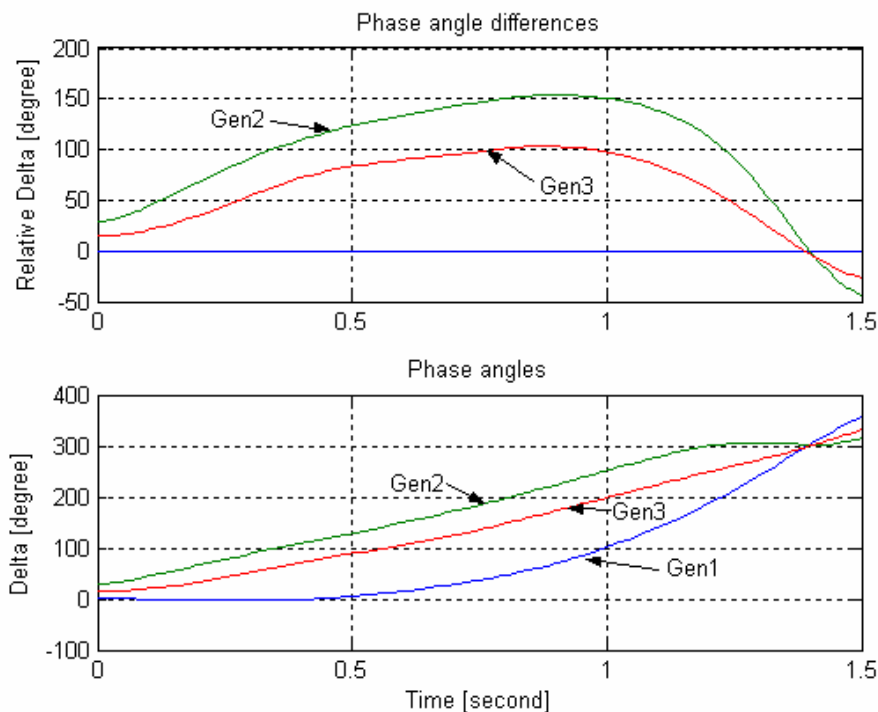
Figure 6.7 Stability Evaluation Illustration-2

System instability is a major disturbance in power systems. This case demonstrates that it is infeasible to sacrifice the system stability to achieve high TTC.

It should be emphasized that in our methodology, stability evaluation is not just based on certain pre-selected fault parameters. On the contrary, the stability evaluation follows

Monte Carlo simulation process which simulates all fault parameters based on real world stochastic features in a power system so that a more practical TTC can be given.

6.3.4.3 TTC Results

The TTC from area-2 to area-3 without considering security constraint is 149.39MW. This value is derived as per the first step of the methodology proposed above. It is also used as a base value for following TTC calculation with consideration of security constraint.

Figure 6.8 illustrates the Monte Carlo simulation process for calculating the final TTC. We can see the TTC converges at the value of 132.44MW, much less than the one without considering security constraint. Since thermal, voltage and transient stability constraints are included, we can conclude that this converged TTC value can represent the practical TTC.
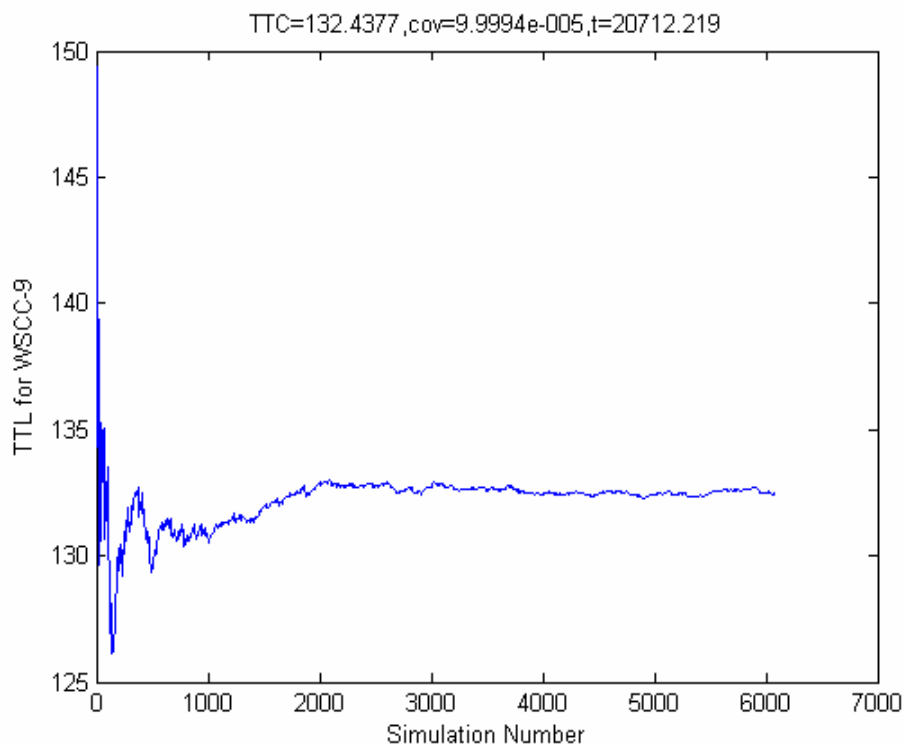
Figure 6.8 TTC by Monte Carlo Simulation

Furthermore, the advantage of Monte Carlo simulation can be taken to provide probability distribution of TTC in Figure 6.9.
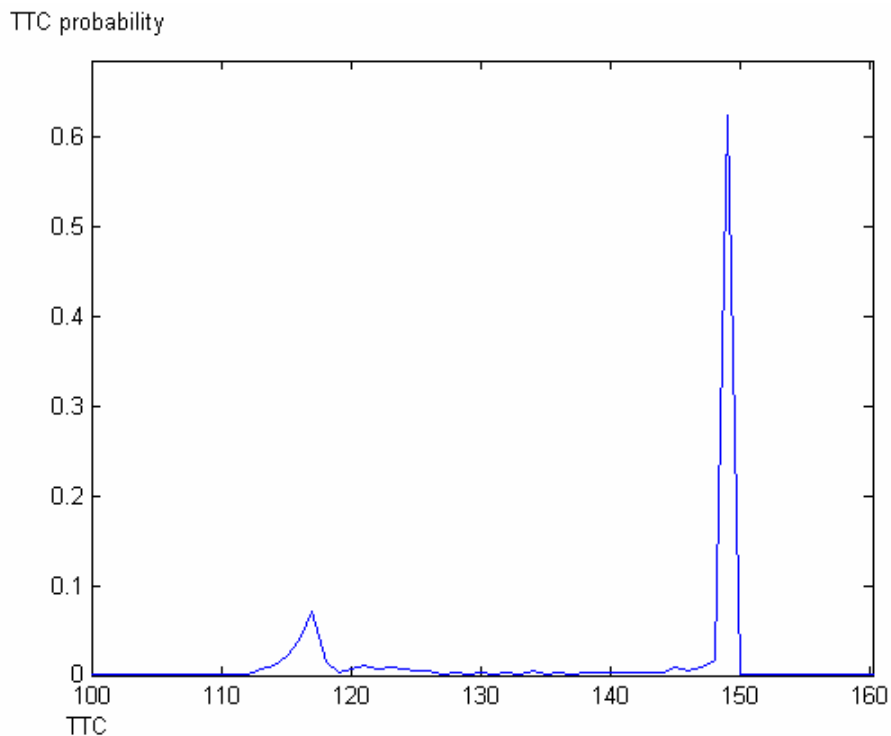
Figure 6.9 Probability Distribution of TTC

The majority of TTC locates in between 145-150 MW. The TTC within this range can withstand most of the transient fault contingencies without violating thermal and voltage limits.

Another peak appears around 110-120MW. This means that the system can withstand some severe transient faults in lower TTC values.

The probability distribution of TTC has useful applications in power system operation. In this case, for example, the probability distribution of TTC implies that the TTC can be held at 145-150MW as normal operating condition. However, in some critical conditions, such

as adverse weather situations in which some severe component contingencies are likely to happen, the TTC can be reduced to around 115MW for the sake of system safety. In addition, the probability distribution of TTC also indicates that the TTC of 120-145MW is not practically economical and effective.

6.3.5 Conclusion

A comprehensive approach for TTC calculation is proposed with consideration of thermal, voltage and transient stability limits. Based on this approach, both steady state and dynamic security assessments are included in the process of obtaining total transfer capability. The studies reported indicate that TTC without considering transient stability limits is prone to give optimistic results and is risky in real application.

Fault conditions such as fault location and fault duration time are major factors in determining the system stability. A fault condition varies greatly based on the nature of fault and protection device/scheme applied. Only probabilistic stability analysis is capable of giving more realistic results in TTC calculations. In addition, the statistical output like probability distribution of TTC can provide guidance in power system operation.

VII.   CONCLUSIONS

7.1 Summary

This dissertation has presented new approaches for power system vulnerability analysis considering protection system failures and total transfer capability analysis. The major contributions of the work can be summarized as below.

1) New component-protection system models including hidden failure modes and mathematical models are established to facilitate power system vulnerability analysis considering protection failures. Since protection system failures are the main cause of cascading outages and system blackouts result from cascading outages, it is important to explore the impact of protection system failures on blackouts. The models proposed provide a solid platform for such an analysis. Based on these models, adequacy and security analysis can be conducted successfully.

2) Based on the explicit reliability models proposed in this dissertation, a comprehensive methodology is developed for power system vulnerability analysis. The methodology deals with detailed cascading outage sequences and comprehensive system probabilistic features. With the proposed methodology, we can not only evaluate common adequacy reliability indices *BIP*, *LOLP*, and *nEPL*, but also analyze the transient stability with the occurrence of cascading outages in the power system. The reliability results based on different individual faulted lines will give us guidelines for the weakest links in a power network.

3) A new vulnerability index, Integrated System Vulnerability (ISV), is introduced to depict the overall severity of the impact of cascading outages. Different reliability indices show different weakest links in the system. We could estimate the system vulnerable point based on individual reliability index with particular emphasis. In a power system, each transmission line has different component failure phenomena, protective device hidden failure probability and protection system scheme. Because

of these variations, *BIP*, *LOLP*, *EPL* or *POS* separately might locate different weak links for the same system. *ISV*, with effects of both adequacy and security performance, represents the integrated vulnerability of a particular system.

4) Two innovative Monte Carlo simulation approaches for vulnerability analysis considering protection system failures are proposed and developed. One is Importance Sampling based Monte Carlo Simulation (IS-MCS) method, which uses varied probability to reveal more rare events. Another one is called SOM-IS-MCS, which combines Self-Organizing Maps (SOM) and IS-MCS to further reduce the simulation time. These two approaches are effective in handling rare event simulation problems.

5) A comprehensive approach for TTC calculation is proposed with consideration of thermal, voltage and transient stability limits. Based on this approach, both steady state and dynamic security assessments are included in the process of obtaining total transfer capability. The studies reported indicate that TTC without considering transient stability limits is prone to give optimistic results and could be risky in real applications. Based on the proposed approach, the effect of FACTS devices on TTC is examined and a new probabilistic TTC methodology is implemented. FACTS devices have both positive and negative effects on system stability depending on their location. In order to evaluate the effects of FACTS devices on TTC, all critical factors need to be taken into account simultaneously. The probability distribution of TTC has useful applications in power system operation. Only probabilistic stability analysis is capable of giving more realistic results in TTC calculations.

7.2 Suggestions for Further Research

The work reported in this dissertation can be an important basis for future research activities related to power system vulnerability analysis and TTC study. In general, future research directions based on this dissertation are summarized below.

1) In this dissertation, the security studies only examine the angle transient stability. As a matter of fact, power system blackouts are complicated phenomena in which a variety of factors are involved. The evaluation of frequency drops following loss of a generator, multi-swing loss of synchronism, and voltage dynamics can also be investigated for including dynamic effects.

2) In vulnerability analysis, the power outage duration is not considered in this dissertation. Future studies are intended to take account of the outage duration for more accurate adequacy analyses.

3) Dynamic voltage stability has not been considered for TTC analysis in this dissertation. Future work need to be done to include voltage stability for a more comprehensive analysis scheme.

4) The WCSS-9 bus system and IEEE RTS-24 have been used to demonstrate the effectiveness and efficiency of the proposed methods. To better verify the capability of methods for blackout simulation, larger networks need to be tested.

REFERENCES

[1]   North America Electric Reliability Council, Reliability assessment 2001-2010: The reliability of bulk electric systems in North America, October, 2001.

[2]   SANDIA, "The impact of restructuring policy changes on power grid reliability," Report SAND98-2187, 1998.

[3]   R. Billinton and S. Aboreshaid, "Security evaluation of composite power systems", *IEE Proc. – Gener. Transm.   Distrib.   * vol. 142, pp. 511-516, Sept. 1995.

[4]   R. Billinton and G. Lian, "Composite power system health analysis using a security constrained adequacy evaluation procedure", *IEEE Trans. Power Systems*, vol. 9, pp. 936-941, May. 1994.

[5]   P. M. Anderson, *Power System Protection*, New Jersey: Wiley-IEEE Press, 1998.

[6]   A. G. Phadke, and J. S. Thorp, "Expose hidden failures to prevent cascading outages," *IEEE Computer Application in Power,* pp. 20-23, Jul. 1996.

[7]   S. Tamronglak, S. H. Horowitz, A. G. Phadke, and J. S. Thorp, "Anatomy of power system blackouts: Preventive relays strategies," *IEEE Trans. Power Delivery*, vol. 11, pp. 708-715, Apr. 1996.

[8]   K. Bae, and J. S. Thorp, "An importance sampling application: 179 bus WSCC system under voltage based hidden failures and relay misoperation," in *Proceedings of the 1998 System Science, Thirty-first Hawaii International Conf.*, vol. 3, pp. 39-46.

[9]   H. Wang, and J. S. Thorp, "Optimal location for protection system enhancement: A simulation of cascading outages," *IEEE Trans. Power Delivery*, vol. 16, No. 4, pp. 528-533, Oct. 2001.

[10]   D. L. Pepyne, C. G. Panayiotou, C. G. Cassandras, and Y. –C. Ho, "Vulnerability assessment and allocation of protection resources in power systems," in *Proceeding 2001 American Control Conference*, pp. 4705-4710R.

[11]   N. Balu, T. Bertram, A. Bose, V. Brandwajn, G. Cauley *et al.*, "On line power system security analysis," *Proceedings of IEEE,* vol. 80, no. 2, pp. 262-280, Feb. 1992.

[12] R. Billinton, "Composite system reliability evaluation," *IEEE Transactions on Power Apparatus & Systems*, vol. PAS-88, no. 4, pp. 276-281, Apr. 1969.

[13] C. Singh and R. Billinton, *System Reliability Modeling and Evaluation*, London: Hutchinson, 1977.

[14] U.S.-Canada Power System Outage Task Force, "Final Report on the August 14, 2003 Blackout in the Unite States and Canada: Causes and Recommendations", April 2004.

[15] West System Coordinating Council, "Final Report, August 10th 1996 Event," Oct. 1996.

[16] C. Singh and A. D. Patton, "Models and Concepts for Power System Reliability Evaluation Including Protection System Failure", *Electrical Power & Energy System*s, vol. 2, No. 4, pp. 161-168, Oct. 1980.

[17] C. Singh and A. D. Patton, "Protection system reliability modeling: Unreadiness probability and mean duration of undetected faults", *IEEE Trans. Reliability*, vol. R-29, No. 4, pp. 339-340, Oct. 1980.

[18] NERC (North Amercan Electric Reliability Council) Disturbance Analysis Working Group Database, 1984-2002. Date accessed: May 25, 2005

[19] Transmission Transfer Capability Task Force, "Transmission Transfer Capability", North American Electric Reliability Council, Princeton, New Jersey, 1995.

[20] I. Dobson, S. Greene, R. Rajaraman, C. L. Demarco, F. L. Alvarado, M. Glavic, J. Zhang, and R. Zimmerman, Electrical Power Transfer Capability: Concepts, Applications, Sensitivity, Uncertainty. Power Systems Engineering Research Center.

[21] V. Ajjarapu, and C. Christy, "The continuation power flow: A tool for steady state voltage stability analysis", *IEEE Transactions on Power System*, vol. 7, pp. 416-423, Feb. 1992.

[22] C. A. Cañizares, and F. L. Alvarado, "Point of collapse and continuation methods for large AC/DC systems", *IEEE Transactions on Power System*, vol.7, pp. 1-8, Feb. .1993.

[23] H. D. Chiang, A. Flueck, K. S. Shah, and N, Balu, "CPFLOW: A practical tool for tracing power system steady-state stationary behavior due to load and generation variations", *IEEE Transactions on Power Systems*, Vol. 10, pp. 623-634, May. 1995.

[24] M. D. Ilic, J. R. Lacalle-Melero, F. Nishinmura, W. Schenler, D. Shirmohammadi, A. Crough, and A. Catelli, "Short-term economic energy management in a aompetitive utility environment", *IEEE Transactions on Power System*, vol. 8, pp. 198-206, Feb. 1993.

[25] A. Papalexopoulos, "Challenges to on-line optimal power flow implementation", *IEEE Transactions on Power System*, vol. 12, pp. 449-451, Feb. 1997.

[26] S. Hao, G.A. Angelidis, H. Singh, and A. D. Papalexopoulos, "Consumer payment minimization in power pool auction", *IEEE Transactions on Power System*, vol. 13, pp. 986-991, Aug. 1998.

[27] H. Singh, S. Hao, and A. Papalexopoulos, "Transmission congestion management in competitive electricity markets", *IEEE Transactions on Power System*, vol. 13, pp. 672-680. May 1998.

[28] M. Pavella, D. Ruiz-Vega, J. Giri, and R. Avila-Rosales, "An Integrated Scheme for ON-line Static and Transient Stability Constrained ATC Calculation", in *Proceedings of the 1999 IEEE/PES Summer Meeting*, vol. 1, pp. 273-276, July 1999

[29] X. Wang and Y. H. Song, "Advanced real-time congestion management through both pool balancing market and bilateral market", IEEE Power Engineering Review, vol. 20. pp. 47-49, Feb. 2000.

[30] C. N. Yu, and M. D. Ilic, "An Algorithm for Implementing Transmission Rights in a Competitive Power INdustry", in *Proceedings of the* 2000 IEEE/PES Winter Meeting, vol. 3, pp. 1708-1714, Jan. 2000.

[31] M. H. Gravener, and C. Nwankpa, "Available transfer capacity and first order sensitivity", *IEEE Transactions on Power Systems*, vol. 14, pp. 512-518, May 1999.

[32] G. M. Huang, and Y. Li, "Power system reliability evaluation including transient faults," in *Proceedings of the 2001 NAPS*, pp.559-563.

[33] IEEE RTS Task Force of APM Subcommittee, "IEEE Reliability Test System", *IEEE Power App. Syst.,* vol PAS-98, pp. 2047-2054, Nov/Dec. 1970.

[34] J. S. Thorp, A. G. Phadke, S. H. Horowitz, S. Tamronglak, "Anatomy of Power System Disturbances: Importance Sampling", *International Journal of Electrical Power and Energy Systems*, vol. 20, no. 2, pp. 147-152, Feb. 1997.

[35] J. Chen, and J. S. Thorp, "A reliability study of transmission systen protection via a hidden failure DC flow model," Power System Management and Control, No. 488, IEE 2002.

[36] A. W. Marshell, "The Use of Multi-Stage Sampling Schemes in Monte Carlo Computations," in Symposium on Monte Carlo Methods, New York, 1956, pp. 123.

[37] R. Billinton, and W. Li, *Reliability Assessment of Electrica Power System Using Monte Carlo Methods*, New York, Plenum Press, 1994, pp. 53-56.

[38] J. A. Bucklew, *Large Deviation Technique in Decision, Simulation, and Estimation*, New York: John Wiley and Sons, Inc. 1990.

[39] S. T. J. A. Vermeulen, H. Rijanto, and F. A. Van der Duyn Schouten, "Modelling the influence of preventive maintenance on protection system reliability performance," *IEEE Trans. Power Delivery*, vol. 13, Oct. 1998.

[40] L. L. Lai, *Intelligent System Applications in Power Engineering*, New York: John Wiley & Sons, Sep. 1998.

[41] D. Neibur and A. Germond, "Power system static security assessment using Kohonen neural network classifier," *IEEE Transactions on Power Systems*, vol. 7, no. 2, pp. 865-872, May 1991.

[42] M. A. El-Sharkawi and R. Atteri, "Static security assessment of power system using the Kohonen neural network," in *Proceedings of the ANNPS'*93, Tokyo, Japan, pp. 373-377, Apr. 1993.

[43] H. Hori, Y. Tamaru and S. Tsuzuki, "An artificial neural-net based techniques for power system dynamic stability with the Kohonen model," *IEEE Transactions on Power Systems*, vol. 7, no. 2, pp. 856-864, May 1992.

[44] T. Baumann, A. Germond, and D. Tschudi, "Impulse test fault diagnosis on power transformers using Kohonen's self-organizing neural networks," in *Proceedings of the 3rd Symposium on Expert System Applications to Power Systems*, Tokyo, Japan, pp. 642-647, Apr. 1991.

[45] A. Germond, N. Macabrey and T. Baumann, "Application of neural networks to load forecasting," in *Proceedings of INNS-Summer Workshop "Neural Networks Computing for the Electric Power Industry,"* Stanford, California, pp. 165-171, Aug. 1992.

[46] X. Luo, C. Singh and A. D. Patton, "Loss-of-load state identification using self-organizing map," in *Proceedings of IEEE Power Engineering Society 1999 Summer Meeting*, vol. 2, pp. 670-675.

[47] SOM Toolbox Team Helsinki University of Technology, "Technical report on SOM toolbox 2.0," April 2000.

[48] T. Kohonen, *Self-Organizing Maps*, Heidelberg, Germany: Springer Series in Information Sciences, vol. 30, Springer Series in Information Sciences, 2nd ed. 1997.

[49] H. Kim, "Evaluation of Power System Security and Development of Transmission Pricing Method," Ph.D. Dissertation, ELEN, Texas A&M University, August 2003.

[50] H. Kim, and C. Singh, "Probabilistic security analysis using SOM and Monte Carlo simulation," in *IEEE PES Winter Meeting*, vol. 2, 2002, pp. 755-760.

[51] Transmission Transfer Capability Task Force, "Available Transfer Capability Definitions and Determination," North American Electric Reliability Council report, June 1996

[52] Y. Ou, and C. Singh, "Assessment of available transfer capability and margins," *IEEE Trans. Power Systems*, vol. 17-2, pp. 463-468, May 2002.

[53] H. Chiang, A. J. Flueck, K. S. Shah, and N. Balu, "CPFLOW: A practical tool for tracing power system steady-state stationary behavior due to load and generation variations," *IEEE Trans. Power Systems*, vol. 10, No. 2, pp 623-634 May 1995.

[54] G. C. Ejebe, J. Tong, and J. G. Waight. etc., "Available transfer capability calculations," *IEEE Trans. Power* Systems, vol. 3, No. 4, pp. 1521-1527, Nov. 1998.

[55] Y. Ou, and C. Singh, "Improvement of total transfer capability using TCSC and SVC," in *IEEE PES Summer Meeting*, vol. 2, 2001, pp.944-948.

[56] P. A. Anderson, *A. A. Fouad, Power System Control and Stability*, New Jersey: IEEE Press, 1994.

[57] J. Machowski, J. Bialek, J. Bumby, *Power System Dynamics and Stability*, John Wiley & Sons, West Essex, England, 1997.

[58] Y. Xiao, and Y. H. Song, "Available transfer capability (ATC) evaluation by stochastic programming", *IEEE Power System Review*, September 2000, pp. 50-52.

[59] F. Xia, and S. Meliopoulos, A.P., "A methodology for probabilistic simultaneous transfer capability analysis", *IEEE Trans. Power Syst*., 1996, 11, (3), pp. 1269-1278.

[60] B. Corniere, L. Matin, S. Vitet, N. Handjsaid, and A. G. Phadke, "Assessment of the congestion cost and the risk of curtailment associated with available transfer capability (ATC)," in *Proceedings of IEEE PES 2000 Winter Meeting*, Singapore, Jan. 2000.

[61] J. C. O. Mello, A. C. G. Melo, and S. Granville, "Simultaneous transfer capability assessment by combining interior point methods and Monte Carlo simulation," *IEEE Trans. Power Syst*., 1997, 12, (2), pp. 736-742.

[62] R. F. Chang, C. Y. Tsai, C. L. Su, and C. N. Lu, "Method for computing probability distributions of available transfer capability," IEE, Proc.-Gener. Transm. Distrib. vol. 149, no. 4, Jul. 2002, pp. 427-431.
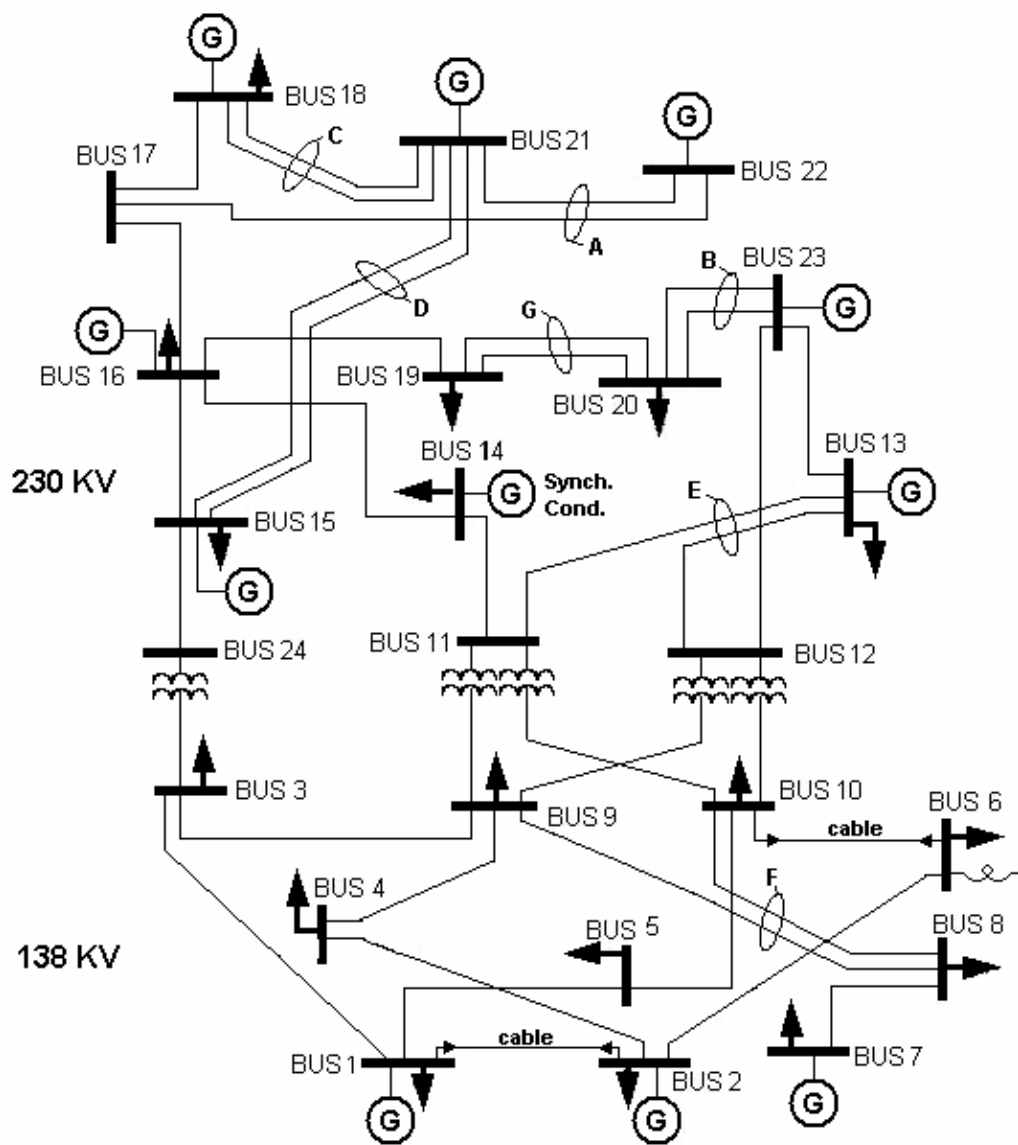
APPENDIX A

IEEE-RTS 24 BUS TEST SYSTEM

Figure A.1 24-bus IEEE Reliability Test System Diagram

Table A.1 Protection Hidden Failure Data

Line	Component		Protection System				P_Z & P_I (x10⁻²)
	λ (1/year)	μ (1/year)	λ_{p1} (1/year) (x10⁻²)	λ_{p2} (1/year) (x10⁻¹)	μ_i (1/year)	μ_I (1/hour)	
1-2	0.24	548	0.86	4.90	4	219	0.19
1-3	3.41	876	0.19	2.00	4	219	0.04
1-5	1.53	876	1.57	4.10	4	219	0.36
2-4	2.09	876	4.08	0.66	4	219	1.00
2-6	3.08	876	1.18	4.22	4	219	0.27
3-9	1.98	876	2.94	1.16	4	219	0.71
3-24	0.02	11.4	4.62	0.37	4	219	1.13
4-9	1.76	876	1.65	1.66	4	219	0.40
5-10	1.54	876	1.03	2.88	4	219	0.24
6-10	0.33	250	1.82	0.68	4	219	0.44
7-8	1.10	876	4.88	4.34	4	219	1.11
8-9	2.74	876	3.59	1.65	4	219	0.86
8-10	2.74	876	3.21	2.44	4	219	0.77
9-11	0.02	11.4	3.91	2.16	4	219	0.92
9-12	0.02	11.4	2.33	1.30	4	219	0.56
10-11	0.02	11.4	1.16	4.92	4	219	0.26
10-12	0.02	11.4	1.59	4.83	4	219	0.35
11-13	1.20	796	3.94	4.74	4	219	0.89
11-14	1.09	796	3.17	2.26	4	219	0.75
12-13	1.20	796	3.30	1.66	4	219	0.79
12-23	2.12	796	2.69	0.04	4	219	0.66
13-23	2.99	796	4.59	0.83	4	219	1.12
14-16	1.08	796	3.91	4.14	4	219	0.89
15-16	0.63	796	1.64	3.22	4	219	0.38
15-21	1.21	796	3.69	1.61	4	219	0.89
15-21	1.21	796	2.19	0.13	4	219	0.54
15-24	1.31	796	2.96	1.78	4	219	0.71
16-17	0.75	796	0.57	3.72	4	219	0.13
16-19	0.74	796	1.59	1.49	4	219	0.38
17-18	0.52	796	3.11	0.91	4	219	0.75
17-22	2.34	796	4.47	2.08	4	219	1.07
18-21	0.75	796	4.82	4.34	4	219	1.09
18-21	0.75	796	0.10	3.13	4	219	0.02
19-20	1.08	796	0.56	0.28	4	219	0.14
19-20	1.08	796	2.02	2.02	4	219	0.48
20-23	0.74	796	0.49	1.51	4	219	0.12
20-23	0.74	796	1.47	0.76	4	219	0.36
21-22	1.65	796	3.40	1.55	4	219	0.82

Table A.2 Important Simulation Parameters

Fault-clearing time	normal distribution
	$\mu = 0.07\text{sec}$ $\sigma = 0.01\text{sec}$
Reclosing time	normal distribution
	$\mu = 0.70\text{sec}$ $\sigma = 0.02\text{sec}$
Trip time when reclosing fail	normal distribution
	$\mu = 0.05\text{sec}$ $\sigma = 0.01\text{sec}$
Backup protection operation time	normal distribution
	$\mu = 0.50\text{sec}$ $\sigma = 0.05\text{sec}$
Fault duration time	Rayleigh distribution
	$\beta = 0.35\text{sec}$

APPENDIX B

WSCC-9 BUS TEST SYSTEM RELIABILITY DATA

Table B.1 Failure Rate and Repair Rate of Each Component

	Bus no.	λ (1/year)	μ (1/year)
Transformer	1-4	4	196
	3-6	4	196
	8-2	4	196
Transmission Line	4-5	10	193
	5-6	23	193
	6-7	7	193
	7-8	5	193
	8-9	19	193
	9-4	6	193

Table B.2 Fault Clearing Time Probability Distribution

Line	Type of distribution	Mean time (s)	Variance (s)
4-5	Normal	0.07	0.01
5-6	Normal	0.07	0.01
6-7	Normal	0.06	0.01
7-8	Normal	0.05	0.01
8-9	Normal	0.04	0.01
9-4	Normal	0.03	0.01

Table B.3 Fault Duration Probability Distribution

Line	Type of distribution	β
4-5	Rayleigh	0.29
5-6	Rayleigh	0.39
6-7	Rayleigh	0.34
7-8	Rayleigh	0.28
8-9	Rayleigh	0.44
9-4	Rayleigh	0.34

Table B.4 Fault Reclosing Time Probability Distribution

Line	Type of distribution	Mean time (s)	Variance (s)
4-5	Normal	0.55	0.03
5-6	Normal	0.75	0.03
6-7	Normal	0.65	0.03
7-8	Normal	0.55	0.03
8-9	Normal	0.85	0.03
9-4	Normal	0.65	0.03

VITA

Xingbin Yu was born in Handan, Hebei Province of P. R. China. He received his Bachelor of Science degree in electrical engineering from Shanghai Jiao Tong University in July 1988. After two years' work at Shiyan Power Industry Bureau as an engineer, he continued his studies as a graduate student and teaching assistant in Shanghai Jiao Tong University and received the Master of Science degree in February 1993. The research of his MS dissertation was on the reliability analyses of power apparatuses. He then worked as an electrical engineer at Qingdao Municipal Power Supply Bureau, where his main duties were power system dispatch and protection system design and management. In September 1996, he started to work as an Industrial Engineer in Enameled Wire & Cable (Singapore) Pte. Ltd., where he was in charge of new product design and process control. Since January 2001, he has been with Texas A&M University, working towards his Doctor of Philosophy degree in electrical engineering. During his Ph.D. program, he worked as Graduate Research Assistant under the guidance of Dr. Singh. His research area is power system reliability analysis. He is a student member of IEEE, the IEEE Power Engineering Society. He joined ERCOT (Electric Reliability Council of Texas) as a market design engineer in 2005.

His permanent address is:

> Xingbin Yu
> #85, Factory 607, Fengfeng Mine District
> Handan, Hebei 056201
> P. R. China